Therapies and Models of Alzheimer's Disease

Dissertation
zur
Erlangung der naturwissenschaftlichen Doktorwürde
(Dr. sc. nat.)

vorgelegt der

Mathematisch-naturwissenschaftlichen Fakultät
der
Universität Zürich

von

Jordan William McAfoose

aus den
Vereinigten Staaten

Promotionskomitee
Prof. Dr. Roger Nitsch (Vorsitz, Leitung der Dissertation)
Prof. Dr. Christoph Hock
Prof. Dr. Burkhard Becher
Prof. Dr. Adriano Fontana
Prof. Dr. Esther Stoeckli

Zürich, 2012

Table of Contents

Summary

Alzheimer's disease (AD) is a neurodegenerative disease that leads to progress cognitive loss and eventually to the complete loss of all daily functions. Described by its distinct neuropathological hallmarks - extracellular deposits of amyloid plaques and intracellular neurofibrillary tangles - the cause of sporadic Alzheimer's disease remains to be fully understood. The misfolding, accumulation and deposition of β-amyloid, however, has emerged as a central component of the disease. Amyloid-lowering therapies are currently, therefore, undergoing wide investigation as a treatment strategy for Alzheimer's disease. Other underlying molecular and cellular mechanisms are likely to be identified as key mediators or causative factors of disease, providing not only better understanding into the pathogenesis and progression of AD, but also drug discovery.

Here we have investigated the therapeutic potential of anti-TNF and amyloid-lowering treatment approaches in transgenic mouse models of brain amyloidosis. In the first study we administered etanercept anti-TNF treatment either directly within the brain by intracerebroventricular (icv) infusion using ALZET osmotic minipumps, or systemically via 4 weekly intraperitoneal injections. Infliximab and PBS treated mice served as controls, along with, non-treated transgenic and wildtype mice. Cognitive assessment of mice demonstrated a treatment dependent improvement in cognitive performance in two hippocampus-dependent cognitive tests. Results from the biochemical analyses indicate that the improvement in cognition was not associated with changes in soluble brain Abeta levels but rather a decrease in formic acid insoluble Abeta levels. Histological analysis using Thioflavin S demonstrated a treatment-induced lowering of plaque number and the percentage area covered by plaques. Upon further histological investigations, etanercept icv-treated mice were further shown to display increased cerebral amyloid angiophathy (CAA) amyloid pathology, as compared to controls, suggesting a redistribution of parenchymal plaques towards the vasculature. The increase in CAA-pathology did not show signs of increased occurrence of micro-bleeds, however, with time, it remains unknown, if these vessels might deteriorate, lose their integrity and begin to bleed. Anti-TNF treatment was further shown to induce a reduction in astrocytosis and increase microglia activation. Our results support clinical findings that TNF-directed immunotherapy may successfully reverse cognitive deficits and provide further evidence into the underlying therapeutic mechanism.

In a second study, we describe the selection of Aβ-specific designed ankyrin repeat proteins (DARPins) as a novel class of therapeutics for Alzheimer's disease. DARPins are small and highly stable proteins with a compact modular architecture ideal for high-affinity protein-protein interactions. Having identified a lead Aβ-specific DARPin candidate (D23) we were able to characterize in great detail the binding affinity, Aβ epitope recognition and binding kinetics of mono- and trivalent D23. We further showed their *in vitro* ability to delay Aβ aggregation and prevent Aβ-mediated neurotoxicity. To demonstrate their *in vivo* therapeutic potential we infused intracerebroventricularly D23 and 3xD23 into brains of 11 months old Tg2576 mice over four weeks. Both D23 and 3xD23 treatment were shown to result in improved cognitive performance and reduced soluble Aβ levels. Collectively, our findings provide proof-of-principle that Aβ-specific DARPins maybe used for the treatment of Alzheimer's disease.

To study the effects of the E693Δ APP mutation on Aβ accumulation and deposition *in vivo*, we generated a novel transgenic mouse model that overexpresses the human APP695 isoform containing the "Swedish" (K670N+M671L) and E693Δ mutations under the control of the mouse PrP promoter. These newly developed E22ΔAβ mice were compared to the well-established Tg2576 mouse line harboring the "Swedish" double mutation alone, and the ArcAβ mice, a mouse model recently developed in our laboratory that overexpresses the

Swedish mutation and the Arctic (E693G) intra-Aβ APP mutation. All transgenic mouse lines and their respective littermate controls underwent extensive cognitive-behavioral assessments at three different ages before they were sacrificed for further biochemical and histopathological analyses. All three transgenic mouse lines, including the E22ΔAβ mice, showed early cognitive impairments in a panel of hippocampus-dependent cognitive tasks. As expected, ArcAβ and Tg2576 mice showed an age-dependent increase in amyloid plaque deposition that was associated with an increase of Aβ in SDS insoluble protein fractions. In contrast, histopathological and biochemical analyses in 15 month-old E22ΔAβ mice revealed a complete absence of extracellular amyloid deposition that was accompanied by prominent accumulation of intraneuronal Aβ species and early decreases in soluble Aβ levels. However, at 24 months of age, prominent vascular amyloid deposits were observed in cortical and – more pronounced – cerebellar leptomeningeal vessels of E22ΔAβ mice. Additional *in vitro* experiments with recombinant E22Δ Aβ peptides clearly demonstrated a strong propensity of the mutated Aβ species to form amyloid fibrils. Moreover, E22Δ Aβ42 showed a unique aggregation kinetics lacking exponential fibril growth and poor seeding effects on wildtype Aβ aggregation. These results provide a possible explanation for the recessive trait of inheritance of the E693Δ APP mutation and place this mutation on the list of other "vasculotropic" intra-Aβ APP mutations.

Zusammenfassung

Die Alzheimer-Krankheit ist die häufigste neurodegenerative Erkrankung und klinisch mit einer progredienten Abnahme kognitiver Fähigkeiten und im Verlauf vollständigem Verlust von Alltagsfunktionen sowie Selbständigkeit assoziiert. Obwohl die neuropathologischen Charakteristika der Erkrankung, extrazelluläre Ablagerungen von Amyloid-Plaques und intrazelluläre Anhäufungen von neurofibrillären Bündeln, bereits seit nunmehr über 100 Jahren bekannt sind, sind die Ursachen der weit verbreiteten sporadischen Form der Alzheimer-Krankheit immer noch unzureichend verstanden und weiterhin Gegenstand intensiver Forschung. Die Fehlfaltung, Akkumulierung und Ablagerung von beta-Amyloid wird heute von den meisten Wissenschaftlern als eine zentrale pathogenetische Komponente der Erkrankung angesehen. Verfahren, die darauf abzielen, beta-Amyloid im Hirn zu reduzieren, gehören daher zu den wichtigsten therapeutischen Strategien gegen die Alzheimer-Krankheit. Daneben ist jedoch davon auszugehen, dass sich mit der laufenden Identifizierung weiterer pathogenetisch wichtiger Krankheitsfaktoren diverse weitere (nicht Amyloid-basierte) Therapieansätze in absehbarer Zeit ergeben könnten.

Im Rahmen dieser Doktorarbeit haben wir die Wirksamkeit zweier unterschiedlicher therapeutischer Ansätze in APP-transgenen Mausmodellen der Alzheimer-Krankheit studiert. In einer ersten Studie wurden die Effekte einer anti-TNF-Behandlung mit Etanercept untersucht, das 4 Wochen lang entweder kontinuierlich intracerebroventrikulär (icv) über ALZET osmotische Minipumpen oder systemisch durch wöchentliche intraperitoneale (ip) Applikationen (ebenfalls 4 Wochen lang) verabreicht wurde. Infliximab- und PBS-Vehikel-behandelte Mäuse sowie unbehandelte und nicht-transgene Mäuse wurden hierbei als Kontrollen herangezogen. Verhaltensanalysen ergaben therapieabhängige positive Effekte in zwei hippokampusabhängigen kognitiven Tests. In der biochemischen Analyse zeigte sich eine Abnahme von Detergens-unlöslichem beta-Amyloid, allerdings unveränderte lösliche beta-Amyloid-Spiegel. Die histologische Analyse ergab eine therapieabhängige Reduktion der Amyloid-Plaque-Zahl sowie des Gesamt-Amyloid-Loads. Darüber hinaus zeigten die APP-transgenen Mäuse, die icv mit Etanercept behandelt worden waren, im Vergleich zu den Kontrollmäusen eine Zunahme von vaskulärem Amyloid (CAA). Letzteres ist ein möglicher Hinweis darauf, dass die Behandlung mit Etanercept zu einer Umverteilung von Amyloid von parenchymalen Plaques zum Gefässamyloid geführt haben dürfte. Die Zunahme von CAA in den behandelten Mäusen war allerdings nicht mit einer Zunahme von Mikroblutungen assoziiert. Desweiteren war die Behandlung mit Etanercept mit einer Abnahme der Astrogliose und einer Zunahme der Mikrogliaaktivierung assoziiert. Zusammengefasst unterstützen die Resultate dieser Studie die aktuellen klinischen Befunde, wonach anti-TNF-basierte Immuntherapien einen günstigen Effekt auf die Kognition bei Patienten mit einer Alzheimer-Krankheit haben können; sie liefern darüber hinaus Einblicke in mögliche zugrundeliegende therapeutische Mechanismen.

In einer zweiten Studie haben wir die therapeutische Wirksamkeit von beta-Amyloid-spezifischen „Designed Ankyrin Repeat Proteins“ (DARPins) in einem Mausmodel

der Alzheimer-Krankheit untersucht. DARPins gehören zu einer neuartigen Klasse von Therapeutika mit verschiedenen vorteilhaften biochemischen Eigenschaften, zu denen neben der relativ kleinen Molekülgrösse und der hohen Stabilität auch der modulare Molekülaufbau gehört, der für die hochaffine Protein-Protein-Interaktion verantwortlich ist. Im Rahmen unserer Experimente haben wir das beta-Amyloid-spezifische DARPin D23 identifiziert, haben dessen Bindungsaffinität, die Abeta-Erkennungsdomäne sowie die Bindungskinetiken von monovalentem D23 versus trivalentem D23 beschrieben. *In vitro*-Analysen konnten einen inhibitorischen Effekt von D23 auf die Abeta-Aggregation und Abeta-vermittelte Neurotoxizität zeigen. Um das therapeutische Potential von Abeta-spezifischen DARPins *in vivo* zu untersuchen, wurden APP-transgene Tg2576-Mäuse 4 Wochen lang mit monovalentem (D23) und trivalentem DARPin (3XD23) icv behandelt. Dabei führte sowohl die Behandlung mit D23 als auch die Behandlung mit 3XD23 zu einer signifikanten Verbesserung der kognitiven Defizite, was mit reduzierten Spiegeln von Detergens-löslichem Abeta einherging. Diese Experimente belegen erstmals *in vivo* den potentiellen therapeutischen Nutzen von Abeta-spezifischen DARPins in der Behandlung der zerebralen Beta-Amyloidose.

Im Rahmen unseres dritten Projekts haben wir die Effekte der erst kürzlich entdeckten familiären APP-Mutation E693Δ auf die Akkumulierung und die Ablagerung von beta-Amyloid *in vivo* untersucht. Dazu haben wir ein neues APP-transgenes Mausmodell generiert, das die humane APP695-Isoform mit der E693Δ-Mutation sowie der Schwedischen (K670N+M671L) Doppelmutation unter der Kontrolle des Maus-PrP-Promotors überexprimiert. Diese neu generierten E22ΔAβ-Mäuse wurden mit dem etablierten Tg2576-Mausmodell, das die Schwedische Mutation allein exprimiert, und dem in unserem Labor entwickelten arcAβ-Mausmodell (Expression von Schwedischer Mutation + „Arctic“ intra-Abeta-APP-Mutation (E693G)) verglichen. Alle drei transgenen Linien, einschliesslich den E22ΔAβ-Mäusen, zeigten frühe kognitive Beeinträchtigungen in einem Panel von hippokampus-abhängigen kognitiven Tests. Wie zu erwarten war, zeigten arcAβ- und Tg2576-Mäuse eine altersabhängige Anhäufung von Amyloid-Plaques, die mit einem Anstieg von Detergens-unlöslichem beta-Amyloid im Hirn korrelierte. Dagegen konnten bei den E22ΔAβ-Mäusen bis zu einem Alter von 15 Monaten überhaupt keine extrazellulären Amyloid-Ablagerungen nachgewiesen werden, dagegen eine frühe Akkumulierung von intrazellulärem Abeta und reduzierte lösliche Abeta-Spiegel. Im Alter von 24 Monaten waren allerdings auch bei den E22ΔAβ-Mäusen prominente extrazelluläre Amyloid-Ablagerungen in Form kortikaler und v. a. cerebellärer leptomeningealer vaskulärer Ablagerungen nachweisbar. Zusätzliche *in vitro*-Experimente konnten zudem zeigen, dass E22Δ-mutierte Aβ-Spezies in der Tat eine hohe Aggregationsbereitschaft und Fähigkeit zur Amyloid-Fibrillenbildung aufweisen. Darüber hinaus konnte bei E22Δ Aβ42 eine einzigartige Aggregationskinetik dokumentiert werden, die u. a. durch ein Fehlen der exponentiellen Wachstumsphase und schlechte „Seeding“-Eigenschaften charakterisiert ist, was eine mögliche Erklärung für das späte Auftreten von extrazellulären Amyloid-Ablagerungen und die rezessive Vererbung der E693Δ-Mutation darstellen könnte.

1 Introduction

1.1 Alzheimer's disease

Alzheimer's disease (AD) is a progressive neurodegenerative disease that results in dementia. The neuropathological hallmarks of AD include β-amyloid plaques, composed of extracellular deposits of the 4 kDa Aβ40 and the more amyloidogenic Aβ42, as well as neurofibrillary tangles (NFT), consisting of intraneuronal filaments of hyperphosphorylated tau protein, as well as, pronounced astrocytosis and activated microglia (Figure 1). These pathological hallmarks were first described in 1906 by the German psychiatrist Alois Alzheimer, following detailed pre-mortem clinical observations and post-mortem neuropathological examination of his patient Auguste Deter. The next major breakthrough in understanding AD pathology came 70 years later when it was discovered that the brains of AD patients demonstrated reduced levels of acetylcholine (for review see, Schliebs et al., 2010). These discoveries lead to the first ever treatment for AD with Tacrine and other cholinesterase inhibitors (Rivastigmine, Donepezil and Galantamine). It was later determined biochemically that beta-amyloid (Aβ) was the pathologic protein constituting extracellular amyloid plaques, leading to the so-called amyloid cascade hypothesis in which amyloid-beta serves a central role in AD pathogenesis (for review see Aguzzi and O'Connor 2010; Hardy et al., 2002).

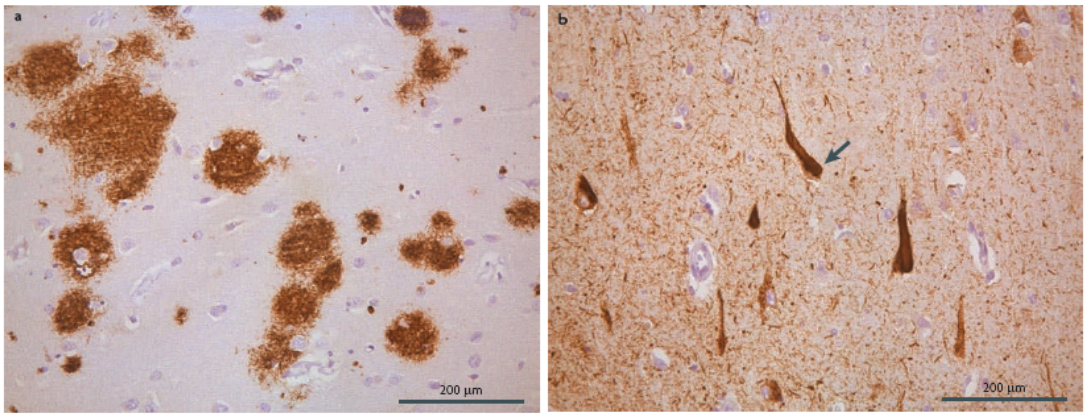

Figure 1. Histopathological hallmarks of AD. A) Photomicrograph depicting extracellular aggregates of β-amyloid in brain parenchyma tissue and B) the intracellular accumulation of hyperphosporylated microtubule associated protein tau as neurofibrillary tangles (NFT) (modified from: Aguzzi and O' Connor, 2010)

Aβ is derived from the amyloid precursor protein (APP), a membrane-spanning protein, by two sequential secretase activities, γ- and β-secretase (Figure 2). In both *in vitro* and *in vivo* experiments, it has been widely shown that synthetic, as well as, naturally derived Aβ peptides can inhibit hippocampal long-term potentiation (LTP) and facilitate long-term depression (Li et al., 2009; Townsend et al., 2006; Walsh et al., 2002), impair memory in animal models (Clearly et al., 2005; Lesne et al., 2006; Shankar et al., 2008) and disrupt synaptic function and structure (Lacor et al., 2007). The most compelling evidence to support the amyloid cascade hypothesis, however, has come from genetic studies in which rare familial early onset autosomal dominant forms of AD (FAD) have been linked to missense mutations in the amyloid beta-peptide precursor protein (APP) or the presenilin (PS1 and PS2) genes (for review see, Bertram et al, 2008; Bertram et al., 2010; Rademakers et al., 2009). All of these FAD mutations were shown to invariably increase the production of Aβ42, the longer and more toxic variant of the Aβ peptide which readily forms amyloid aggregates. The Swedish double mutation (K670N/M671L), for example, located upstream from the Aβ N-terminus adjacent to the β-cleavage site, results in an increased production of both Aβ40 and Aβ42 species, whereas mutations located at the γ-cleavage site of APP cause an increase of the Aβ42/Aβ40 ratio and, as a consequence of this, result in increased Aβ aggregation and deposition (Bertram et al, 2008; Bertram et al., 2010; Rademakers et al., 2009). The recently discovered E22Δ (E693Δ) mutation (Tomiyama et al., 2008) is one of the six so-called "intra-Aβ" mutations clustered around the hydrophobic core of the Aβ sequence (at position 22±1). Position 22

seems to be a critical site involved in pathogenic aggregate formation since mutations at or (±1) around this site including the Dutch (E22Q) (Levy et al., 1990), Flemish (A21G) (Hendriks et al., 1992), Italian (E22K) (Miravalle et al., 2000), Iowa (D23N) (Grabowski et al., 2001) and Arctic (E22G) (Nilsberth et al., 2001) mutations have been reported to result in an increase in total Aβ production (Haass et al., 1994) and – with the exception of the Flemish mutation – enhance Aβ aggregation and toxicity (Fraser et al., 1992; Murakami et al., 2003).

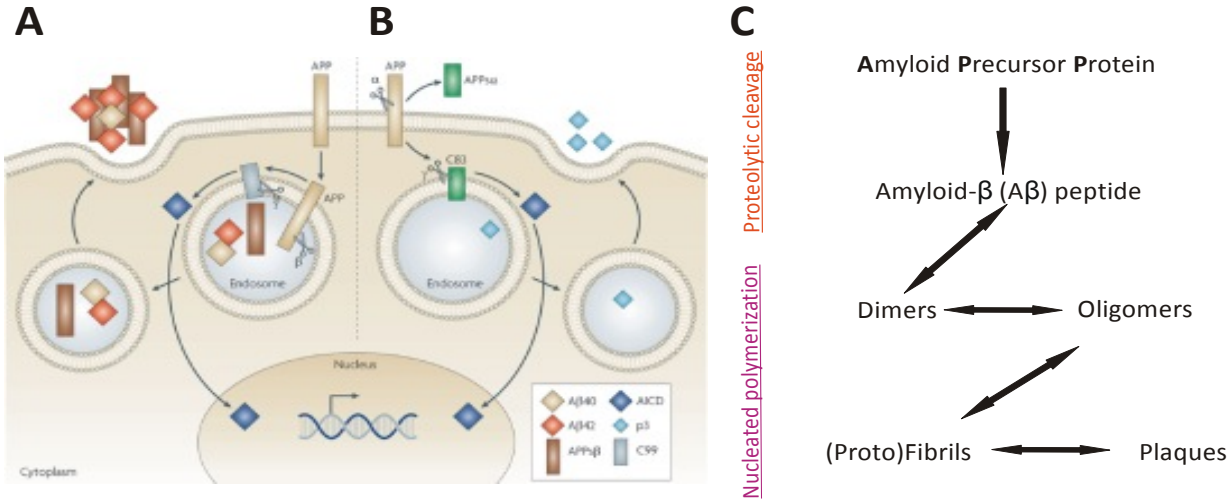

Figure 2. Amyloid-β formation. A) Amyloid-β (Aβ) peptide is generated following the serial proteolytic cleavage of the amyloid precursor protein (APP) by β- and γ-secretases. B) The non-amyloidogenic pathway results in the formation of secreted APP (APPsα) and internalized C83 following α-secretases cleavage, in which subsequently γ-cleavage takes place and the formation of p3 and APP intracellular domain (AICD) occurs (modified from: Aguzzi and O' Connor, 2010). C) Proposed mechanisms leading to Aβ fibrillization, in which following the proteolytic cleavage of APP, soluble Aβ peptides begin to form abnormal β-sheet conformations which increase their likelihood of forming more structured dimer aggregates and small oligomers, these aggregates then act as seeds promoting the formation of protofibrils and fibrils and the eventual formation of insoluble extracellular amyloid plaques.

1.2 Brain aging and neurodegeneration

Aging is a major risk factor for the development of Alzheimer's disease, as well as other neurodegenerative disease including, Parkinson's disease, amyotrophic laterals sclerosis and others. Because the prevalence of both genetic and sporadic forms of most neurodegenerative diseases increases with age, factors associated with senescence are involved in their etiologies. An emerging body of evidence indicates that immune senescence plays an important role in modulating age-associated changes in neuronal function. Immune senescence results in progressively impaired functions of innate and adaptive immunity, but also in

decreased tolerance, chronic inflammation, and accelerated inflammatory-stress responses. Dysfunctional senescent microglia up-regulate pro-inflammatory cytokines maintaining low-grade inflammation within brain and reactive astrocytosis impairs neurovascular coupling and synaptic regulation. As a result, the expression in the central nervous system of genes related to stress, oxidative damage and inflammatory response pathways increase with progressive aging (Lu et al., 2004; Yanker et al., 2008).

The aging brain is further challenged by progressive DNA damage (McKinnon, 2009), mitochondrial dysfunction (DiMauro et al., 2008), oxidative stress (Barnham et al., 2004), environmental and stress-induced epigenetic changes, altered gene and regulatory RNA expression (Bushati et al., 2008; Nelson et al., 2008; Yanker et al., 2008), impaired protein degradation processes (autophagy and proteasome pathways) (Rubinsztein, 2006) and the accumulation of iron, among others. In short, age-dependent accumulation of mitochondrial DNA mutations has been associated with mitochondrial dysfunction, ATP/energy deficits, oxidative stress, impaired Ca^{2+} homeostasis, brain aging and neurodegeneration (Lin et al., 2006: Reeve et al., 2008). Moreover, with age iron accumulates progressively within the brain and in Parkinson's disease, Alzheimer's disease and other neurodegenerative diseases, iron promotes inflammation, oxidative stress, neuronal dysfunction and the production and aggregation of misfolded proteins (Zecca et al., 2004). Protein-degradation activities, including, autophagy (macroautophagy, microautophagy and chaperone-mediated autophagy) and ubiquitin-proteasome pathways, decrease with age and are commonly associated with neurodegenerative diseases, including Alzheimer's disease, Parkinson's disease, and Huntingtin's disease (Rubinsztein, 2006; Wong et al., 2010). These compromised protein-degradation pathways result in the accumulation of misfolded aggregation-prone proteins, intracellular aggregates and cell death (Martinez-Vicente et al., 2007). Lastly, the role of misfolded protein aggregates in neurodegenerative disease has long been postulated, with some of the first neuropathological descriptions of intracellular inclusion bodies and extracellular plaques being described in postmortem brains of neurodegenerative patients over a century ago. Extensive molecular, cellular and genetic evidence has since accumulated to support the role of misfolded aggregation-prone proteins with neurotoxic properties in neurodegenerative diseases (Aguzzi et al., 2010; Forman et al., 2004; Haass et al., 2007), including β-amyloid in Alzheimer's disease (AD); tau in

AD, frontotemporal dementia (FTD), progressive supranuclear palsy (PSP), Pick's disease and other tauopathies; α-synuclein in Parkinson's disease (PD) Lewy body dementia (LBD) and Multiple Systems Atrophy (MSA); huntington in Huntington's disease; and superoxide dismutase in Amyotrophic lateral sclerosis; among others.

1.3 Immune Senescence and neurodegeneration

With progressive aging, the production of naïve lymphocytes decreases, thymic involution occurs, peripheral lymphoid tissues shrink in volume and the accumulation of incompetent memory lymphocytes increases resulting in reduced adaptive immunity, poor vaccination response and greater susceptibility to infection and disease (Nikolich-Zugich, 2008). Compromised B and T cell functions can also lower the immune system's ability to differentiate 'self' from 'foreign' antigens, thus leading to the development of 'destructive' autoimmune responses. Alternatively, these changes in B and T cell function may lead to decreased 'protective' autoimmunity, with less B-cell and T-cell reactions against brain antigen and reduced naturally-occurring human conformation-specific antibodies (Szabo et al 2008; Neff et al., 2008, Kellner et al., 2009) reacting with pathology aggregates of misfolded proteins with toxic properties and thus impaired protection against the development of neurodegenerative diseases (Bhat et al., 2009; Diamond et al., 2009).

In addition to reduced adaptive immunity, progressive aging is associated with impaired innate immunity and a low-grade chronic inflammatory state (Shaw et al., 2010). Senescence of brain-to-immune communication pathways activate the hypothalamus-pituitary-adrenal axis and increase glucocorticoids to neurotoxic concentrations resulting in neuronal damage, hippocampal atrophy, cognitive decline, depressive episodes and the risk of developing neurodegenerative diseases, such as AD (Sorrells et al., 2007; Sotiropoulos et al., 2008). Furthermore, age-related changes in microglia function can promote low-grade inflammation, exaggerate cognitive liabilities following inflammatory responses and promote neurodegeneration (Block et al., 2007; Fiala et al., 2007). Indeed, chronic low-grade inflammation during aging has been associated with increased mortality, cognitive decline and neurodegeneration, with numerous results indicating increased levels of such pro-inflammatory cytokines as IL-1, IL-6 and TNF, chemokines and acute phase proteins, in serum, plasma and CSF of elderly subjects (Alvarez et al., 2007; Bermejo et al.,

2008; Schram et al., 2007; Gimeno et al., 2008; Reuben et al., 2002). Not surprisingly, systemic immune and inflammatory alterations have been described in Alzheimer's disease and ALS (Mantovani et al., 2009; Zhang et al., 2005) among others, with acute systemic immune challenges often reported as the main cause of delirium in elderly populations (Perry et al., 2007). Immune interventions that target these age-associated immunological components are of therapeutic importance for neurodegenerative diseases and currently the subject of considerable investigation (Dorshkind et al., 2009; Popovich et al., 2008; Weksler et al., 2009).

1.4 Role of glial cell-related immunosenescence in neurodegeneration

Glial cells are essential for normal brain development and function; they actively participate in neuronal plasticity and repair (Halassa et al., 2007), neurotrophic support, myelination, neurovascular coupling and the formation of the blood-brain barrier (BBB) (Zlokovic, 2008) and immune surveillance (Bains et al., 2007; Barres, 2008; Allen et al., 2009). During disease states, however, compromised glial cell function can have detrimental consequences on brain function and cognition. Age-related changes in glial function can also impair neuronal function, exaggerate inflammatory responses following infection or CNS injury and contribute to neurodegeneration (Jimenez et al., 2008; Solano et al., 2008). Microglia serve multiple functions as resident macrophages within the CNS that express Fc receptors for IgG uptake, MHC glycoproteins, complement components and scavenger receptors, as well as, the secretion of cytokine and chemokine (Barres, 2008; Ransohoff et al., 2009). Evidence strongly supports the important role of microglial in immune surveillance, phagocytosis and immunological defense against pathogens and environmental insults within the CNS (Graeber, 2010; Hanisch et al., 2007; Kettenmann, 2007). In health, during 'resting' and 'surveying' states, microglia display neuroprotective properties, release growth factors, repair local microenvironment damage and continuously monitor their surroundings by extending and retracting their processes. However, following injury or immune activation, 'activated' microglia become highly mobile and migrate to areas of injury, where they participate in phagocytosis and repair. Activated microglia also exert inflammatory responses characterized by the upregulation and secretion of pro-inflammatory cytokines (IL-1, IL-6 and TNF), chemokines and reactive oxygen species. Age-related

changes in microglia structure and phenotype (Figure 3) include spheroidal swelling, beaded or deramified processes (Streit, 2006; Streit et al., 2008), and associated impairment in phagocytic functions, heightened inflammatory responses and decreased production of neurotrophic factors (Jimenez et al., 2008).

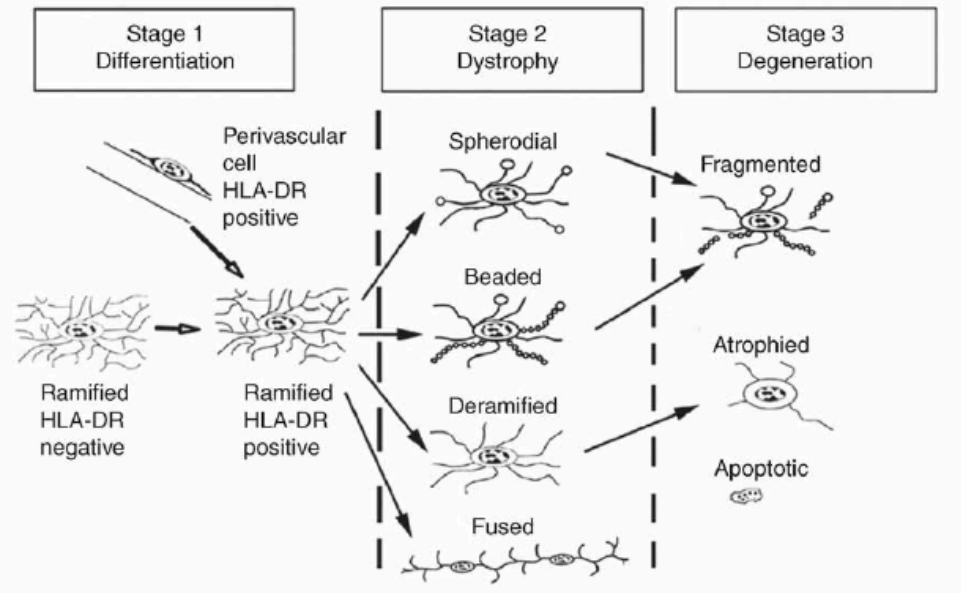

Figure 3. Microglial structure and phenotypes. Resident microglia can become activated to adopt one of many diverse phenotypes throughout aging, stage of disease and many other variables. The first phase of the microglial life cycle during stage 1 involves acquisition of the HLA-DR-positive phenotype. There are two possible pathways: HLA-DR-positive perivascular cells differentiate to become HLA-DR-positive ramified microglia and/or HLA-DR-negative microglia become HLA-DR-positive. Trans-differentiation of perivascular cells into ramified microglia is likely to be a minor pathway. During stage 2, ramified HLA-DR-positive microglia begin to show dystrophic changes by developing spheroidal swellings and beaded or deramified processes. They might also aggregate to form rod cells or other multi-cellular aggregates. During stage 3, degenerative changes such as fragmentation (cytorrhexis), loss of processes (atrophy) and apoptosis can occur. The exact sequence of this progression has not yet been determined. Adopted from Streit, 2006.

Given the essential role microglia-mediated phagocytosis serves in clearance of cellular debris and triggering repair following injury, impaired phagocytosis has profound implications for the accumulation of abnormal deposits of misfolded proteins associated with neurodegenerative diseases (Neumann et al., 2009: Perry et al., 2010). In a mouse model of brain amyloidosis newly formed beta-amyloid plaques recruit microglia to the site and induce microglia activation (Meyer-Luehmann et al., 2008). Microglia-mediated clearance of beta-amyloid is strongly activated in the presence of specific IgG antibodies allowing for substrate recognition and Fc-mediated phagocytosis (Bard et al., 2000). Indeed, following the administration of immunotherapy in both humans and mice, microglia have been demonstrated to participate in the phagocytosis of Abeta (Wisniewski et al., 2008).

Moreover, immunization may alter phagocyte functions, enabling microglia to efficiently phagocytose Abeta through both Fc-mediated phagocytosis and Fc-independent mechanisms (Boche et al., 2008; Brody et al., 2008; Koenigsknecht-Talboo et al., 2008). Finally, evidence indicates that the trafficking of peripheral monocytes into the brain promotes the clearance of Abeta, provides neuroprotective support and delays the progression of AD (El Khoury et al., 2008; El Khoury et al., 2007; Simard et al., 2006); however some experimental confounds have been raised (see Davoust et al., 2008; Ransohoff, 2007; Ransohoff and Perry, 2009).

In the presence of toxic misfolded forms of Abeta, aged microglia react with exaggerated inflammatory responses, increased reactive oxygen species production and neurotoxicity, as compared to young microglia (Leung et al., 2009). In support of these findings, a clinical study by Edison et al (2008), demonstrated using PiB-PET and [11C](R)PK11195-PET that microglial activation was associated with increased beta-amyloid plaque load and cognitive dysfunction. Taken together, these findings suggest that while there are roles of microglia in surveying the brain for, and clearing of, toxic misfolded proteins, their age-related changes predispose them for overshooting responses to misfolded proteins with detrimental downstream consequences for neuronal function and integrity. Impaired phagocytosis, chronic inflammation and microglia-mediated neurotoxicity might therefore represent three aspects of age-dependent changes in microglia function that result in accumulation of misfolded proteins and neurodegeneration (Block et al., 2007; Fiala et al., 2007). However the involvement of microglia in the formation, maintenance and clearance of misfolded protein monomers, higher-order aggregates and plaques remains to be fully understood (Grathwohl et al., 2009; Mandrekar et al., 2009; Ransohoff and Perry, 2009).

Similarly, astrocyte functions can deteriorate during aging, leading to compromised BBB function, impaired neurovascular coupling, decreased neurotrophic support, excitotoxicity and compromised neuronal transmission and synaptic regulation (Wang et al., 2008). Astrocytes are the most abundant glial cell in the brain and have been widely recognized to serve several physiological functions that are necessary for brain development, function and repair (see Wang et al., 2008 for a review). Besides their roles in neuronal processing, synaptic integration, synaptogenesis, synaptic plasticity (Bains et al., 2007; Halassa et al., 2007; Turrigiano, 2006), astrocytes also

serve a key role in CNS innate immunity and inflammatory responses, by expressing Toll-like receptors involved in pathogen recognition and participating in phagocytosis (Farina et al., 2007: Wyss-Coray et al., 2003). Indeed, under pathophysiological conditions such as infection, injury and neurodegeneration, reactive astrocytes can exert immune and inflammatory responses by expressing and secreting a wide range of immunological factors, such as, complement factors, acute phase reactants, adhesion molecules, major histocompatibility complex (MHC) class I and II glycoproteins, cytokines and chemokines. Reactive astrocytes can also aid the recruitment of immune cells from the periphery by modifying BBB permeability. Finally, astrocytes serve an important role in neuronal survival and regeneration by providing neurotrophic support with growth factors, such as NGF, BDNF, GDNF and IGF-1. Loss of neurotrophic support can induce DR6-mediated axonal self destruction and neuronal death (Nikolaev et al., 2009); at least during neurodevelopment. More specifically, neurotrophic deprivation triggers the release of N-APP, a 35kDa APP fragment generated from sAPPbeta by an unknown mechanism, following the cleavage of APP by beta-secretase. N-APP then binds DR6 to induce axonal self destruction via caspase 6 and neuronal death via caspase 3).

1.5 Role of inflammatory cytokines in physiology and neurodegeneration

1.5.1 Cytokines, synaptic plasticity and cognitive function

Immune signalling factors including cytokines, chemokines, complement proteins and other immune molecules serve essential roles within the brain such as neuronal development and synaptic plasticity (Di Filippo et al., 2008; McAfoose et al., 2009; Yanamadala et al., 2010). Chemokines, in particular, exert neuromodulator properties (Rostene et al., 2007) and cytokines, namely IL-1, IL-6 and TNF, under non-immune challenged conditions participate in several forms of synaptic plasticity such as, Hebbian plasticity (Malenka et al., 2004), synaptic scaling (Burrone et al., 2003; Perez-Otano et al., 2005; Turrigiano, 2007), and adult neurogenesis (Bruel-Jungerman et al., 2007a; Bruel-Jungerman et al., 2007b), that promote memory consolidation and cognition; for review see (Di Filippo et al., 2008; McAfoose et al., 2009).

For example, growing evidence (Balschun et al., 2004; Li et al., 1997; Tancredi et al., 2000; Jankowsky et al., 2000; Avital et al., 2003; Schneider et al., 1998; Spulber et al., 2009) suggests that IL-1 and IL-6 participates in long-term potentiation (LTP), a form of Hebbian synaptic plasticity, and memory consolidation processes. Essentially this process can be divided into three stages (Figure 4). In stage 1, the simultaneous neuronal activity (firing) of both pre-synaptic and post-synaptic neurons results in the induction of LTP. This induction of LTP, in stage 2, can lead to the production of both IL-1 and IL-6 (Jankowsky et al., 2000). Finally in stage 3, LTP maintenance is fine-tuned by the overall level or net expression of both IL-1 and IL-6. More specifically, evidence (Schneider et al., 1998; Coogan et al., 1999; Ross et al., 2003) suggests that increased local production of IL-1 in the hippocampus facilitates LTP maintenance, whereas, IL-6 blocks LTP maintenance by opposing, in a negative feed-back fashion, the effects of IL-1 on LTP maintenance (Balschun et al., 2004). Collectively, these processes interact to influence memory consolidation and learning processes.

Indeed, cognitive-behavioural research in mice and rats has demonstrated that IL-1 and IL-6, under physiological conditions, participates in hippocampal-dependent memory processes (Brennan et al., 2003; Yirmiya et al., 2002; Hryniewicz et al., 2007; Baier et al., 2009), with evidence (Avital et al., 2003) to support the link between synaptic plasticity and memory function. However, during stress, aging and disease, increased levels of IL-1 and IL-6 appear to elicit memory impairment (Godbout et al., 2004; Pugh et al., 2001), suggesting that deviations in physiological IL-1 and IL-6 concentrations result in impaired memory (Goshen et al., 2007; Avital et al., 2003).

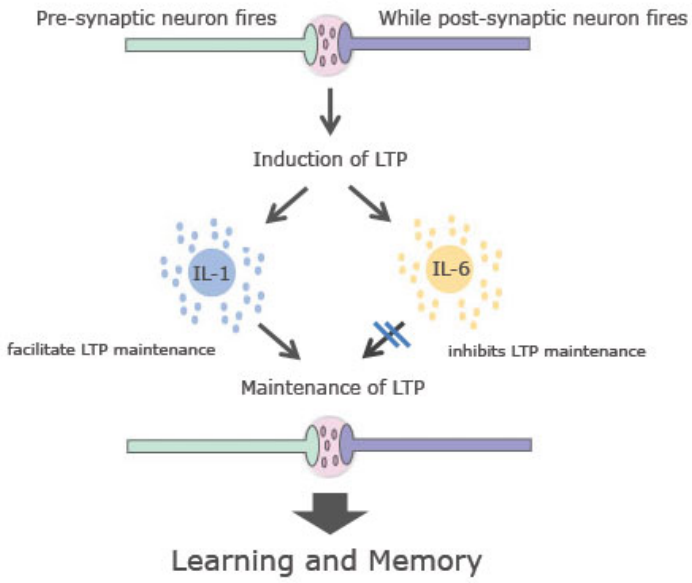

Figure 4. Schematic showing the involvement of IL-1 and IL-6 in long-term potentiation (LTP) synaptic plasticity. In short, the simultaneous neuronal activity (firing) of both pre-synaptic and post-synaptic neurons results in the induction of LTP. This induction of LTP leads to the production of both IL-1 and IL-6, which according to the overall level of expression of both IL-1 and IL-6 will either facilitate or inhibit the maintenance of LTP, respectively. This fine-tuning of LTP by IL-1 and IL-6 ultimately influences the consolidation of learning and memory. Adapted from McAfoose & Baune, 2009.

Tumor necrosis factor alpha (TNF) also exerts multiple biological functions within the brain, including, neuromodulation (Szelenyi, 2001; Vitkovic et al., 2000a; Vitkovic et al., 2000b), glutamate transmission (Pickering et al., 2005), dendritic branching (Neumann et al., 2002) and both Hebbian and non-Hebbian (synaptic scaling) synaptic plasticity (Albensi et al., 2000; Beattie et al., 2002; Stellwagen et al., 2005; Stellwagen et al., 2006). In particular, TNF participates in synaptic scaling, a non-Hebbian form of synaptic plasticity which has been shown to stabilize the activity of neurons and networks (Bains et al., 2007; Stellwagen et al., 2006; Turrigiano, 2007) (Figure 5). In short, during prolonged neuronal inactivity, which leads to a decrease in synaptic strength, the release of TNF by astrocytes is induced by glial-neuronal communication processes (Stellwagen et al., 2006). In a hemeostatic fashion, the released TNF by astrocytes increases post-synaptic neuron activity, thus, increasing or scaling-up the synaptic strength of the post-synaptic neuron. Collectively, this helps to maintain neuronal activity and learning and memory functions.

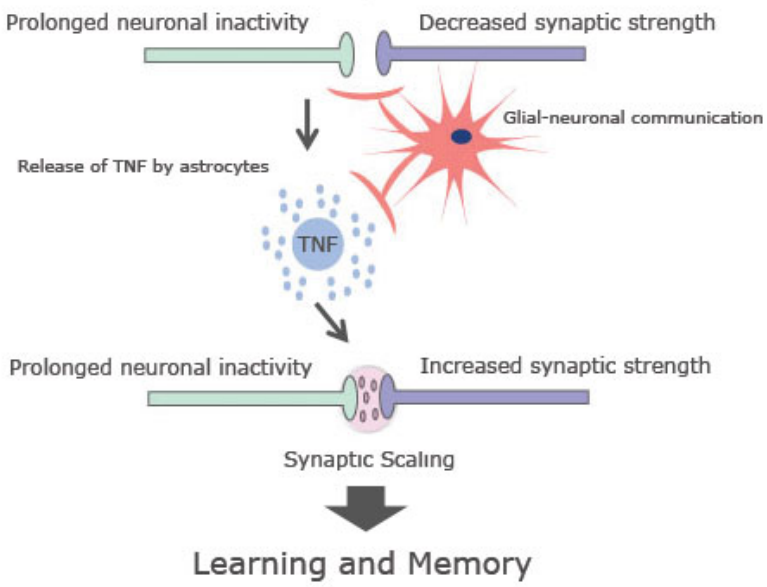

Figure 5. Schematic showing the involvement of TNF in synaptic scaling. In brief, a prolonged period of neuronal inactivity leads to a decrease in synaptic strength, which triggers, via glial–neuronal communication, the release of TNF by astrocytes. The released TNF by astrocytes in turn induces an increase in synaptic strength of the post-synaptic neuron; which helps to maintain neuronal activity (synaptic scaling) and promote learning and memory functions. Adapted from McAfoose & Baune, 2009.

As shown by Baune and others (2008a), the presence of TNF, in mice, during physiological conditions is essential for normal functions of memory and learning. Subsequent research by McAfoose et al (2008), showed that although the initial absence of TNF in transgenic knockout mice (TNF-/-) is cognitively detrimental, with age TNF deficiency appears to be cognitively beneficial. Although the biological mechanisms underlying this change in cognitive profile remain to be determined, the behavioural results alone suggest a possible role for TNF in neurocognitive aging. Indeed, in healthy elderly humans it was reported (Baune et al., 2008b) that genetic variants of TNF may have protective effects in cognitive function. In transgenic mice the over-expression of TNF is detrimental, with both pathological changes in brain and cognitive impairment demonstrated (Aloe et al., 1999; Campbell et al., 1997).

1.5.2 Neurodegenerative Properties

Within the brain inflammatory factors can exert physiological, protective and neurodegenerative properties (see Figure 6). Indeed, chronic inflammation has been widely characterized in neurodegenerative diseases, however, some debate remains as to whether these inflammatory processes play a causal, bystander or beneficial

role in disease (Wyss-Coray, 2006). What is known is that with age levels of inflammatory factors, such as pro-inflammatory cytokines (IL-1, IL-6 and TNF) and chemokines, increase resulting in chronic low-grade inflammation. In particular, glial-mediated chronic inflammation can exert neurotoxicity, promote the production and aggregation of abnormal proteins, disrupt neurogenesis and impair synaptic plasticity. Moreover, microglial senescence and associated chronic inflammation, can profoundly impair brain function and contribute to cognitive decline and the development of neurodegenerative diseases (Streit, 2006; Streit et al., 2008). Toxic soluble and aggregated proteins associated with neurodegenerative diseases, such as beta-amyloid (Aβ), tau, alpha-synuclein and prion protein can activate glia cells and induce neuroinflammation and brain pathology.

In Alzheimer's disease, for example, oligomeric forms of Aβ can activate the innate immune system and trigger inflammatory responses in microglia and astrocytes that can lead to further Aβ accumulation, tau phosphorylation, neurotoxicity, oxidative stress and synaptic dysfunction (Salminen et al., 2009). In particular, cytokines IL-1, TNF and IFN-γ can modulate γ-secretase activity and the production of Aβ via JNK-dependent MAPK pathway (Liao et al., 2004). In transgenic mice harboring the Swedish mutation, TNF and IFN-γ regulate Aβ deposition and β-secretase (BACE1) expression (Yamamoto et al., 2007). NFκB-mediated pathways and peroxisome proliferated activated receptor-γ (PPARγ) serve an important role in pro-inflammatory cytokine modulation of BACE1 activity and expression (Sastre et al., 2008). Similarly, research by Medeiros and colleagues (2007) demonstrated in mice that both pharmacological (anti-TNF antibody and aminoguanidine) and genetic (knockout mice) blockage of TNF and iNOS reduced cognitive deficits evoked by Aβ. In support of such findings, He et al. (2007) demonstrated that the deletion of TNF R1 gene in APP23 transgenic mice (APP23/TNFR1-/-) inhibits Aβ generation and prevents memory deficits.

Given the role of cytokines in synaptic plasticity and learning and memory processes (Di Filippo et al., 2008; McAfoose et al., 2009), it is not surprising that increased cytokine levels in the brain have been shown to disrupt synaptic plasticity and cognitive functioning (Butler et al., 2004; Goshen et al., 2007). In Alzheimer's disease, evidence indicates that TNF mediates Aβ induced suppression of long-term potentiation (LTP) (Wang et al., 2005). In support of these findings it was recently

demonstrated by Rowan and colleagues (2007) that neutralizing TNF using infliximab, thalidomide and a TNF peptide antagonist prevented Aβ induced inhibition of LTP. It was also shown by these authors that mice deficient in TNF receptor 1 (TNF R1 knockout mice) do not display any Aβ inhibitory effects on LTP induction; suggesting a key role of TNF R1 in TNF-mediated inhibition of LTP. It is also thought that prolonged Aβ induced suppression of synaptic activity can lead to excessive release of TNF by astrocytes, resulting in synaptic dysregulation (Small, 2008; Tobinick, 2008). Interestingly, this would suggest that a physiological function of TNF (synaptic scaling) and not an inflammatory or pathophysiological process of TNF, might be contributing to AD pathology and cognitive dysfunction. Although this remains to be fully clarified, cognitive-behavioural data obtained from mice indicated that anti-TNF treatment using thalidomide prevents Aβ induced memory impairment (Alkam et al., 2008). Moreover, it was demonstrated in a recent study by Tobinick and others (Tobinick et al., 2008) , that once weekly perispinal injection of etanercept (a TNF antagonist) resulted in rapid cognitive improvement in a late-onset AD patient.

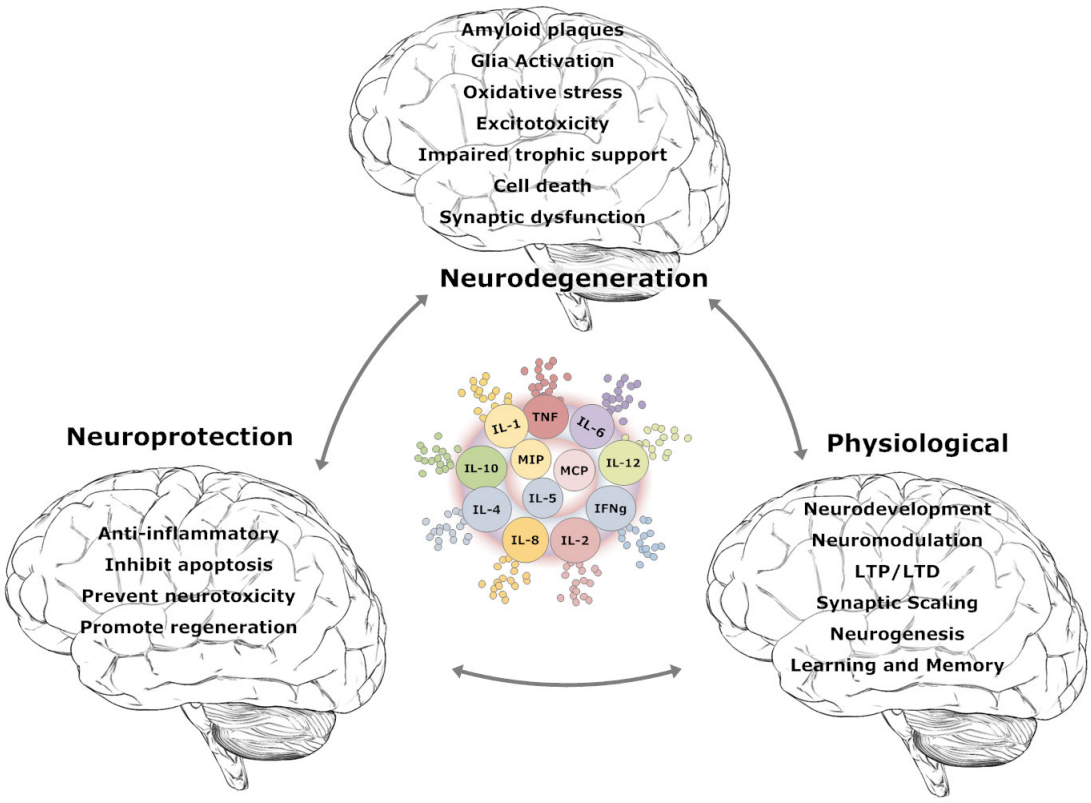

Figure 6. Schematic showing neurodegenerative, neuroprotective and physiological properties of cytokines and chemokines, within the central nervous system. During pathological conditions activated microglial and reactive astrocytes release 'pro-inflammatory' cytokines, such as, IL-1, IL-6 and TNF, that

interact with neurons and other glial cells, to induce a neuroinflammatory response that leads to the production of reactive oxygen species and lowered neurotrophic factors levels (i.e. NGF, BDNF and GDNF). Collectively, these inflammatory processes alter the normal balance and physiological function of neurons resulting in synaptic dysfunction, excitotoxicity and cell death. In Alzheimer's disease it is believed that an up-regulation of cytokines can exacerbate or facilitate the production of amyloid beta peptides, their fibrillization, and amyloid deposition. This positive feedback loop leads to further activation of glial cells and further up-regulation of cytokines. These same cytokines can also exert neuroprotective properties within the CNS; although typically such properties are attributed to the release of 'anti-inflammatory' cytokines, such as, IL-4 and IL-10. Moreover, during normal physiological conditions the release of IL-1, IL-6 and TNF participate in several forms of synaptic plasticity thought to facilitate learning and memory.

1.6 Brain-immune interactions in the protection against neurodegeneration

Brain-immune functions are governed by complex bi-directional communication pathways between the immune and central nervous system and specialized mechanisms for the tight control of immune responses. While there is no equivalent to lymphatic vessels in the brain, evidence indicates that cerebrospinal fluid (CSF) flow and periarterial interstitial fluid (ISF) drainage pathways connect the CNS to the lymphatic system; thus facilitating CNS immune surveillance (Engelhardt et al., 2005; Johnston et al., 2004; Ransohoff et al 2003; Schwartz et al., 2010). Clearance of soluble proteins, especially toxic misfolded proteins, from ISF drainage pathways to lymph nodes may represent one pathway by which antigenic material from the brain parenchyma can access lymphoid tissue and induce antigen-specific responses by naïve or memory B and T cells (Ransohoff et al 2003). Immune surveillance of the CNS parenchyma maybe further facilitated by T lymphocyte trafficking in and out of CSF-filled ventricle, subarachnoid and perivacular spaces where contact with antigen presenting cells of the CNS (subarachnoid-space macrophages and pericytes embedded in the basal membranes of CNS microvasculature) can take place (Engelhardt and Ransohoff, 2005). The blood brain barrier (BBB) serves, therefore, a fundamental role in regulating brain-immune processes (Banks et al., 2010) and protecting the brain against the detrimental effects of brain-reactive autoantibodies and cytotoxic T cells that might otherwise lead to autoimmune-associated neurological and neuropsychiatric diseases, such as those known in multiple sclerosis, paraneoplastic syndromes, neuromyelitis optica, limbic encephalitis, Guillian-Barré syndrome, systemic lupus erythematosus (Bhat et al., 2009; Diamond et al., 2009).

On the other hand, both T- and B-cells together with phagocyte functions of brain-resident microglia against misfolded protein antigens can protect neurons from

degeneration. Accumulating evidence suggests roles for naturally-occurring antibodies in the delay - or the prevention of – clinically overt neurodegenerative disease (Diamond et al., 2009; Neff et al., 2008; Rodriguez et al., 2009; Schwartz et al., 2008a; Schwartz et al., 2008b; Szabo et al., 2008). Protective immunity could be mediated by conformation-specific antibodies reacting with pathologic misfolded protein oligomers, neutralizing their toxic properties, accelerating their microglia-mediated clearance, or preventing their growth.

Indeed, the presence of auto-antibodies against Abeta, alpha-synuclein and PrP have been documented in the blood and CSF of healthy individuals and patients (Geylis et al., 2005; Papachroni et al., 2007). These auto-antibodies can bind, and neutralize, conformation-specific epitopes of misfolded proteins, inhibit fibrillization and aggregation, block oligomeric induced neurotoxicity, facilitate microglia-mediated phagocytosis and promote neuroprotection (Szabo et al 2008; Neff et al., 2008, Kellner et al., 2009). Although previous findings have been controversial over the years, with earlier papers reporting either no decline or an increase in autoantibodies in AD patients, recent studies provide more conclusive evidence.

Recent work by Britschgi and colleagues (2009), in particular, provides convincing evidence that autoantibodies against a broad range of amyloidogenic peptides are naturally present in human plasma and CSF and that these autoantibodies display conformational-specific reactivity to misfolded proteins with neurotoxic properties. The authors also elegantly demonstrate that these autoantibodies display neuroprotective properties, with naturally occurring antibodies against Aβ protecting primary neurons against Aβ toxicity and that immunization with full-length Aβ can induce an enhanced cross-reactive autoantibody response against not only other Aβ species but also other toxic amyloidogenic peptides. In support of these findings, it was shown that autoantibodies levels decrease with age with even further reductions being described in AD patients. Kellner et al (2009) have also reported on the effects of auto-antibodies against Abeta on beta-amyloid plaque removal in non-immunized AD patients and age-matched non-demented controls. In this study, AD patients with high IgG-labeled neuritic beta-amyloid plaques demonstrated reduced beta-amyloid plaque load along with signs of increased phagocytic microglia; suggesting that the presence of anti-Abeta antibodies may be a naturally occurring protective factor against beta-amyloid pathology in AD. Indeed, in comparison to non-demented

healthy elderly subjects, AD patients exhibit lower serum titers levels of naturally occurring anti-Abeta antibodies (Du et al., 2001; Weksler et al., 2002). Catalytic IgM antibodies against Abeta have been additionally found in human sera and show high specific anti-Abeta activity but low capacity to clear the BBB compared to IgG anti-Abeta antibodies; raising the possibility that IgM anti-Abeta antibodies might prove to be therapeutically effective in the blood (Szabo et al., 2008). As recently reported by Marcello and colleagues (2011), reduced plasma levels of IgM autoantibodies against N-truncated pyroglutamate Abeta were found in AD patients compared to healthy controls, along with a significant correlation between levels of these IgM autoantibodies and cognitive status in MCI patients.

The presence of brain reactive antibodies in human sera may represent two aspects of immune response: a destructive autoimmune response that contributes to disease pathology resulting in *antibody-mediated brain dysfunction*, or alternatively, a protective autoimmune response that serves a protective role against disease processes resulting in *antibody-mediated neuroprotection*. Understanding the protective and detrimental aspects of brain reactive auto-antibodies, the mechanisms mediating their entry into the brain and their consequences on brain development and function during health and disease, will provide new insight into the pathogenesis and treatment of several neurodegenerative diseases. The advent of molecular imaging technology together with therapeutic immunization strategies targeting neurotoxic misfolded proteins provides new aspects for the treatment and prevention of neurodegenerative diseases including AD, prion disease, PD and ALS.

1.7 Immune-modulatory strategies for Alzheimer's disease

Rejuvenating and harnessing the aged immune system is of therapeutic importance and the subject of considerable investigation (Dorshkind et al., 2009; Popovich et al., 2008; Ron-Harel et al., 2009). Indeed, the last decade has seen tremendous advancement in the development of immune-based treatment intervention for neurodegenerative diseases. To-date, several anti-amyloid immunotherapy strategies have been developed for the treatment of Alzheimer's disease (Citron, 2010; Lemere et al., 2010), with many currently under extensive pre-clinical and clinical testing. In addition to these therapeutic initiatives, new therapies are being investigated that target cytokines (Chadwick et al., 2008; Tweedie et al., 2007) and

other inflammatory processes in Alzheimer's disease that result in neuronal injury, neurodegeneration and cognitive dysfunction.

In a pilot study, Tobinick and others (2006) demonstrated that once weekly perispinal injection of etanercept (a TNF antagonist) in 15 mild-to-severe AD patients resulted in significant improvement in cognitive function at 6 months follow-up. In a subsequent study (Tobinick et al., 2008), the same authors demonstrated that perispinal anti-TNF treatment results in rapid cognitive improvement in a late-onset AD patient. Based on the reported rapid improvement in cognitive function following treatment and the known involvement of TNF in synaptic plasticity, it has been suggested that perispinal administration of etanercept might 'reverse' the synaptic dysregulation caused by TNF over-expression (Griffin, 2008; Tobinick, 2008; Tobinick, 2009). Alternatively, etanercept might be a combined TNFalpha neutralizing/"passive immunization" agent with rapid efficacy due to its anti-TNF properties and long-term efficacy resulting from engagement of Fc receptor-mediated effector functions (Griffin, 2008). Future research should therefore seek to identify the biological mechanisms underling the 'rapid' and 'long-term' therapeutic efficacy of etanercept treatment. Ideally such research should utilize mouse models in which the expression of TNF (and other cytokines) can be characterized throughout aging (wildtype mice), disease progression (transgenic AD mouse models) and following therapeutic intervention, especially in relation to cognitive function (cognitive-behavioural testing), neurobiological processes (synaptic scaling) and disease pathology (Aβ formation and deposition). Such findings are particularly important, as other research (Taoufik et al., 2008), investigating the therapeutic efficacy of anti-TNF treatment in MS patients, indicated that the net outcome of TNF neutralization is harmful. Furthermore, it has been reported that following anti-TNF treatment for rheumatoid arthritis, patients have been shown to develop neurological problems and demyelinating lesions (Richez et al., 2005; Sicotte et al., 2001). Animal research (Aloe et al., 1999; Baune et al., 2008a, McAfoose et al., 2008) has additionally demonstrated that both the absence and overexpression of TNF in mice is associated with cognitive dysfunction and disease pathology; thus highlighting the physiological, neuroprotective and neurodegenerative properties of TNF.

As mentioned earlier, microglia activation and microglia-mediated neuroinflammation are important factors in AD pathophysiology that can result in neuroprotection and

the clearance of Ab (phagocytosis) or neuronal damage. Developing treatment approaches that successfully control microglia activation and pro-inflammatory cytokine expression while promoting neuronal protection are therefore of therapeutic significance and currently under extensive investigation (Landreth et al., 2008; Shie et al., 2009). Of particular importance here is the recent discovery that 1) peroxisome proliferator-activated receptor gamma (PPARγ) activation inhibits microglia activation promotes anti-inflammation and induces Aβ clearance (Camacho et al., 2004) and 2) PPARγ agonists (pioglitazone and rosiglitazone) might serve as useful therapeutics for the treatment of AD (see for Landreth et al., 2008; Shie et al., 2009 a review). In transgenic AD mouse models it has been shown that treatment with risoglitazone results in improved learning and memory (Escribano et al., 2009; Pedersen et al., 2006) and a restoration of LTP (Loane et al., 2007). In humans, it has also been reported, in two clinical trial studies, that AD patients receiving rosiglitazone treatment showed improved cognitive function at 6 month follow-up (Risner et al., 2006; Watson et al., 2005). Although the exact mechanisms remain to be fully characterized evidence (Loane et al., 2007) suggests that IL-4 mediates the anti-inflammatory and neuroprotective effects of rosiglitazone.

Another therapeutic approach, alpha-lipoic acid (LA), has been shown to be beneficial in the treatment of AD. Indeed, a 48 month study conducted by Hager et al. (2007) showed that treatment with LA slowed the rate of disease progression (cognitive decline) in mildly demented AD patients. These therapeutic effects have been contributed to LA ability to exert anti-inflammatory and neuroprotective properties. Other metal chelator and anti-oxidant treatment approaches, such as M-30 and HLA-20 (Mandel et al., 2007), have demonstrated therapeutic efficacy in AD patients.

Evidence (Nizri et al., 2006) suggests that in addition to their known ability to enhance cholinergic production, acetylcholinesterase inhibitors (AChEIs) can also exert anti-inflammatory effects, both peripherally and within the CNS. More specifically, it has been shown that peripheral administration of galantamine reduces serum TNF levels and that these effects are mediated via the vagus nerve signalling “cholinergic anti-inflammatory pathway” (Pavlov et al., 2009). These authors further demonstrated (Parrish et al., 2008; Pavlov et al., 2009) that this anti-inflammatory process (vagus nerve-based cholinergic anti-inflammatory pathway) is mediated by

the alpha7 subunit-containing nicotinic acetylcholine receptor (α7nAChR). Such findings raise the possibility that at least some of the therapeutic effects of AChEIs might be due to their anti-inflammatory properties.

1.8 Amyloid-lowering immunotherapeutic strategies for Alzheimer's disease

Based on the effective clearance of beta-amyloid from brain upon repeated Abeta immunization in mouse models for AD, along with restoration of neuronal morphology and behavioural functions, clinical trials in humans were initiated (for review see: Brody et al., 2008; Lemere et al., 2010). More than one dozen clinical trials testing both passive immunotherapy and active vaccination strategies are currently underway.

Clinical trials of active immunization were first done with aggregated Abeta42 combined with the adjuvant QS-21 (Elan/Wyeth AN1792 trial) (Bayer et al., 2005; Gilman et al., 2005). During the later stages of the phase I trial, the emulsifier polysorbate 80 was added to the active vaccine formulation after which the observed immune responses shifted from a predominantly Th2 biased response to a proinflammatory Th1 response (Pride et al., 2008). This change in formulation was associated with the occurrence of a case with aseptic meningoencephalitis in phase I (Nicoll et al., 2003), and further 18 patients in the phase II trial corresponding to 6% of the patients treated with the active vaccine (Orgogozo et al., 2003). Unrelated to the T-cell mediated side-effect of meningoencephalitis, patients with AD responded to the active vaccination by generation of highly specific antibodies against beta-amyloid plaques (Hock et al., 2002; Gilman et al., 2005), along with better memory performance in a cohorts of patients with high antibody titers (Hock et al., 2003). Long-term follow-up of the actively immunized AN1792 cohort of patients revealed reduced cognitive decline in immunization responders with increased antibody titers up to 5 years after the initial immunizations (Vellas et al., 2009). Autopsy analyses consistently showed signs of clearance of beta-amyloid from brain (Ferrer et al., 2004; Masliah et al., 2005) and the magnitude of beta-amyloid clearance apparently was correlated serum titers of antibodies against beta-amyloid (Holmes et al., 2008). In addition, increased titers of antibodies against beta-amyloid was associated with decreased CSF levels of the intraneuronal protein tau, possibly as an indication of

slowed neuronal disintegration following attenuated neurodegeneration (Gilman et al., 2005).

Whether clearance of beta-amyloid from brain in patients with AD will be associated with sufficient clinical benefits over time may depend largely on the disease stage at which the treatment is initiated, as implied by recent reports on individual AD patients who received active vaccination (Holmes et al., 2008; Vellas et al., 2009). If these initial findings hold true in larger patient populations, it may turn out that Abeta immunotherapy is most effectively applied in non-demented subjects with preclinical brain beta-amyloidosis, referred to as *primary progressive brain amyloidosis*. Emerging longitudinal imaging studies of brain beta-amyloid with PET indicate that 67% of amyloid-positive non-demented subjects with mild cognitive impairment (MCI) converted to AD within 5 years, as compared to 0% of amyloid-negative non-demented subjects with MCI (Nordberg, ICAD2009). Taken together, this population of elderly subjects with primary progressive brain amyloidosis may turn out to be a prime target population for secondary prevention of AD by using Abeta immunotherapy.

1.9 Aims of thesis

1.9.1 Anti-TNF project

This project was designed to test the following **Working Hypothesis,** that anti-TNF therapy can lower amyloid pathology, ameliorate neuroinflammatory responses and rescue cognitive deficits in 12 month old arcAb transgenic mice.

Specific Aims:

1. To identify the effects TNF deficiency (TNF ko models) on AD pathology in arcAb mice.

2. To determine if anti-TNF therapy (etanercept) will rescue cognitive deficits in arcAb mouse.

3. To determine the therapeutic outcome of icv vs. ip administration of etanercept.

4. To determine the underlying therapeutic mechanisms of etanercept anti-TNF therapy on amyloid pathology and neuroinflammation (astrocytosis and microgliosis).

1.9.2 DARPin project

This project was designed to test the following **Working Hypothesis,** that selected DARPins with Abeta-binding properties could be used as a therapeutic approach to lower amyloid pathology and rescue cognitive deficits in 12 month old transgenic mouse models of Alzheimer's disease.

Specific Aims:

1. To determine if DARPin therapy will rescue cognitive deficits in Swedish and arcAb mouse.

2. To determine the underlying therapeutic mechanisms of DARPin therapy on amyloid pathology and neuroinflammation (astrocytosis and microgliosis).

1.9.3 Delta project

This project was designed to test the following **Working Hypothesis,** that the specific conformational change induced by the E22Δ mutation causes the formation of soluble oligomeric derivatives with synaptotoxic activities that cause cognitive decline in the absence of amyloid plaque formation and deposition.

The **Specific Aims** of this project are:

1. To determine the effects of E22Δ Aβ on cognitive performance in E22Δ transgenic mice expressing the mutation, as compared to arcAb and Swedish (tg2576) mice.

2. To determine the histological and biochemical properties of E22Δ Aβ-pathology overtime, as compared to arcAb and Swedish mutations.

3. To elucidate the aggregation propensity of E22Δ Abeta species, as compared to arcAb and wildtype Abeta species.

2

Effects of anti-TNF therapy on amyloid pathology and neuroinflammation in 12 month old arcAß transgenic mice

Jordan McAfoose, Luka Kulic, Tobias Welt, Claudia Späni, Rebecca Derungs, Armanda Pfister, Salome Zeller & Roger M. Nitsch

Abstract

Alzheimer's disease (AD) is a neurodegenerative disease associated with the accumulation of misfolded Abeta-amyloid aggregates and glia-mediated neuroinflammatory processes. The overexpression of tumor necrosis factor alpha (TNF), in particular, may promote amyloid plaque deposition and mediate Abeta-related synaptotoxicity. The use of Etanercept anti-TNF therapy for the treatment of AD is therefore currently under Phase II clinical trial investigation. In this study we investigated the intracerebroventricular (icv) infusion of Etanercept, Infliximab and PBS for 28 days via using ALZET osmotic minipumps, and 4 weekly intraperitoneal (ip) injections of Etancercept, Infliximab and PBS, with an additional 15 non-treated transgenic and wildtype mice as a further controls. All mice (n=120) underwent general health and neurological examination, as well as, cognitive assessment before they were sacrificed for further biochemical and histological analyses. ArcAβ/TNF knock out mice were also generated to investigate the long-term effects of TNF deficiency on amyloid pathology. ArcAβ/TNF knock out mice and control littermates were tested at 12 months of age for cognitive-behavioral changes and differences in underlying pathology. Immunohistochemical analyses confirmed ventricular placement of the brain infusion cannula and the ubiquitious distrubtion of Etanercept throughout the brain for intracerebroventricular, with CNS entry of peripherally administered Etanercept via leakage in the blood brain barrier. Cognitive-behavioral assessment of mice demonstrated a treatment dependent improvement in cognitive performance in two hippocampus-dependent cognitive tests. Results from the biochemical analyses indicate that the improvement in cognition was not associated with changes in soluble brain Abeta levels but rather a decrease in Formic acid insoluble Abeta levels. Thioflavin S histological analysis demonstrated a treatment-induced lowering of Abeta plaque number and percentage area covered by plaques. Results further demonstrated an increase clearance of Abeta plaques towards the vasculature, as shown by higher relative area covered by CAA. Immunohistochemical staining against GFAP and Iba1 demonstrated reduced astrocytosis but increased microglia activation. Our results indicate that TNF-directed immunotherapy may successfully reverse Abeta-related cognitive deficits in a transgenic mouse model of AD.

2.1 Introduction

Alzheimer's disease (AD) is a progressive neurodegenerative disease that leads to serve cognitive impairment and behavioural disturbances. Neuropathologically, AD is characterized by extracellular accumulation of β-amyloid protein (Aβ), intracellular neurofibrallary tangles (NFT), cerebral amyloid angiopathy, granulovacular degeneration, Hirano bodies, neuropil threads and activated glial cells (chronic, localized non-immune mediated inflammation). Although the pathogenesis of AD remains to be fully clarified, current evidence suggests that Aβ plays a central role in the complex and multifactoral mechanisms that underlie AD; the so-called amyloid cascade hypothesis. Although the pathways controlling production and aggregation of Aβ are well studied, the mechanisms that drive the spread of neurodegeneration in the brain are unclear. One possible mechanism that is gaining wide acceptance is that Alzheimer's disease involves an orchestrated cytokine and/or 'inflammatory' process that culminates in neuronal injury and destruction (Rojo et al., 2008).

In particular, there is now substantial and accumulating, basic science, and clinical evidence that excess TNF is centrally involved in the pathogenesis of dementia and other neuropsychiatric conditions. In Alzheimer's disease it is thought that the over-expression of TNF may give rise to the development of amyloid plaques and subsequently mediate amyloid interference with memory (He et al., 2007; Rowan et al., 2007; Wang et al., 2005). Findings by Medeiros and colleagues (2007) has demonstrated that TNF signaling pathways and iNOS act as central mediators of Aβ action in a mouse model of AD. Their research demonstrated that both pharmacological (anti-TNF antibody and aminoguanidine) and genetic (knockout mice) blockage of TNF and iNOS reduced cognitive deficits evoked by Aβ. In support of these findings, He et al. (2007) demonstrated that the deletion of TNF R1 gene in APP23 transgenic mice (APP23/TNFR1-/-) inhibits Aβ generation and prevents memory deficits. Moreover, it has recently been suggested that the progression of AD might be the consequence of exaggerated TNF-mediated synaptic scaling during prolonged neuronal inactivity caused by Aβ (Small, 2008). The concept of TNF-alpha-inhibition for the treatment of AD has, therefore, been recently reviewed (Tweedie et al., 2007; Tobinick, 2008). In a pilot study, Tobinick and others (2006) demonstrated that once weekly perispinal injection of etanercept (a TNF antagonist) in 15 mild-to-severe AD patients resulted in significant improvement in cognitive

function at 6 months follow-up. In a subsequent study (2008), the same authors demonstrated that perispinal anti-TNF treatment results in rapid cognitive improvement in a late-onset AD patient. Given TNFs involvement in synaptic plasticity (Beattie et al., 2002; Stellwagen et al., 2005; Stellwagen et al., 2006) it is thought that this rapid improvement in cognition results from 'reversed' excess TNF-mediated synaptic plasticity dysregulation (Griffin, 2008; Tobinick, 2008; Tobinick, 2009). Alternatively, etanercept might be a combined TNFalpha neutralizing/"passive immunization" agent with rapid efficacy due to its anti-TNF properties and long-term efficacy resulting from engagement of Fc receptor-mediated effector functions (Griffin, 2008). Animal research (Aloe et al., 1999; Baune et al., 2008a, McAfoose et al., 2008) has additionally demonstrated that both the absence and overexpression of TNF in mice is associated with cognitive dysfunction. Such findings highlight the physiological, neuroprotective and neurodegenerative properties of TNF.

The aim of the study was to investigate, in a preclinical study, the efficacy of directly infused and systemically administered etanercept anti-TNF therapy using ArcAβ transgenic mice as an AD mouse model. A primary outcome of this study was to assess the effects of anti-TNF treatment on cognitive performance and patho-biological measures suggestive of a disease-modifying mechanism, in particular the effects of anti-TNF treatment on Aβ levels, as well as, plaque deposition, astrocytosis and microglia activation. The long-term effects TNF deficiency on amyloid pathology was investigated using ArcAβ/TNF ko transgenic mice.

2.2 Materials and Methods

2.2.1 Animals

This study used a recently published (Knobloch et at., 2008) AD transgenic mouse model expressing human APP with the combined Swedish and Arctic mutations (arcAβ) that develop Abeta plaque pathology between the ages of 9 to 12 months of age. As part of this study, arcAβ mice were crossed with TNF knockout mice to generate both arcAβ/TNF knockout mice (arcAβ/TNF-/-), arcAβ/TNF +/- mice and arcAβ/TNF +/+ control littermates. Mice were bred, held and kept at the Neurodegenerative and Biobehavioral Research (NBR) Facility of the Division of Psychiatry Research under specific pathogen free (SPF) conditions, temperature

controlled (22 °C±1 °C), 3 to 5 animals per cage, with sawdust as bedding and tissue as nesting material. All housing boxes were under individual air ventilation. A 12 hour light–dark cycle beginning at 7:00 h was maintained in the housing room and except for the time of testing, water and food was provided *ad libitum*. Cognitive-behavioral testing was performed in a separate room within the NBR Facility specifically designed for cognitive-behavioural investigations (minimal stress, quite room, controlled lighting, etc.). Experiments were approved by the veterinary office of the Cantonal Health Department and efforts were made to minimize the number and suffering of the animals in these experiments.

2.2.2 Cognitive-behavioural testing

A battery of well-validated and carefully controlled tests were used to behaviorally assess mice for motoric and cognitive performance (Crawley, 2007). At the time of testing, mice were weighed and examined for general health measures to ensure that the mice were physically able to conduct the cognitive-behavioral test and to rule out any adverse side effects due to the surgical procedure or anti-TNF treatment; supplementary material.

Grip Strength Analysis

Grip strength was measured using a Grip strength Meter apparatus that measures the gripping strength of mice. The system is supplied with a grid which connects to the sensor. Animals were lowered down until the paws grasped the gird and then gently pulled back until the grip was released. The maximal force achieved by the animal was recorded electronically over three trials.

Paw grip endurance test (PaGE) Using a stainless steel mesh grid, mice were suspended upside down over a foam landing pad for 120s and the longest latency to fall over three trials is recorded.

Extension reflex

Extension of the hindlimbs is normally observed when a mouse is suspended in the air by its tail. However, in mice with motoneuron disease, retraction of the hindlimb is more commonly seen. A score of 0 indicates normal extension reflex of both

hindpaws, whereas, a score of 1 corresponds with extension reflex of only one hindpaw, and 2 is the absence of any hindlimb extension.

Rotarod test

In the rotarod test a mouse has to keep its balance on a horizontal rotating rod (diameter 3 cm). A trial starts when the mouse is placed on the rotating rod, and stops when the mouse falls down. Five mice are simultaneously placed on the rotarod apparatus with the rod rotating at 4 rpm (rotations/minute) during the first minute, with an increase in rotation speed every 30 seconds thereafter. A trial ends for a mouse when it falls down or when 5 minutes are complete.

Locomotor Activity

Open Field Test: According to published procedures (Crawley, 2007) mice are placed in the center of a brightly lit white Plexiglas box (50x50cm), and their movements (distance traveled and average speed) were tracked using ANY-maze video tracking software (Stoelting Co., USA) for 5 min.

Y-maze

Spatial working memory was assessed in mice using the Y-maze (Y-shaped plastic maze, with 40 cm x 20 cm x 10 cm arm sizes). During a 5 minute trial, the sequence of arm entries was recorded using the ANY-maze Video Tracking System (Stoelting Co., USA). The percent alternation was calculated as the ratio of actual to possible alternations (defined as the total number of arm entries -2) x 100%.

Novel Object Recognition

The Novel Object Recognition task is undertaken in accordance to published protocols (Winters et al., 2008). In brief, following a habituation period, mice are exposed to two novel objects placed within the open-field box, then after a 5 minute delay, one of the familiar objects is replaced with a new novel object, and the time spent exploring each object is recorded electronically. A preference index, or time spent exploring the novel object over the time spent exploring the familiar object, is used to measure recognition memory.

2.2.3 Biochemical and Immunohistochemical analyses

Mice were deeply anesthetized and blood collected from the right ventricle using a syringe with EDTA and samples were centrifuged at 8'000 rpm for 8 minutes at 4C and plasma extracted using a sterile pipette and stored at -80C for later batch analysis. Following the collection of blood, mice were transcardially perfused with PBS and their brains rapidly removed. Brains were dissected in two hemispheres with the left hemisphere being placed in 4% PFA and post-fixed overnight at 4C° and then transferred to 30% sucrose for 72 hours (cyroprotection) for later histological analysis. PFA-fixed and cryoprotected hemibrains were cut in 35 µm thick coronal slices at -80C using a microtome (Leica Jung HN40) and kept at -20C in an anti-freeze solution (phosphate buffer 0.50 M in MilliQ water: ethyleneglycol: glycerol = 1.3:1:1) until staining was performed. The right hemibrain was dissected for biochemical purposes and immediately frozen in liquid nitrogen and stored at -80C°. Brain tissue was later homogenized using a sequential extraction protocol in which tissue was homogenized using a glass-Teflon homogenizer (20 strokes, 315 rpm) in RIPA buffer containing complete protease inhibitor tables (Sigma-Aldrich), centrifuged at 100,000 x g (53,000 rpm) at 4C for 1 hour and supernatant extracted and stored at -80C for later biochemical batch analysis. The remaining pellet was frozen on dry ice, resuspended in 70% formic acid, sonicated for 30s at 30% power, ultracentrifuged (100,000 x g @ 4C for 30 minutes), supernatant extracted, lyophilized, reconstituted in RIPA buffer and stored at -80C for later batch analysis.

Beta-amyloid analysis.

Abeta levels were measured in plasma and brain homogenates using a MSD 3plex multi-SPOT Abeta human kit (MesoScale Discovery, USA) for $A\beta_{38}$, $A\beta_{40}$ and $A\beta_{42}$, in accordance to manufacturer's instructions. MSD SECTOR Imager 6000 reader was used for analysis and the MSD DISCOVERY WORKBENCH software (Version 3.0.17) with Data Analysis Toolbox was used to calculate sample concentrations by comparing them against a standard curve (five-parameter logistic curve).

Immunohistochemistry.

All immunohistochemical stainings were executed using the free-floating method. Washing steps were carried out between all incubations using washing buffer (TBS pH 7.4 containing 0.2%Triton X-100) at RT. Slices were blocked for 1 hour at RT

using blocking buffer (5.0% goat serum 5.0% donkey serum in washing buffer). Blocked slices were incubated overnight at 4C with slight agitation in primary antibody incubation buffer (2.5% goat serum and 2.5% donkey serum in washing buffer) containing the primary antibody/antibodies. Primary antibodies were: rabbit anti- Iba1 (Wako Chemicals, Osaka, Japan) and goat anti-GFAP (Advanced ImmunoChemical Inc.). Subsequently, secondary antibody incubations were carried out for 2 hours at RT using fluorophor-conjugated antibodies. Slices were washed in washing buffer, mounted on chrom-gelatin-coated microscopy slides (Super-frost-plus, Menzel, Braunschweig, Germany) and glass-covered using Hydromount® (National Diagnostics, Hull, UK). Thioflavin S staining was done according to standard protocol. In short, floating sections were washed in KPBS and mounted on chrom-gelatin coated glass slides before being processed. After treatment for 20 min with 0.25% potassium permanganate, sections were washed in d.d. H_2O and incubated in 2% potassium disulfide and 1% oxalic acid until they appeared white. Sections were then floated 3 seconds in 0.25% acetic acid, washed in d.d. H_2O and stained for 5 min with a solution of 0.015% Thio-S in 50% ethanol. Finally, sections were washed in 50% ethanol and in d.d. H_2O, then dried, and glass-covered using Hydromount® (National Diagnostics, Hull, UK). For detection of micro-hemorrhages Prussian Blue staining was performed in which sections were incubated in a mixture of equal volumes of 10% potassium ferrocyanide ($K_4Fe(CN)_6$ trihydrate) in d.d. H_2O and 20% hydrochloric acid (HCl) in d.d. H_2O for 30 min. Brain sections were subsequently washed with d.d. H_2O, counterstained with nuclear fast red solution for 10 min and washed with d.d. H_2O, then dried, and glass-covered using Hydromount® (National Diagnostics, Hull, UK). All chemicals were purchased from Sigma-Aldrich, Switzerland.

2.2.4 Treatment and Surgical Implantation of Alzet® osmotic minipumps

Twelve-month-old arcAβ mice were deeply anaesthetized (fentanyl/midazolam/medetomidin), a small midline incision was made to expose the skull, and a subcutaneous pocket was prepared in the midscapular area of the back of the mice so that a sterile Alzet® minipump (model 2004, 3.0 cm. in length, 0.7 cm. in diameter and weighing 1.1 g empty weight) filled with antibody solution or vehicle could be inserted. Mice were then head fixed within a stereotaxic apparatus and the bone suture junction bregma was used as a reference point to drill a hole in the skull

and lower an Alzet Brain infusion kit 3 cannula into the left lateral ventricle; coordinates according to bregma; AP, -0.2 mm; ML, 0.9 mm; and DV, 2.5 mm. Following the placement of the cannula, two small screws were placed within the skull and dental cement applied to firmly attach to the skull. Naloxon, flumazenill/atipamezol and metacam was given subcutaneously as an antidote and post-operative analgesic, with further metacam and buprenorphine / phenylbutazon / aminophenazon / benzylpenicillin / dihydrostreptomycin provided within the drinking water for 2 weeks as an analgesic /antibiotic. Post-operatively, mice were housed for three days on heat pads and moist food placed at the floor of the cage to promote recovery and to reduce drop-outs. Groups of 15 transgenic arcAβ mice were used per treatment condition, with mice either receiving icv-infusion over 28 days (10mg/ml concentration, ~26.4 μg per day; 740 μg over 28 days infusion) or weekly intraperitoneal injections of 5 mg/kg for 4 weeks of anti-TNF therapy (Etanercept), anti-TNF control (Infliximab) or PBS control. Additionally, non-treated transgenic and wildtype littermates were included as controls.

2.2.5 Image analysis

Immunohistochemical quantification was performed using ImageJ software (http://rsb.info.nih.gov/ij/), in which all images were first converted into grayscale images (8-bit). Subsequently, all images were further adjusted to a defined grayscale threshold. For each investigation, the grayscale threshold was held constant for all groups to allow comparison between images. Quantification of plaque load and CAA (ThioS), astrocytosis (GFAP) and activated microglia (Iba1) was reported as the area positive for the staining in a determined area of the cortex (% area).

2.2.6 Statistical analysis

Data analysis was performed using the Statistica 10.0 statistical software. Tests for normal distribution were performed before statistical testing, according to the results of the Shapiro-Wilk- and the Kolmogorov-Smirnov-Test for normality, either T- or Mann-Whitney-U-Test for 2 sample groups or one-way ANOVA was performed (followed by post-hoc Fischer LSD analysis). For NORT a Wilcoxon-Test was performed to test if the ratio differed significantly from 1, +$P < 0.05$. A p-value < 0.05

was considered statistically significant. *P < 0.05, **P < 0.01, ***P < 0.001 indicate significantly different performances. Error bars are SEM.

2.3 Results

2.3.1 Cognitive-behavioural assessment

There were no differences in general health measures across all experimental groups, with both i.c.v. treated, i.p. treated and non-treated arcAβ mice displaying similar, general health measures, healthy appearance of fur, appropriate social behaviors and handling responses, auditory-visual sensory integrity, comparable grip strength, intact righting and extension reflexes (see supplementary material, Table 1). All groups were further monitored for possible treatment-induced side effects, drop outs, or specific technical failures, with no treatment group specific differences being reported (see supplementary material, Table 2*).* Assessment of body weight, demonstrated equivalent body weights across all experimental groups, for both males and females*.* Locomotor examination using the open field test demonstrated comparable locomotor activity across all groups, including total distance travelled, maximum speed and time immobile (data not shown). Similarly, all experimental groups exhibited comparable performance on the rotarod, grip strength and paw grip endurance (data not shown).

Cognitive assessment in the Y-maze demonstrated that both etanercept icv- and ip-treated mice displayed a significant increase in the percentage of spatial alternations, compared to PBS treated mice (p<.05, see Figure 1 B). Results further demonstrate that treated mice performed better than non-treated transgenic mice comparable of wildtype performance, indicating a treatment-induced improvement in spatial working memory (Figure 1 B). The increase in spatial alternations could not be attributed to an increase in exploration, as the number of total arm entries and distance travelled did not differ between groups (data not shown). ArcAβ/TNF -/- mice ($t_{(16)}$=1.554, p=0.069; Figure 1 A) and arcAβ/TNF -/+ ($t_{(12)}$=1.613, p=0.066; Figure 1 A) also showed non-significant trends towards better cognitive performance than arcAβ mice, with similar performance compared to wildtype mice. Novel object recognition (NORT) assessment demonstrated non-significant improvements in performance for both icv- and ip-treated etanercept mice compared to Infliximab and PBS treated

mice and non-treated controls (Figure 1 B). Similar results were shown for arcAβ/TNF -/- and arcAβ/TNF -/+ mice, as compared to arcAβ controls (Figure 1 D). Collectively, these results suggest an improvement in performance comparable to wildtype mice.

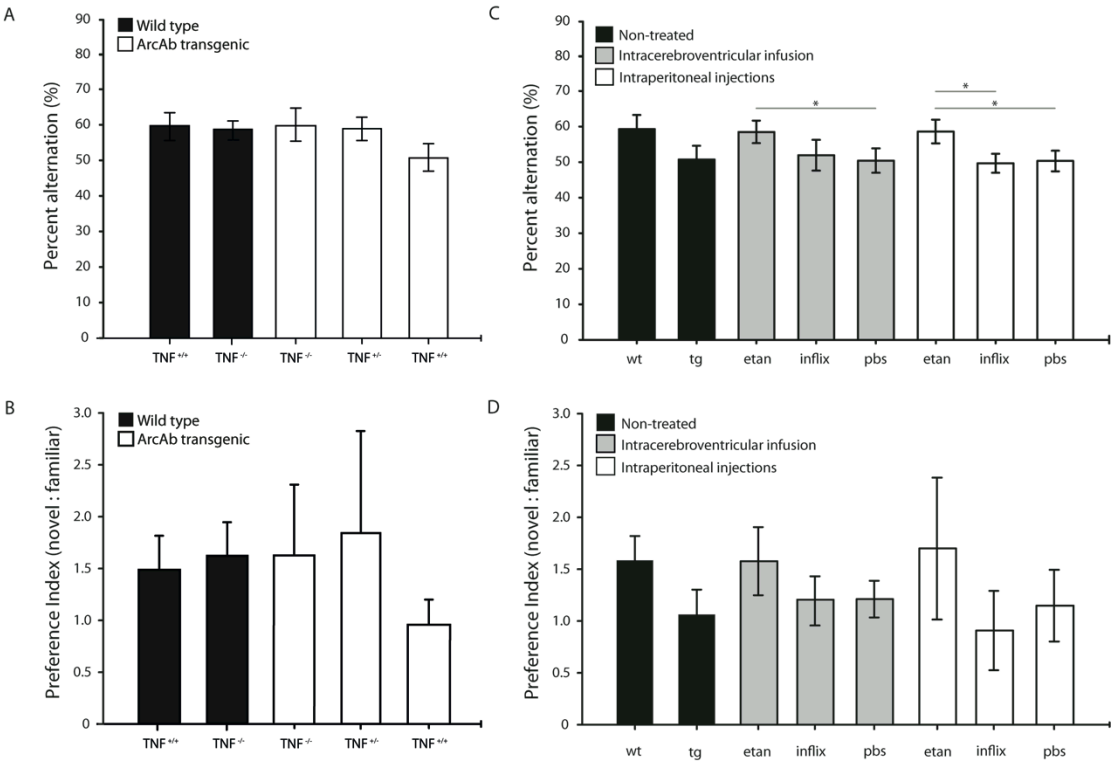

Figure 1. TNF deficiency and Etanercept Anti-TNF therapy improves cognitive performance in arcAb transgenic mice. A. ArcAβ transgenic mice on TNF deficient background (arcAβ/TNFko) demonstrate comparable spatial alternations on Ymaze as wildtype mice, whereas, arcAb control mice show decreased spatial alternation. B. ArcAβ/TNFko mice perform similar to wildtype mice on the NORT, with a higher preference index for the novel object than the familiar object, whereas, arcAβ controls show nearly an equal preference for novel and familiar objects. C. Etanercept icv-treated and ip-treated mice display comparable spatial alternation performance as wildtype mice, whereas, Infliximab and PBS icv-treated and ip-treated controls display similar spatial alternation performance as non-treated arcAβ control mice. D. Etanercept icv-treated and ip-treated mice show higher preferences for the novel object than familiar objects comparable to wildtype mice, whereas, Infliximab and PBS icv-treated and ip-treated controls show decreased preference for the novel object. n = 12-15 per group.

2.3.2 Histological analysis for cannula placement, mIgG and distribution of anti-TNF biologics

To confirm the correct stereotactic surgical placement of the brain cannulas into left lateral ventricle, the brains of all icv-treated mice were microscopic analyzed (Figure 2 A) and mice identified with misplaced cannula were excluded from further analyses (see *supplementary material, Table 2*). As a further control measure, we investigated

the distribution of icv-infused etanercept in all treated mice. Results from anti-hIgG immunohistological analysis demonstrated a diffused expression of etanercept anti-TNF biologic, extending from the site of infusion throughout the brain of icv-treated mice (Figure 2 B). These findings confirm sufficient distribution of therapeutic biologic throughout the brain and exclude failure to continually infuse biologic over the 28 days of the osmotic minipumps. To confirm whether peripherally administered etanercept would remain systemically or potentially cross the blood brain barrier (BBB), anti-hIG stainings were additionally carried out on ip-treated mice. Anti-hIgG stainings in ip-treated arcAβ mice revealed entry of biologic into the CNS via leakages in the blood brain barrier, as compared to ip-injected wildtype controls in which the biologic remained within the vasculature (Figure 2 C). Anti-mIgG immunohistological analysis revealed no difference in mIgG presence between treatment groups and PBS treated controls (Figure 2 D), suggesting no MAHA response to the treatment biologic.

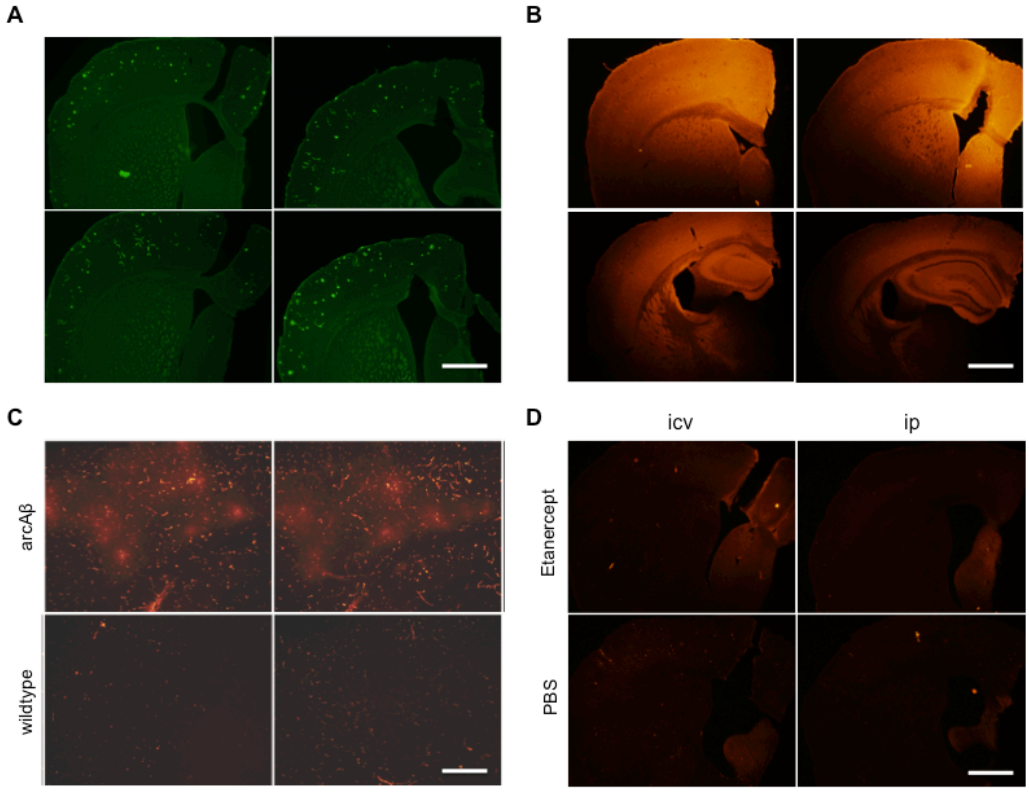

Figure 2. Histological analysis of brain cannula placement, biologic distribution, entry into CNS and MAHA response. A. Placement of the brain cannula within the lateral ventricle was confirmed histologically. B and C. Representative microphotographs of sections stained for anti-human IgG to measure the distribution of biologic throughout the brain in icv-treated mice (B) and ip-treated mice (C). D. The lack of mIgGs in brains of both etanercept icv and ip-treated as compared to PBS controls, suggests that there was no MAHA responses generated by treated mice. Scale bars: 1 mm (A, B and D) and 250 µm (C).

2.3.3 Histological analysis for amyloid plaques, CAA and micro-bleeds

Histological analysis of fibrillar Aβ and CAA demonstrated that arcAβ mice on TNF deficient backgrounds (arcAβ/TNFko), as compared to arcAβ controls, showed a significant decrease in plaque number ($t_{(94)}$=-2.028, p=0.023; data not shown), but comparable percentage plaque load ($t_{(94)}$=-0.014, p=0.494; Supplementary Figure 1). Further analysis demonstrated a significant increase in CAA in arcAβ TNF deficient mice, as compared to arcAβ mice ($t_{(94)}$=-2.004, p=0.025; Supplementary Figure 1). Thioflavin S histological analysis also demonstrated a treatment-induced significant lowering in the number of Abeta plaques ($f_{(3,131)}$=11.665, p<0.001), with etanercept icv-treated mice as compared to infliximab and PBS treated mice, as well as, non-treated transgenic controls (all p's<0.001) showing significantly lower number of plaques (Figure 3 A). Fischer LSD post-hoc analysis showed no significant difference between infliximab and PBS icv-treated mice, or non-treated transgenic mice. Further investigation demonstrated a significant difference in percentage area covered by plaques ($f_{(3,131)}$=2.643, p=0.05), with reduced plaque area for etanercept icv- treated mice as compared to infliximab icv- treated mice (p=0.034), PBS icv-treated mice (p=0.045) and non-treated transgenic mice (p=0.009). No other significant differences were found between treatment groups (Figure 3 A). Quantification of the percentage CAA revealed a significant difference ($f_{(3,131)}$=12.449, p<0.001), with etanercept icv-treated mice showing higher percentage CAA as compared to all other treatment groups (all p's <0.001) (Figure 3 A and B). Post-hoc analysis further demonstrated a significant difference between both infliximab icv-treated and non-treated mice and PBS icv-treated mice (p=0.037 and p=0.039, respectively), but no significant difference between infliximab icv-treated mice and non-treated transgenic controls. Histological analysis further demonstrated a significant reduction in plaque number for etanercept ip-treated mice ($t_{(86)}$=-3.869, p<0.001) in comparison to PBS controls, as well as lower percentage plaque area ($t_{(88)}$=-1.798, p=0.037; data not shown). Prussian Blue staining combined with Thioflavin S co-staining revealed plaque- and CAA-related micro-bleeds in both etanercept and PBS icv-treated mice, as well as, non-treated transgenic controls (Figure 3 C). Further analysis under higher magnification showed that micro-bleeds were not associated with all CAA and did not present in higher frequencies for etanercept icv-treated mice.

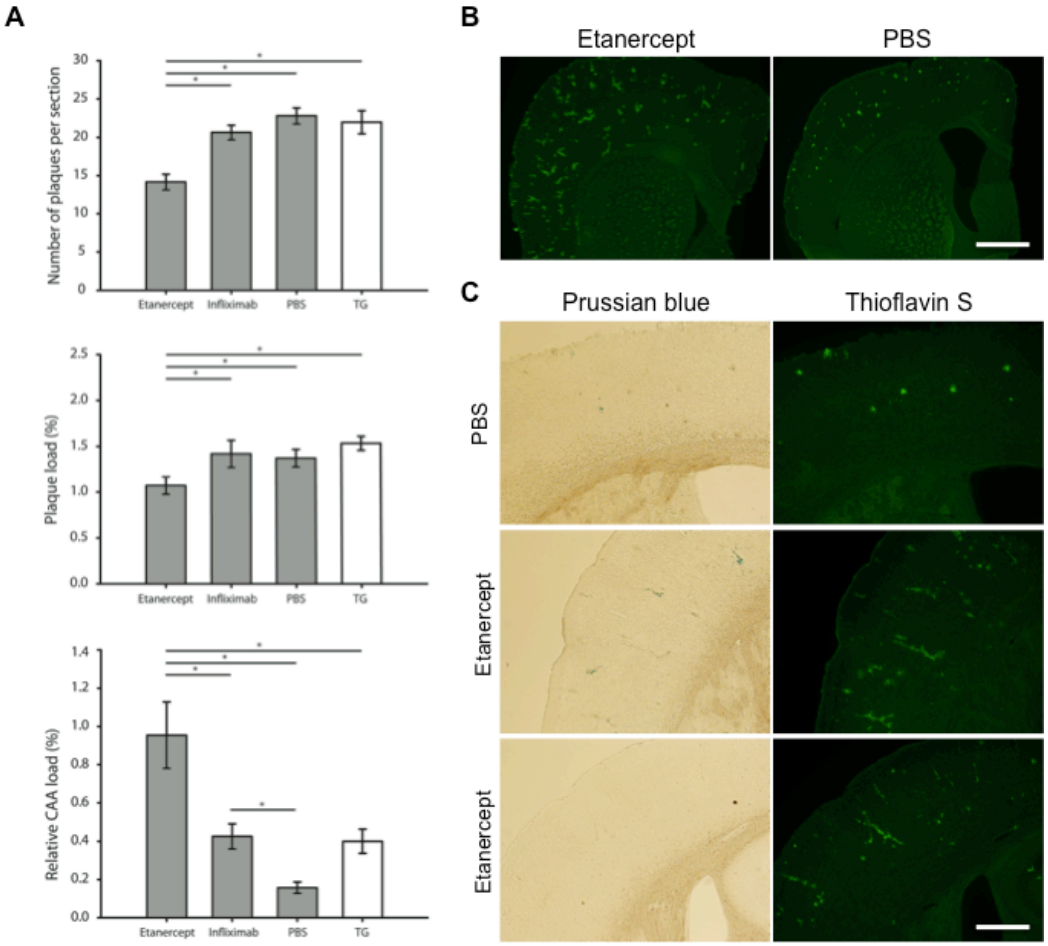

Figure 3. Anti-TNF therapy and genetic deletion leads to lower amyloid plaques but higher CAA. A. ArcAβ/TNFko mice show less number of plaques as compared to arcAβ controls but higher over all plaque load, suggesting the development of larger plaques. These mice also display higher amounts of CAA then arcAβ control mice, suggesting an increased tendency for vascular deposition of amyloid. B. Etanercept icv-treatment results in significantly reduced number of plaques and overall plaque load, as compared to Infliximab and PBS icv-treated mice, as well as, non-treated transgenic controls. Etanercept icv-treated mice further display increased CAA as compared to controls, suggesting a redistribution of parenchymal plaques towards the vasculature. C. Representative photomicrographs demonstrating the increased CAA in Etanercept icv-treated mice, as compared to controls. D. Histological analysis demonstrated plaque- and CAA- associated micro-bleeds in both PBS and Etanercept-treated mice. The frequency and severity of micro-bleeds was not correlated with increased CAA in Etanercept icv-treated mice, with many CAA pathologies not being associated with micro-bleeds, suggesting an amyloid-induced risk for micro-bleeds and not a treatment-induced risk for micro-bleeds, despite increased CAA in treated mice. Scale bars: 1 mm (B) and 250 µm (C).

2.3.4 Brain homogenate and plasma Abeta peptide anaylsis

Biochemical analysis of Abeta levels in brain homogenates from icv- and ip-treated mice showed a non-significant increase in RIPA soluble Abeta 40 levels, as compared to both icv- and ip-PBS treated mice and non-treated transgenic controls (Figure 4 A). No other changes were shown in RIPA solube Abeta 38 or 42 levels in icv- and ip-treated mice, as compared to icv- and ip-PBS and non-treated controls (Figure 4 A). Icv-treated mice did however demonstrate a significant reduction in the

formic acid fraction of Abeta 38, 40 and 42, as compared to icv-PBS treated mice and non-treated transgenic controls (Figure 4 B, $p<0.05$). Ip-treated mice showed similar Abeta patterns in the formic acid fraction with a significant reduction in Abeta 38 levels and non-significant reductions in Abeta 40 and 42 levels, as compared to both ip PBS treated mice and non-treated controls (Figure 4 B). No significant difference where seen in the plasma Abeta levels amongst all treatment groups (data not shown).

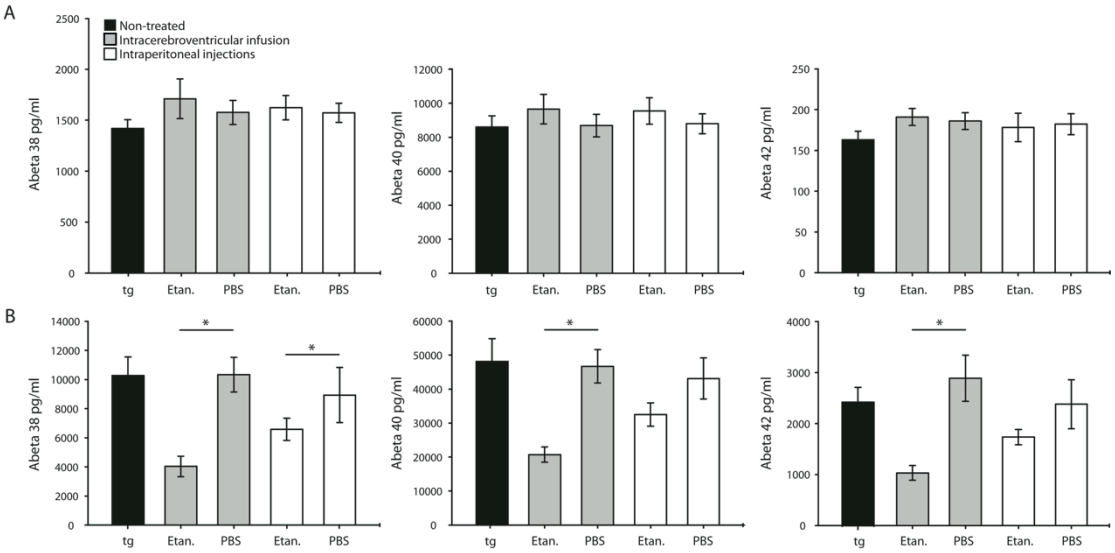

Figure 4. Anti-TNF therapy results in reduced formic acid Abeta levels. A. Biochemical analysis using MSD 3-plex Abeta plates revealed no significant difference in RIPA soluble Abeta 38, 40 or 42 levels across all experimental groups. There was however, a slight trend towards increased RIPA soluble Abeta 40 levels in both Etanercept icv- and ip-treated mice. B. Etanercept icv- and ip- treatment did however result in significantly lower Abeta 38, 40 and 42 levels in the formic acid insoluble fraction.
n = 6-8 per group.

2.3.5 Microglia and Astrocyte analysis

Immunohistochemical staining against GFAP and Iba1 demonstrated strong astrocytosis and microgliosis in all transgenic mice, whereas age-matched wt mice were almost devoid of any reactive astrocyte or activated microglia (data not shown). ArcAβ mice on a TNF knockout background (arcAβ/TNFko) did however show a slight but non-significant reduction in astrocytosis and a non-significant trend towards increased microglia activation, as compared to arcAβ mice (Figure 5 B and E). Etanercept icv-treated mice did, however, show significantly lower astrocytosis, as compared to PBS icv-treated mice (($t_{(70)}$=-2.43, p=0.002; Figure 5 C), and a non-significant trend towards lower astrocytosis, as compared to Infiximab icv-treated mice (Figure 5 C). Histological analysis of Iba1 demonstrated a significantly higher

relative increase in activated microglia in Etanercept icv-treated mice, as compared to Infliximab icv-treated (($t_{(70)}$=2.271, p=0.026; Figure 5 F) and PBS icv-treated mice ($t_{(70)}$=2.354, p=0.021; Figure 5 F).

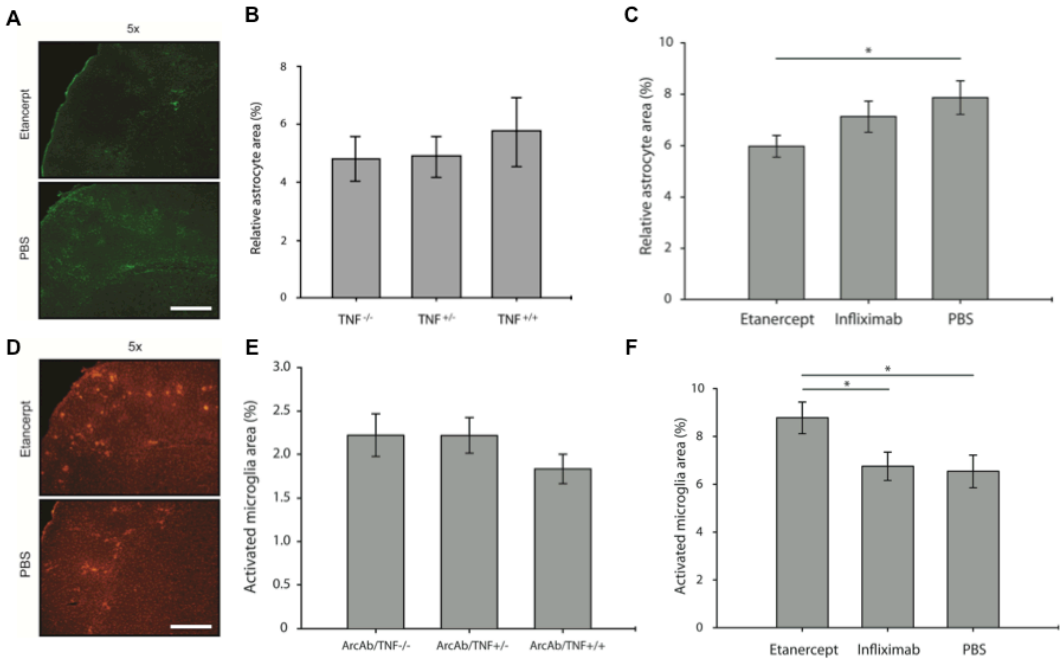

Figure 5. Anti-TNF therapy leads to reduced astrocytosis and increased microgliosis. A. Representative photomicrograph of GFAP staining in Etanercept and PBS icv-treated mice. B. ArcAβ mice on TNF deficient backgrounds display lower astrocytosis than arcAβ controls. C. Etanercept icv-treated mice display significantly lower levels of astrocytosis, as compared to Infliximab and PBS icv-treated controls. D. Representative photomicrograph of Iba1 staining in Etanercept and PBS icv-treated mice. E. ArcAβ mice on TNF deficient backgrounds show a non-significant trend towards increased activated microglia. F. Etanercept icv-treated mice have significantly increased levels of activated microglia, as compared to both Infliximab and PBS icv-treated mice. Scale bars: 500 μm (A and D).

2.4 Discussion

Our findings demonstrate, in a preclinical study, that anti-TNF etanercept therapy, administered intracerebroventricularly (28 days infusion) or intraperitoneally (4 weekly ip injections) can rescue cognitive deficits, as well as, reduce amyloid plaque deposition in 12 month old arcAβ mice. Here we sought to differentiate the therapeutic efficacy of direct modulation of TNF-mediated responses within the central nervous system (CNS) versus systemic TNF-mediated inflammatory or brain-immune communication mechanisms. As such, we either administered anti-TNF therapy directly into the CNS via icv-infusion or systemically through weekly ip-injections. As a control, therefore, all icv-treated mice included in this study were examined both macro and microscopically to confirm correct cannula placement

within the left ventricle and that following 28 days infusion there was wide distribution of the biologic throughout the entire brain of treated animals. Similarly, it was demonstrated that ip-treated mice showed diffusion of the biologic within the brain at sites of impaired blood-brain-barrier (BBB); a widely reported characteristic of arcAβ mice (Knobloch et al., 2007; Merlini et al., 2011). The entry of peripherally administered etanercept within the brain excluded any restricted systemic effect of anti-TNF treatment and lends support towards a CNS-delivered therapeutic approach, as originally demonstrated by Tobinick et al (2006 and 2008) in which the authors treated Alzheimer's disease patients with once weekly perispinal injection of etanercept. However, with Phase II clinical trials underway to investigate the therapeutic potential of subcutaneously administered etanercept in Alzheimer's disease patients, it will be possible to determine in human subjects if systemic anti-TNF therapy may have beneficial effects as well.

All mice tolerated treatment and surgery well, with no aversive side effects observed and no signs towards a MAHA response against the treatment biologic. Cognitive assessment within the Y-maze and Novel Object Recognition Task (NORT) demonstrated improvements for both icv- and ip- treated mice, as compared to controls. These treated mice showed performance levels comparable to wildtype mice, suggesting a complete rescue in cognitive deficits following treatment. Such findings support previous studies in mice, as well as, the cognitive improvements demonstrated in Alzheimer's disease patient following weekly perispinal injections (Tobinick et al., 2006; Tobinick et al., 2008). Given the short duration of treatment (1 month), our findings also support the rapid cognitive rescue observed in human following etanercept anti-TNF treatment (Tobinick et al., 2008). Similarly, it was shown that arcAβ mice deficient in TNF (ArcAβ/TNF-/- mice) displayed better cognitive performance than arcAβ transgenic mice, suggesting long-term benefits of TNF modulation.

These behavioral findings were supported by histological reductions in the number of plaques, as well as, lower percentage area covered by plaques in icv- and ip-treated mice, as compared to controls. Upon further histological investigations, etanercept icv-treated mice were further shown to display increased CAA as compared to controls, suggesting a redistribution of parenchymal plaques towards the vasculature.

As micro-bleeds have been widely described to occur at sites of extensive CAA it was anticipated that the redistribution of amyloid to the vessels in icv-treated etanercept mice would lead to increased occurrence of micro-bleeds. However, histological analysis indicated that micro-bleeds were associated with plaque- and CAA-pathology irrespective of treatment, with frequency and severity of micro-bleeds showing no correlation with increased CAA in etanercept icv-treated mice. In particular, it was shown that many areas of heavy CAA deposition in etanercept icv-treated mice did not show signs of micro-bleeds, suggesting an amyloid-induced risk for micro-bleeds and not a treatment-induced risk for micro-bleeds, despite increased CAA in treated mice. However, it could be that these micro-bleed free areas of heavy CAA deposition might reflect newly formed CAA following anti-TNF treatment induced redistribution of amyloid towards the vasculature and that with time, if not cleared efficiently, these vessels might deteriorate, lose their integrity and begin to bleed.

As a next step, we used MSD analysis to determine Aβ levels in two sequentially extracted protein fractions from hemi brain tissue. In agreement with our histological findings, icv- and ip-treated etanercept mice showed a significant reduction of Aβ in the detergent insoluble formic acid fraction, as compared to control mice. Collectively, these findings provide evidence that anti-TNF etanercept treatment may successfully reverse Aβ-mediated cognitive deficits in a transgenic mouse model of brain amyloidosis and that the continuous infusion of etanercept may have a modulatory effect on brain Aβ levels, as well as, amyloid deposition. Indeed, it has been widely shown that TNF over-expression may promote amyloid plaque deposition, as well as, mediate amyloid induced cognitive dysfunction (He et al., 2007; Rowan et al., 2007; Wang et al., 2005). Medeiros and colleagues (2007) demonstrated that TNF signaling pathways and iNOS act as central mediators of Aβ with both pharmacological and genetic blockage of TNF and iNOS improving cognitive deficits evoked by Aβ. Other evidence supports the role of TNF-mediated synaptic dysfunction in the progression of AD following prolonged Aβ-induced neuronal inactivity (Small, 2008).

Our histological findings demonstrated that icv-treatment was able to lower astrocytosis, as compared to control mice. These results were similarly shown in ArcAβ mice on a TNF knockout background. Such findings suggest a normalization

of reactive astrocytes towards physiological conditions and lend support for an anti-TNF therapy mediated reversal of TNF-mediated synaptic dysfunction. Microglia investigations showed a treatment-induced increase in active microgliosis, with similar founding in ArcAβ TNF knockout mice. These findings suggest that excessive TNF expression might interfere with microglia activation and the potential clearance of amyloid plaque by microglia. Combined, our results indicate that anti-TNF therapy may restore physiological astrocyte functions, promote microglia activation, reduce amyloid burden and successfully reverse abeta-induced cognitive deficits in 12 month old arcAβ transgenic mice.

2.5 Acknowledgements

We thank members of the NBR group, Daniel Schuppli and the rest of the Mouse Facility at the Division of Psychiatry Research for expert technical support and animal care giving support. This study was supported in by a Forschungskredit UZH grant.

2.6 Supplementary Material

General health, sensory-motor and mini-neurological examination. Mice were weighed and their coat appearance, handling responses and home cage social behavior registered. More specifically, coat appearance was assessed for matted, discolored fur, bald patches, missing whiskers, scarring, or wounds, which might otherwise indicate poor health, insufficient grooming, overgrooming and fighting. Unusual responses to handling including, extreme jumping, vocalizations, and attempts to bite the human handler may indicate poor health and were regarded as poor handling responses. Nesting patterns, sleeping in a huddle, allogrooming and normal social interaction behaviors were considered as good home cage social behaviors, whereas, social withdrawal or isolation, excessive fighting, over grooming was regarded as inappropriate home cage social behaviors. Any deviations from good coat appearance and appropriate handling responses and home cage social behavior would be regarded as poor health and scored as a fail, thus excluding the mouse from cognitive-behavioral testing. Successful righting reflex was recorded if the mouse was able to right itself when placed on its back and/or since mice able to right themselves often can't be placed on their backs, the inability to place the mouse on its back was considered successful righting as well. Grip strength was determined

by placing the mouse on a grid and gently inverting the grid and observing whether or not the mouse was able to hold on will suspended upside down. The visual forepaw test involved holding the mouse by its tail at a height of about 15cm above a flat surface and noting the limbs held close to the body. As the mouse was gradually lowered to the surface, successful visual forepaw response was considered if the mouse extended its forepaws for a “soft landing” on the horizontal surface before or without the whiskers or nose touching. Acoustic startle reflex provides a good measure of gross hearing ability and was considered successful if the mouse displayed a flinch response to a loud hand clap. All abovementioned assessments were measured as a pass-or-fail or yes-or-no response by the human observer.

Supplementary Table 1. General health, sensory-motor and mini-neurological examination. All experimental groups had normal coat appearances, appropriate handling responses and home cage behavior, intact visual-auditory function and normal basic reflexes, including visual forepaw response, acoustic startle and righting reflexes.

Experiment group	Administration	Coat appearance	Handling response	Home cage behavior	Visual forepaw	Acoustic startle	Grip test	Extension reflex	Righting reflex
Etanercept	icv	Good (15/15)	Good (15/15)	Good (15/15)	Pass (15/15)	Pass (15/15)	Good (15/15)	Pass (15/15)	Pass (15/15)
	ip	Good (15/15)	Good (15/15)	Good (15/15)	Pass (15/15)	Pass (15/15)	Good (15/15)	Pass (15/15)	Pass (15/15)
Infliximab	icv	Good (15/15)	Good (15/15)	Good (15/15)	Pass (15/15)	Pass (15/15)	Good (15/15)	Pass (15/15)	Pass (15/15)
	ip	Good (14/14)	Good (14/14)	Good (14/14)	Pass (14/14)	Pass (14/14)	Good (14/14)	Pass (14/14)	Pass (14/14)
PBS	icv	Good (15/15)	Good (15/15)	Good (15/15)	Pass (15/15)	Pass (15/15)	Good (15/15)	Pass (15/15)	Pass (15/15)
	ip	Good (15/15)	Good (15/15)	Good (15/15)	Pass (15/15)	Pass (15/15)	Good (15/15)	Pass (15/15)	Pass (15/15)
Non-treated	none	Good (15/15)	Good (15/15)	Good (15/15)	Pass (15/15)	Pass (15/15)	Good (15/15)	Pass (15/15)	Pass (15/15)
Wildtype	none	Good (15/15)	Good (15/15)	Good (15/15)	Pass (15/15)	Pass (15/15)	Good (15/15)	Pass (15/15)	Pass (15/15)

Supplementary Table 2. Drop-outs and technical failures including, cannula misplacement or dislodgement, incorrect ip injections or wrongful genotyping.

Experiment group	Administration	Start	Drop-out	Technical Failures	Finished
Etanercept	icv	15	3	2	10
	ip	15	0	1	14
Infliximab	icv	15	1	3	11
	ip	14	0	0	14
PBS	icv	15	1	1	13
	ip	15	1	1	13
Non-treated	none	15	2	0	13
Wildtype	none	15	0	0	15

3

Aβ-specific DARPins as a novel class of therapeutics for Alzheimer's disease

Michael Hanenberg, Jordan McAfoose, Luka Kulic, Tobias Welt, Fabian Wirth, Petra Parizek, Lisa Strobel, Susann Cattepoel, Claudia Späni, Rebecca Derungs, Marcel Maier, Andreas Plückthun & Roger M. Nitsch

Abstract

With the advent of recombinant protein expression and efficient *in vitro* selection technologies, a novel class of designed ankyrin repeat proteins (DARPins) are beginning to present attractive opportunities for both diagnostic and therapeutic use. DARPins are small and highly stable proteins with a compact modular architecture ideal for high-affinity protein-protein interactions. In this report we describe the selection of Aβ-specific DARPins, determination of their affinities, Aβ epitope recognition and binding kinetics. We further showed their *in vitro* ability to delay Aβ aggregation and prevent Aβ-mediated neurotoxicity. To demonstrate their *in vivo* therapeutic potential mono- and trivalent Aβ-specific DARPins (D23 and 3xD23) were infused intracerebroventricularly into brains of 11 months old Tg2576 mice over four weeks. Both D23 and 3xD23 treatment were shown to result in improved cognitive performance and reduced soluble Aβ levels. These findings demonstrate the therapeutic potential of Aβ-specific DARPins for the treatment of Alzheimer's disease.

3.1 Introduction

The accumulation of misfolded aggregation-prone proteins as intracellular inclusion bodies and extracellular plaques within the brain is a common pathological feature of many neurodegenerative diseases. In contrast to their physiological precursors, these misfolded proteins often acquire β-sheet structural changes that promote and stabilize oligomeric and fibril aggregate formation, as well as, the resistance to natural degradation processes and ultimately the gain of toxic properties that lead to neurodegeneration. Other shared mechanisms include the cell-to-cell propagation of these misfolded proteins (Aguzzi et al., 2009; Lee et al., 2010). From a therapeutic point of view, these emerging concepts strongly support the use of immunotherapeutic strategies with antibodies that can bind, neutralize, and prevent the aggregation and propagation of misfolded proteins throughout the brain.

Based on the effective clearance of β-amyloid from the brains of mouse models of brain amyloidosis upon repeated Aβ immunization (Schenk et al., 1999; Morgan et al., 2000), numerous immunotherapy clinical trials in humans have subsequently been initiated (Rinne et al., 2010; Siemers et al., 2010; Relkin et al., 2009). To-date, more than one dozen anti-amyloid immunotherapy clinical trials testing both passive immunotherapy and active vaccination strategies are currently underway for the treatment of AD (Delrieu et al., 2012). Apart from relatively high costs associated with immunoglobulin production and challenges in quality assurance, complex glycosylation patterns, the inability to reach intracellular targets and the sensitivity to reducing environments may place serious constraints on the use of antibody-based immunotherapies. As an alternative, designed ankyrin repeat proteins (DARPins), which can be effectively selected *in vitro* for binding affinities against a broad variety of target proteins have begun to provide new therapeutic opportunities (Stumpp et al., 2008).

DARPins are built by several ankyrin repeat (AR) modules that are tightly packed and capped by terminating capping repeats that shield the hydrophobic core (Binz et al., 2003). Moreover, DARPins can be conveniently produced in *E. coli* and the lack of cysteines in their primary amino acid sequence provides them with stability in harsh intracellular conditions, high thermostability and good solubility with low aggregation tendency (Binz et al., 2003; Binz et al., 2004). At one-tenth the molecular weight of

IgGs, DARPins are likely to exhibit a higher degree of tissue penetration and might cross the blood brain barrier (BBB) more efficiently upon peripheral administration. Combined with their ability to rapidly diffuse throughout tissue and an accelerated serum half-life (Zahnd et al., 2010), DARPins bound to Aβ could be potentially removed quickly and efficiently making them ideal amyloid-lowering therapeutics with lower risk for immunogenicity, potential aversive immune reactions and the production of neutralizing antibodies following repeated administration.

Here we describe the selection of a novel class of Aβ-specific DARPins, their affinity determination and binding kinetics, as well as, their ability to prevent Aβ aggregation, reduce Aβ-mediated neurotoxicity and *in vivo* therapeutic potential in Swedish (Tg2576) transgenic mice.

3.2 Materials and Methods

3.2.1 Preparation of the amyloid-β peptides.

The full length recombinant Aβ1-42 peptide was purchased from rPeptide (Bogart, USA). All biotinylated variants (biot.-Aβ1-28, Aβ1-40-biot. and biot.-Aβ1-42) were obtained from Anaspec (Fremont, USA). The lyophilized peptide was prepared as previously described (Stine et al., 2003; Wood et al., 1996). Briefly, the peptide was dissolved in 1,1,1,3,3,3-hexafluoro-2-propanol (HFIP) to yield a final concentration of 1 µg/µL. The peptides were distributed into 10 – 50 µg aliquots and the HFIP completely evaporated under a constant stream of nitrogen. The tubes were snap-frozen in liquid nitrogen and stored at -80°C until further use. For resuspension, the Aβ aliquots were thawed on ice and dissolved in 10 mM NaOH under vigorous vortexing and sonication (30 s) to yield a final concentration of 10 – 250 µM. From these stock solutions, the peptides were finally diluted into the experimental buffer.

3.2.2 Ribosome display selection of DARPins.

The enrichment of anti-Aβ DARPins was performed using previously described cDNA libraries with two randomised repeat units (N2C) flanked by N- and C-terminal capping repeats (Binz et al., 2004). As reported previously, the library was subjected to a total of four selection cycles with modifications as follows (Zahnd et al., 2007).

A microtiter plate (Nunc, Langenselbold, Germany) was coated with 100 µL of a 66 nM solution (Tris-buffered saline; pH 7.4) of neutravidin overnight at 4°C. Subsequently, wells were blocked with 0.5% bovine serum albumin (BSA) in TBS and 100 µL of a solution of C-terminally biotinylated Aβ1-28 (250 nM, in TBS) was immobilized. From cycle two onwards, the selection was performed in solution and ternary complexes were pulled down with 20 µL of streptavidin (SV) coated magnetic particles (Roche, Rotkreuz, Switzerland). Prior to the incubation step with the peptide target, the DARPin subpool was depleted from unspecific binders by preabsorption to empty SV particles. Selection stringency was increased by a decreased amount of biotinylated Aβ1-28 (400 nM in cycle 1, 100 nM in cycles 2 to 4), extended washing time and a decreasing number of PCR cycles (40, 35, 30, 28) for re-amplification of the reverse-transcribed mRNA pool. After cycle 4, the cDNA was subcloned into expression vector pQE-30ss (Huber et al., 2007) and transformed into competent *E.coli* XL-1 Blue.

3.2.3 Screening ELISA.

Individual clones were picked and grown in deep-well microtiter plates (Nunc, Langenselbold, Germany) in 1 mL of LB medium containing 100 µg/mL ampicillin. DARPin expression and cell lysis were performed as described by Eggel et al (Eggel et al., 2009). For the analysis of individual DARPin clones microtiter plates (Corning, Amsterdam, The Netherlands) were coated with 66 nM neutravidin (30 µL/well) overnight and 250 nM of the target peptides (30 µL of biotinylated Aβ1-28, Aβ1-40 or Aβ1-42) were immobilized for 1 h at 4°C. Binding of the crude extracts to wells containing the peptides was compared to wells containing biotin-blocked neutravidin alone. After extensive washing with TBS-T (TBS supplemented with 0.05% Tween 20) bound DARPins were detected via an anti-RGS-His_6 antibody (Qiagen, dilution 1:1000) and an anti-mouse-HRP conjugate (GE Healthcare, dilution 1:2000). The assay was developed using 20 µL of a mixture of tetramethylbenzidine (TMB) with 30 mM citric acid (1:20) and stopped with 20 µL of 1 M H_2SO_4. The absorbance at 450 nm was recorded against a reference wavelength of 690 nm with a standard ELISA reader Sunrise™ (Tecan, Männedorf, Switzerland).

3.2.4 Titration ELISA.

Biotinylated antigens (biotinylated Aβ1-28 or Aβ1-42) were immobilized on neutravidin coated plates in triplicates as described before. Purified DARPins were serially diluted in TBS and applied to the wells with previously coated antigen. The wells were washed three times with TBS-T between every incubation step and detection of bound complexes was performed with an anti-RGS-His_6 primary antibody (Qiagen, 1:1000) and an anti-mouse-HRP conjugate (GE Healthcare, 1:2000), diluted in TBS-B (TBS supplemented with 0.5% BSA). After addition of the TMB substrate, the signal was recorded at 450 nm against a reference wavelength of 690 nm. The signals were normalized to the highest absorbance and plotted against the logarithm of the DARPin concentration. The data were fitted to a sigmoid dose-response equation using Graph Pad Prism 5 (GraphPad Software, USA) to calculate the half-maximal effective concentration (EC_{50}).

3.2.5 Competition ELISA.

The competition ELISA was performed as originally described by Friguet et al*.,* (1985). with the following modifications: a constant concentration of DARPin (10 nM) was incubated with various quantities of soluble Aβ1-42 ranging from 0 to 5000 nM in TBS150 for 1 h at 4°C in order to achieve equilibrium. A total of 30 µL of these DARPin-antigen mixtures was then transferred into the wells of a microtiter plate previously coated with Aβ1-28-biotinyl (30 µL per well at 250 nM in TBS150 for 1 h at 4°C) and incubated for 30 min at 4°C. In order to probe any readjustment of equilibrium, the content of each well was transferred to identically coated wells of a second microtiter plate, incubated for the same time and processed as the first plate. After three washing steps with TBS-T, bound DARPins were detected using an anti-RGS-His_6 antibody (dilution 1:1000) and an anti-mouse-HRP conjugate (GE Healthcare, dilution 1:2000). The fractions of DARPins retained in the first wells was computed as described by Friguet et al., (1985) ($f < 0.2$ was considered a still acceptable shift in equilibrium). The absorbance was recorded at 450 nm (reference 690 nm) and plotted versus the concentration of the competitor.

3.2.6 Epitope mapping by monoclonal antibodies.

Biotinylated DARPin D23 was diluted to 500 nM in TBS150 and immobilized on neutravidin-coated wells of a 96-well microtiter plate for 1 h at 4°C. Unbound surface sites were blocked with 0.5% BSA dissolved in TBS150. A 50 µg aliquot of Aβ1-42 was dissolved in 10 mM NaOH to yield a final concentration of 100 µM. The sample was vigorously vortexed and sonicated for 30 s and diluted in PBS (137 mM NaCl, 2.7 mM KCl, 10 mM Na_2HPO_4, 1.38 mM K_2HPO_4, pH 7.4) to a final concentration of 200 nM. The peptide was incubated in the DARPin-coated wells for 1 h at 4°C. The bound peptide was probed with varying concentrations from 10 ng/µL to 0.1 ng/µL of monoclonal antibody 6E10, 4G8 (Covance, Basel, Switzerland) and 22C4 (in-house). These antibodies are known for their differing linear epitopes on the Aβ1-42 peptides comprising residues 1-16, 17-24 and 30-42, respectively (Kim et al., 1988; Mohajeri et al., 2002). The antibodies were detected with an anti-mouse-IgG-HRP conjugate (GE Healthcare, 1:2000) and revealed colourimetrically using TMB diluted in citric acid.

3.2.7 Epitope mapping by peptide competition.

Aβ1-28-biotin (250 nM) was surface-immobilized on a neutravidin layer in a 96-well format as described previously. DARPin D23 was diluted to 50 nM in TBS150 and pre-incubated with a 50-fold molar excess of the peptide fragments Aβ(-4-6), Aβ (-3-7), Aβ(-2-8), Aβ(-1-9), Aβ(1-8), Aβ(2-11), Aβ(3-12), Aβ(4-13), Aβ(5-14), Aβ(6-15) (peptides&elephants, Potsdam, Germany), Aβ(1-11), Aβ(1-16), Aβ(12-28), Aβ(17-28), Aβ(29-40), Aβ(31-35), Aβ(33-42), Aβ(1-28), Aβ(1-28) (Bachem, Bubendorf, Switzerland) and scrambled Aβ1-42 (rPeptide, Bogart, USA). The lyophilized peptides were dissolved in DMSO to a final concentration of 1 mM and stored at -20°C until further use. Bound DARPin was detected with an anti-hexahistidine antibody (dil. 1:1000, Qiagen, Hildesheim, Germany) and a subsequent anti-mouse IgG-HRP conjugate (dil. 1:2000, GE Healthcare,). Revelation was done using TMB diluted in citric acid as described before.

3.2.8 Aβ aggregation assays.

The rate of spontaneous aggregation of the monomeric Aβ peptide into fibrillar amyloid structures was monitored via thioflavin T (ThT) fluorescence as described

previously (Finder et al., 2010). Briefly, the recombinant Aβ1-42 peptide was dissolved in 10 mM NaOH under vigorous vortexing and sonification (1 min) to a final concentration of 250 µM. The concentration of the Aβ stock solutions was determined spectrophotometrically (ε = 1730 $M^{-1}cm^{-1}$) as described (Finder et al., 2010). The stock solutions were kept on ice und used within 24 h of preparation. The aggregation kinetics were performed and monitored in stirred fluorescence quartz cuvettes (1 mL) at 25°C using a CaryEclipse fluorescence spectrophotometer (Varian, Agilent Technologies, Basel, Switzerland) with external temperature control. Unless indicated otherwise, the aggregation mixtures consisted of 50 µM Thioflavin T, 150 mM NaCl, 10 mM phosphate with a pH of 7.4. In case of inhibition studies, equimolar (5 µM) amounts of DARPin D23 or E2_5 were also included in the assay mix. As a last step, the monomeric Aβ1-42 peptide was added freshly to the tempered mix at a final concentration of 5 µM. The samples were zeroed and aggregation kinetics were immediately monitored by exciting the sample at λ_1 = 456 nm and recoding the emission at λ_2 = 489 nm every 2 min (optimal wavelengths experimentally determined in pre-experiments with amyloid fibres).

3.2.9 Neurotoxicity assays.

Primary neurons were isolated from the cortex of rat embryos (day E18). Therefore the brains were dissected in ice-cold PBS supplemented with 1 mg/mL glucose according to standard protocols (Freshney, 2010). Briefly, the cortices were removed from the brains and collected in ice-cold PBS/glucose. After removal of the meninges, they were minced and incubated in Dispase II (2.4 U/ml, Roche, Mannheim, Germany) at 37°C for 10 min. The enzyme was discarded and the tissue was washed with DMEM, supplemented with 10% FCS. After thorough trituration, the number of living cells was determined via Trypan Blue staining. The cells were pelleted (5 min, 1000 rpm), the medium was removed and diluted to the desired density in Neurobasal medium (Invitrogen, Basel, Switzerland), supplemented with 2% B27 and 125 µM L-glutamine (Invitrogen, Zug, Switzerland). The cells were seeded in poly-ornithine-coated plates (either 96-well plates or 24-well plates with 12 mm round coverslips) at 1 x 10^3 cells/well (96-well plates) or 1 x 10^5 cells/well (24 well plates). The cells were kept in culture for 5 days (days in vitro, DIV) at 37°C and 7% CO_2. The cytotoxicity experiments were started on DIV 6. For this purpose, Aβ was prepared as previously described and premixed with Neurobasal medium,

DARPin D23 or DARPin E2_5, respectively. Half of the cell culture medium was removed and the Aβ / DARPin pre-mix was added onto the cells. Controls were treated either with vehicle or with scrambled Aβ (both in 10 mM NaOH / Neurobasal medium). The plates were incubated for another 48 h before either the cytotoxic effect or neuromorphological changes were measured. For toxicity studies, the CytoTox-Glo™ Cytotoxicity assay (Promega, Madison, USA) was used according to the manufacturer's instructions. Three wells per treatment were measured and the assay repeated two more times. Data are given as means ± SEM.

3.2.10 Cloning strategy for multivalent DARPins.

The DARPin CDS was excised from the expression plasmid pQE30 (Qiagen, Hildesheim, Germany) using the restriction enzymes BamHI and HindIII (New England Biolabs, Ipswich, USA). The recipient plasmid (pQI-bi-1_1) was opened with the same restriction enzymes. DARPins were first inserted into cassette 1 via a BamHI/Hind III restriction digestion and in a separate restriction digestion into cassette 2 through the compatible restrictions sites for BgLII and BsaI downstream of the linker sequence. An $MRGSH_6$ tag located 5' of the first expression cassette allowed purification and detection of the fusion constructs. For the construction of trivalent DARPins, the bivalent construct was PCR amplified using the primers MVD3_forw (5'-AAAGAGGAGAAATTAACTATGAGAGGATC-3') and QiBi_MVD_rev (5'-AAGGATAGGTCTCAAGCTAGAGAGTCATTACCCCAGGCGTTTAAGG-3'). The reverse primer has a 5'-overhang with a *BsaI* restriction site (underlined, overhang restriction). The resulting amplificate was digested using BamHI / BsaI and inserted into the pQI-bi-1_1 recipient vector via the restriction sites for BgLII and BsaI. The vector had previously been modified to already contain a DARPin in the 5'-expression cassette. The resulting trivalent DARPin codes for three in-frame monomer units connected by two 10-AA-linkers. The cloning strategy introduced an additional transcription termination region (TTR) at the 3' of the expression cassettes.

3.2.11 Surface plasmon resonance.

SPR was recorded with a Biacore T100 instrument (GE Healthcare) similarly to previous descriptions (Binz et al., 2004). A streptavidin SA chip (GE Healthcare) was coated with 170 RU Aβ1-28-biotinyl or 250 RU Aβ1-42-biotinyl in 10 mM NaOH. For

all subsequent experiments a HBS-EP running buffer (10 mM HEPES, 150 mM NaCl, 3.4 mM EDTA, 0.05% Tween 20, pH 7.4) was used. Association and dissociation events were measured at a constant flow rate of 30 µL/min. Analytes were injected at increasing concentrations doubling from 0.5 nM to 512 nM for 12 min and the dissociation phase was recorded for 30 - 70 min. Wherever possible, concentrations were assessed in duplicates and binding stability monitored to exclude target loss. As a correction for non-specific binding, the signal of an uncoated reference cell was subtracted from all measurements. The kinetic data obtained were evaluated via global fit using the BIAevaluation software 2.0.3 (GE Healthcare).

3.2.12 Animals.

This study used Swedish tg2576 transgenic mice expressing human APP with the Swedish mutation. Mice were bred, held and kept at the Division of Psychiatry Research mouse facility under specific pathogen free (SPF) conditions, temperature controlled (22 °C±1 °C), 3 to 5 animals per cage, with sawdust as bedding and tissue as nesting material. All housing boxes were under individual air ventilation. A 12 hour light–dark cycle beginning at 7:00 h was maintained in the housing room and except for the time of testing, water and food was provided *ad libitum*. Cognitive-behavioral testing was performed in a separate room within the mouse facility specifically designed for cognitive-behavioral investigations. Experiments were approved by the veterinary office of the Cantonal Health Department.

3.2.13 Cognitive-behavioural testing.

At the time of testing, mice were weighed and examined for general health measures to ensure that the mice were physically able to conduct the cognitive-behavioral test and to rule out any adverse side effects due to the surgical procedure or DARPin therapy; supplementary material. Spatial working memory was assessed in mice using the Y-maze (Y-shaped plastic maze, with 40 cm x 20 cm x 10 cm arm sizes). During a 5 minute trial the sequence of arm entries was recorded using the ANY-maze Video Tracking System (Stoelting Co., USA). The percent alternation was calculated as the ratio of actual to possible alternations (defined as the total number of arm entries -2) x 100%.

3.2.14 DARPin icv administration via surgical Implantation of Alzet® osmotic minipumps.

Twelve-month-old tg2576 mice were deeply anaesthetized, a small midline incision was made to expose the skull, and a subcutaneous pocket was prepared in the midscapular area of the back of the mice so that a sterile Alzet® minipump (model 2004, 3.0 cm. in length, 0.7 cm. in diameter and weighing 1.1 g empty weight) filled with DARPin solution or vehicle could be inserted. Subsequently, an Alzet Brain infusion kit 3 cannula was lowered into the left lateral ventricle (coordinates according to bregma; AP, -0.2 mm; ML, 0.9 mm; and DV, 2.5 mm) and two small screws were placed within the skull and dental cement applied to firmly attach to the skull. Post-operatively, mice were housed for three days on heat pads and moist food placed at the floor of the cage to promote recovery and to reduce drop-outs. Groups of 19-23 mice received icv-infusion over 28 days (equimolar concentration of 50μM) of either D23, 3xD23, E2_5 or PBS control.

3.2.15 Biochemical and Immunohistochemical analyses.

Mice were deeply anesthetized and blood collected from the right ventricle using a syringe with EDTA and samples were centrifuged at 8'000 rpm for 8 minutes at 4°C and plasma extracted using a sterile pipette and stored at -80°C for later batch analysis. Following the collection of blood, mice were transcardially perfused with PBS and their brains rapidly removed. Brains were dissected in two hemispheres with the left hemisphere being placed in 4% PFA and post-fixed overnight at 4C° and then transferred to 30% sucrose for 72 hours (cyroprotection) for later histological analysis. PFA-fixed and cryoprotected hemibrains were cut in 35 μm thick coronal slices at -80°C using a microtome (Leica Jung HN40) and kept at -20°C in an anti-freeze solution (phosphate buffer 0.50 M in MilliQ water: ethyleneglycol : glycerol = 1.3:1:1) until staining was performed. The right hemibrain was dissected for biochemical purposes and immediately frozen in liquid nitrogen and stored at -80°C. Brain tissue was later homogenized using a sequential extraction protocol in which tissue was homogenized using a glass-Teflon homogenizer (20 strokes, 315 rpm) in RIPA buffer containing complete protease inhibitor tables (Sigma-Aldrich, Switzerland), centrifuged at 100,000 x g (53,000 rpm) at 4°C for 1 hour and supernatant extracted and stored at -80°C for later biochemical batch analysis. The remaining pellet was frozen on dry ice, resuspended in 70% formic acid, sonicated

for 30s at 30% power, ultracentrifuged (100,000 x g @ 4°C for 30 minutes), supernatant extracted, lyophilized, reconstituted in RIPA buffer and stored at -80°C for later batch analysis.

3.2.16 Beta-amyloid analysis.

Aβ fragments were measured in plasma and brain homogenates using a MSD 3plex multi-SPOT Abeta human kit (MesoScale Discovery, USA) for Aβx-38, Aβx-40 and Aβx-42, in accordance to manufacturer's instructions. MSD SECTOR Imager 6000 reader was used for analysis and the MSD DISCOVERY WORKBENCH software (Version 3.0.17) with Data Analysis Toolbox was used to calculate sample concentrations by comparing them against a standard curve (five-parameter logistic curve).

3.2.17 Immunohistochemistry.

Thioflavin S staining was done according to standard protocol. In short, floating sections were washed in KPBS and mounted on chrom-gelatin coated glass slides before being processed. After treatment for 10 min with 0.25% potassium permanganate, sections were washed in KPBS and incubated in 1% potassium metabisulfite and 1% oxalic acid until they appeared white. Sections were then floated 3 seconds in 0.25% acetic acid, washed in water and stained for 5 min with a solution of 0.015% Thio-S in 50% ethanol. Finally, sections were washed in 50% ethanol and in water, then dried and coverslipped with Hydromount® (National Diagnostics, Hull, UK). All chemicals were from Sigma (St. Louis, MO).

3.2.18 Statistical analysis.

Data analysis was performed using the Statistica 10.0, SPSS 19.0 statistical software and GraphPad Prism 4.03 software. Tests for normal distribution were performed before statistical testing, according to the results of the Shapiro-Wilk and the Kolmogorov-Smirnov Test for normality, either Student's t Test or Mann-Whitney U Test for 2 sample groups or ANOVA was performed (followed by post-hoc Fischer LSD analysis or Tukey's test). A p-value < 0.05 was considered statistically significant. Error bars are SEM.

3.3 Results

3.3.1 DARPin D23 specifically binds to soluble monomeric Aβ.

Ribosome display was used to enrich specific DARPins against the Aβ peptide. A cDNA library with two randomized repeat units (N2C) was subjected to surfaces coated with C-terminally biotinylated Aβ1-28. This truncated Aβ variant was chosen over Aβ1-42 for its reduced propensity to form aggregates. In every round, the selection pressure was increased through a decrease in the amount of target peptide, increased washing stringency and a reduced number of PCR cycles to re-amplify the selected subpool. An alternate use of neutravidin and streptavidin excluded the erroneous selection against scaffolding proteins. From cycle 2 onwards, selection was performed in solution to drive the selection of DARPins recognizing soluble Aβ species (Figure 1 A). After four cycles, a screening ELISA revealed 30 out of 96 clones as positive (~ 31%) with negligible reactivity to control proteins (Supplementary Figure 1). DNA sequence analysis of twenty randomly selected Aβ binders confirmed differences mainly at the variable interaction residues and with lower frequency also in the N-terminal cap. Due to best performance in a series of competition experiments, the DARPin termed D23 was selected as a lead candidate for further characterization. A titration ELISA (Figure 1 B) demonstrated that the selected clone also recognizes the pathologically relevant variant Aβ1-42 with a comparable EC_{50} in the nanomolar range (17 nM for Aβ1-28 and 31 nM for Aβ1-42). The binding of DARPin D23 to surface-immobilized Aβ was specifically competed using a molar excess of soluble Aβ1-42 with a 50% drop in binding signal at a competitor concentration of approximately 50 nM suggesting that D23 specifically binds soluble Aβ1-42 in the low nanomolar range (Figure 1 C).

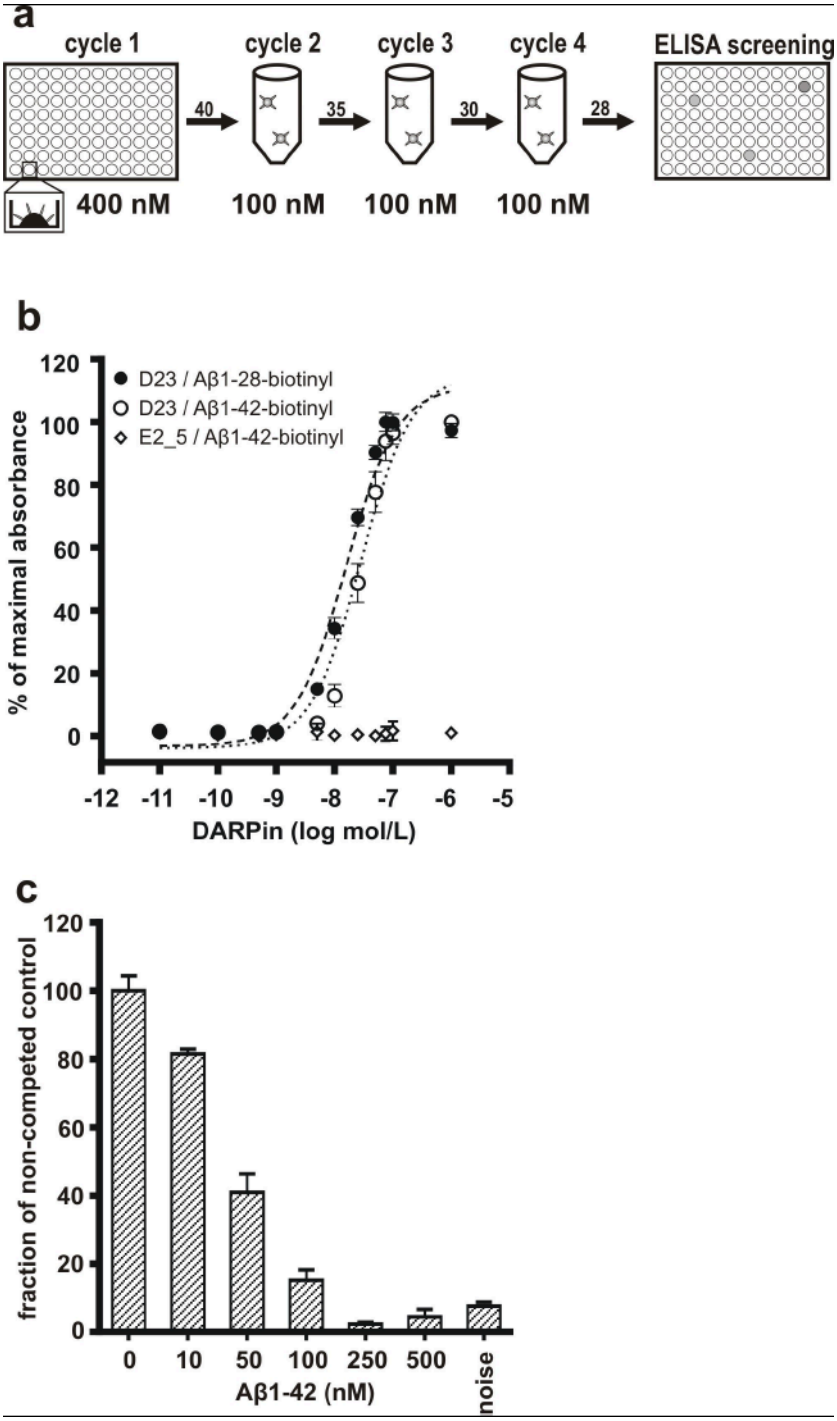

Figure 1. A specific anti-Aβ DARPin was selected *in vitro* through ribosome display. (a) A DARPin N2C library was selected against decreasing amounts of the biotinylated Aβ1-28 peptide via ribosome display in four selection cycles. Peptides were presented via neutravidin (cycle 1) or recovered from solution through streptavidin-coated particles in all subsequent rounds. DNA was re-amplified at the end of each cycle with decreasing numbers of PCR cycles (arrow numbers). After four cycles, individual clones were analyzed for Aβ binding activity through ELISA. (b) DARPin D23 showed a superior binding profile as compared to other clones and bound both Aβ1-28 and Aβ1-42 in the nanomolar range with an EC_{50} of 17 nM (Aβ1-28) and 31 nM (Aβ1-42). A non-selected library member, E2_5, did not bind Aβ1-42 at any concentration. (c) DARPin D23 binding to immobilized Aβ1-28-biotin can be inhibited by increasing concentrations of the soluble peptide Aβ1-42. The competition shows half-maximal inhibition at approximately 50 nM Aβ1-42. Data represented as means ± SD.

3.3.2 D23 binds a conformational Aβ epitope involving the free N-terminus.

D23 bound three C-terminally biotinylated variants (Aβ1-28, Aβ1-40 and Aβ1-42) with similar affinities, but did not recognize N-terminally biotinylated Aβ1-42 in ELISA (Supplementary Figure 2). We utilized the three monoclonal antibodies 6E10 (N-terminus), 4G8 (central domain) and 22c4 (C-terminus) with known epitopes on the Aβ peptide to thoroughly analyze the DARPin-bound epitope. The addition of these antibodies to a DARPin-immobilized Aβ coat revealed that the DARPin-Aβ interaction strongly interfered with peptide recognition by antibody 6E10 and to a lesser extent by 4G8 suggesting that the N-terminal Aβ stretch was already bound by DARPin D23 (Figure 2 A). The use of truncated Aβ1-28 during ribosome display selections precluded the interference of DARPin D23 with the C-terminal antibody 22c4 and served as maximal readout control for this assay. To dissect the DARPin-Aβ interaction more closely, a peptide scanning approach with soluble short Aβ fragments was used to compete the DARPin-Aβ1-28 interaction (Figure 2 B). A 50-fold molar excess of partially overlapping peptide fragments was used for competition and only signals above those of scrambled Aβ1-42 were regarded as specific inhibition. Not only was the importance of the N-terminal aspartate residue confirmed for high affinity binding, but also we observed that longer peptide fragments (Aβ1-16, Aβ1-38) inhibited the interaction more effectively than shorter ones suggesting that the N-terminal stretch is part of a conformational, rather than a linear epitope. The binding mode of D23 is probably different from that of previously mentioned monoclonal antibodies that recognize a linear stretch of the Aβ peptide and also cross-react to APP (Tampellini et al., 2007) (at least 6E10 and 4G8). This particular DARPin binding modality is advantageous as the conformation of the monomeric Aβ peptide is most likely different from the one in its parental protein and also limits cross-reactivity to APP (data not shown). In an immunohistochemical analysis of brain sections from APP transgenic mice, we observed the specific staining of parenchymal and vascular amyloid deposits through D23 but not by E2_5 (Figure 2 C). Importantly, D23 does not cross-react to other brain structures in wild-type mice (WT).

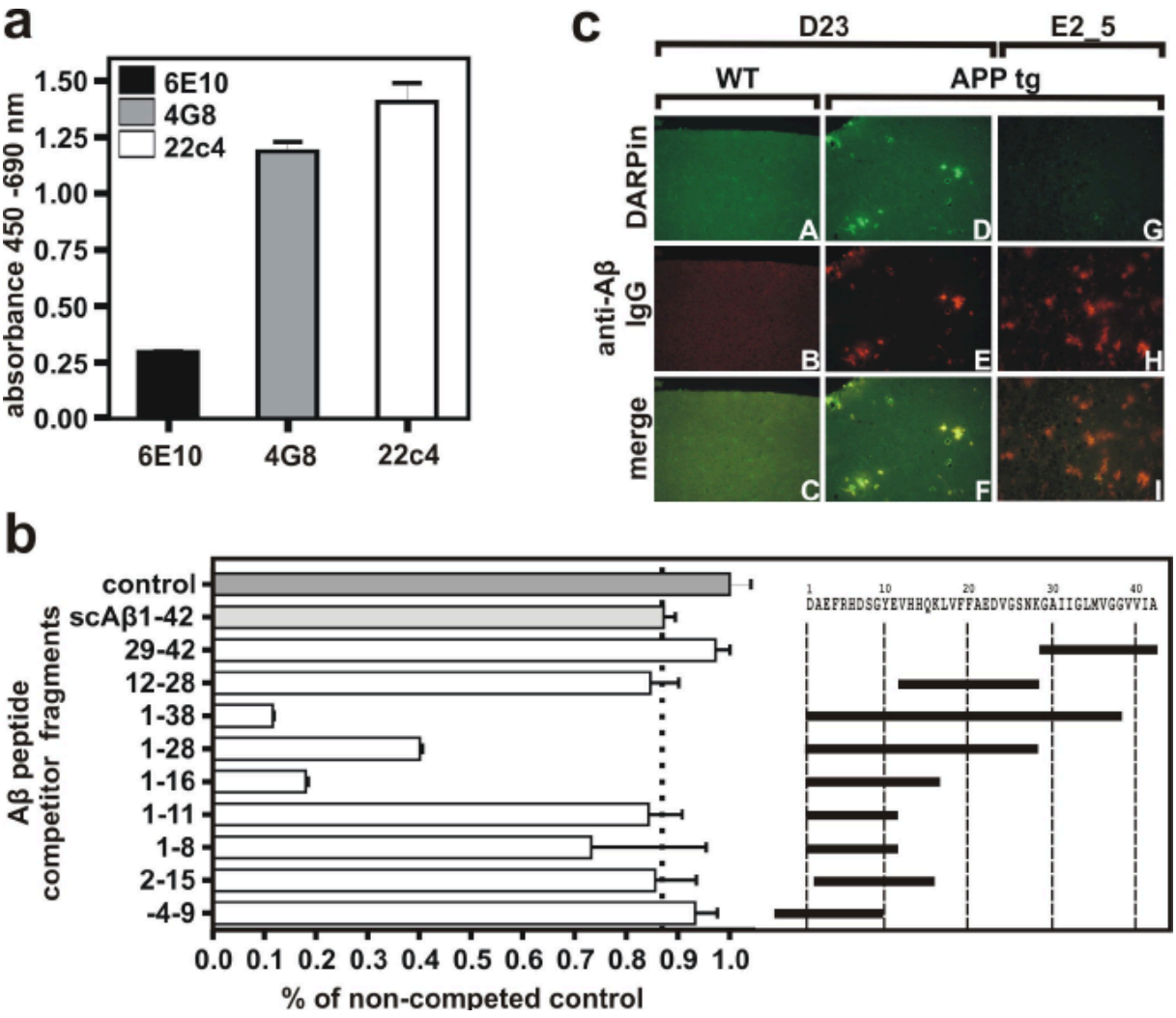

Figure 2. DARPin D23 recognizes a conformational Aβ epitope and binds amyloid deposits in *ex vivo* murine brain tissue. (a) In a direct ELISA with immobilized DARPin D23, the accessibility of bound Aβ1-42 was probed with monoclonal anti-Aβ antibodies directed against the N-terminus (6E10), central part (4G8) or C-terminus (22c4) of the peptide. Binding of the N-terminus specific antibody 6E10 to the Aβ peptide was impaired most. (b) To further determine the Aβ epitope recognized by D23, a 50-fold molar excess of Aβ-derived peptide fragments was used to compete DARPin binding to immobilized Aβ1-28 peptide and ELISA signals normalized to a non-competed control. Inhibition was considered specific if signals were below the one of scrambled Aβ1-42 control (dotted line). A free N-terminus aspartate residue was required for efficient inhibition, whereas central or C-terminal fragments did not show any inhibitory effect. Competition with longer fragments involving a free N-terminus (Aβ1-16, Aβ1-28, Aβ1-38) showed best inhibition of up to 80%. (c) GFP-fused DARPin D23 specifically recognizes amyloid-β plaques in brain slices from transgenic ArcAβ mice. The specificity of plaque binding by the selected DARPin D23 was confirmed by applying DARPins C-terminally fused to superfolder GFP (sfGFP) onto brain sections from wildtype mice (A-C) and ArcAβ (D-F) transgenic mice and. D23 recognized vascular and parenchymal amyloid deposits without cross-reactivity to WT brain structures. The control DARPin E2_5 did not show any binding activity. First row: DARPin binding (GFP channel); middle row: α-Aβ antibody binding (Cy3 channel); bottom row: merge of GFP- and Cy3-channel.

3.3.3 D23 prevents Aβ aggregation and –mediated neurotoxicity

To study the DARPin's functional effect on Aβ aggregation, equimolar concentrations of Aβ1-42 were incubated under constant agitation either alone or with DARPins D23 and E2_5, and thioflavin T (ThT) fluorescence signals were recorded over time (Figure 3 A). Whereas a 5 µM preparation of monomeric Aβ1-42 readily aggregates into fibrils, the addition of equimolar amounts of D23 – but not E2_5 – is able to significantly delay both the lag time and steepness of the aggregation curve. We hypothesize that D23 stabilizes the monomeric form of Aβ peptide and sequesters it from the dynamic aggregation equilibrium. This idea is underscored by the observation that D23 does not interfere with the Aβ aggregation process if added during log-phase or after the plateau has been reached, but delays the aggregation process if supplemented in substoichiometric amounts at the beginning of the assay (data not shown). To analyze the DARPin's effect on toxicity mediated by soluble Aβ species, we determined a 48 hours incubation of 5 µM Aβ as most toxic to a culture of rat primary cortical neurons, whereas a preparation of similarly composed scrambled Aβ did not induce any toxicity (Supplementary Figure 3). Aβ-mediated neurotoxicity was quantified either alone or in equimolar combination with DARPin D23 or its control version E2_5. The latter did not show any effect on neurotoxicity, while the anti-Aβ DARPin could reduce toxicity by about 40% (Figure 3 B).

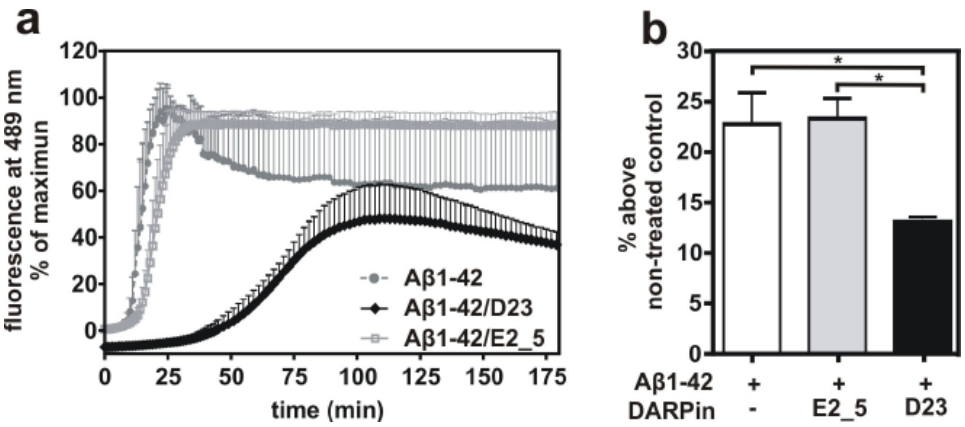

Figure 3. Aβ aggregation and -mediated neurotoxicity can be inhibited through D23 addition. (a) The inhibitory effect of DARPin D23 on Aβ1-42 aggregation was monitored by thioflavin T fluorescence (ThT). Equimolar concentrations of Aβ1-42 and DARPins D23 or E2_5 were co-incubated and ThT fluorescence monitored for 3 hours at 489 nm. DARPin D23 delays Aβ aggregation, whereas E2_5 has no effect on the Aβ1-42 aggregation profile. The assays were performed in triplicates in stirred cuvettes. Data presented as means ± SD. (b) Primary rat neurons (day in vitro 5) were co-incubated with equimolar amounts of recombinant Aβ1-42 and DARPins D23 or E2_5 (all components 5 µM). After 48 hours the level of Aβ1-42-mediated toxicity was assessed by luminescence emitted from released neuronal protease activity. D23 is able to significantly decrease Aβ1-42-mediated cytotoxicity as compared to controls (mean ± SEM; * $p < 0.05$; One-way ANOVA, followed by Tukey's test).

3.3.4 Multivalent DARPins improve binding kinetics for immobilized Aβ1-42.

To further optimize Aβ binding, we constructed bi- and trivalent DARPins that were connected by flexible amino acid linkers. DARPins were genetically engineered as end-to-head fusions and expressed in a single open reading frame (ORF) as previously described (Zahnd et al., 2010). As for the monovalent DARPin D23, multivalent constructs were efficiently expressed and purified in a single IMAC-procedure from bacterial crude cell lysates (Figure 4 A, inlay). Size exclusion chromatograms (SEC) confirmed that all constructs eluted as single peaks with apparent molecular weights of 12 kDa (D23), 30.4 kDa (2xD23) and 44.3 kDa (3xD23) from a SEC column (Figure 4 A). Only minor differences in their corresponding EC_{50} values were observed, when comparing Aβ binding in ELISA (Supplementary Figure 4), but a separate kinetic analysis of the association and dissociation phases via surface plasmon resonance, revealed substantial differences in the on- and off-rates of the individual constructs (Figure 4 B-D). While the monovalent DARPin D23 (Figure 4 B) showed a very fast on-rate (k_{on} = 1.26 x 10^6 $M^{-1}s^{-1}$), the association kinetics were decreased by a factor of 40 for the bivalent DARPin 2xD23 (k_{on1} = 3.72 x 10^4 $M^{-1}s^{-1}$, k_{on2} = 4.19 x 10^{-5} $M^{-1}s^{-1}$), but only three times for the trivalent construct 3xD23 (k_{on1} = 4.03 x 10^5 $M^{-1}s^{-1}$, k_{on2} = 8.02 x 10^{-4} $M^{-1}s^{-1}$; Figure 4 C,D). This suggests that DARPin association kinetics are influenced by the sterical accessibility to the Aβ peptide rather than by a limited diffusion due to the increased molecular weight of the multivalent constructs. The high off-rates of D23 (k_{off} = 7.3 x 10^{-2} s^{-1}) indicate that the monovalent DARPin dissociates from its target in proportion to its association velocity limiting its affinity to a two-digit nanomolar range. An apparent increase in overall affinity of the multivalent constructs 2xD23 (k_{off1} = 2.8 x 10^{-3} s^{-1}, k_{off2} = 6.3 x 10^{-4} s^{-1}) and 3xD23 (k_{off1} = 1.3 x 10^{-3} s^{-1}, k_{off2} = 2.0 x 10^{-3} s^{-1}) is due to their built-in avidity allowing frequent re-binding to the sensor-surface. Kinetic data suggest that the construction of the trimeric derivative 3xD23 best combined a slightly decreased on-rate with a strongly improved off-rate, even though this effect can only be exploited in polymeric Aβ species such as oligomers or fibrils. Motivated by the promising *in vitro* features of the selected DARPins, we investigated the long-term stability of D23 under physiological conditions (Supplementary Figure 5) and were reinforced to investigate the effect of

intracerebroventricular infusions of mono- and trivalent DARPin constructs in SweAPP transgenic mice.

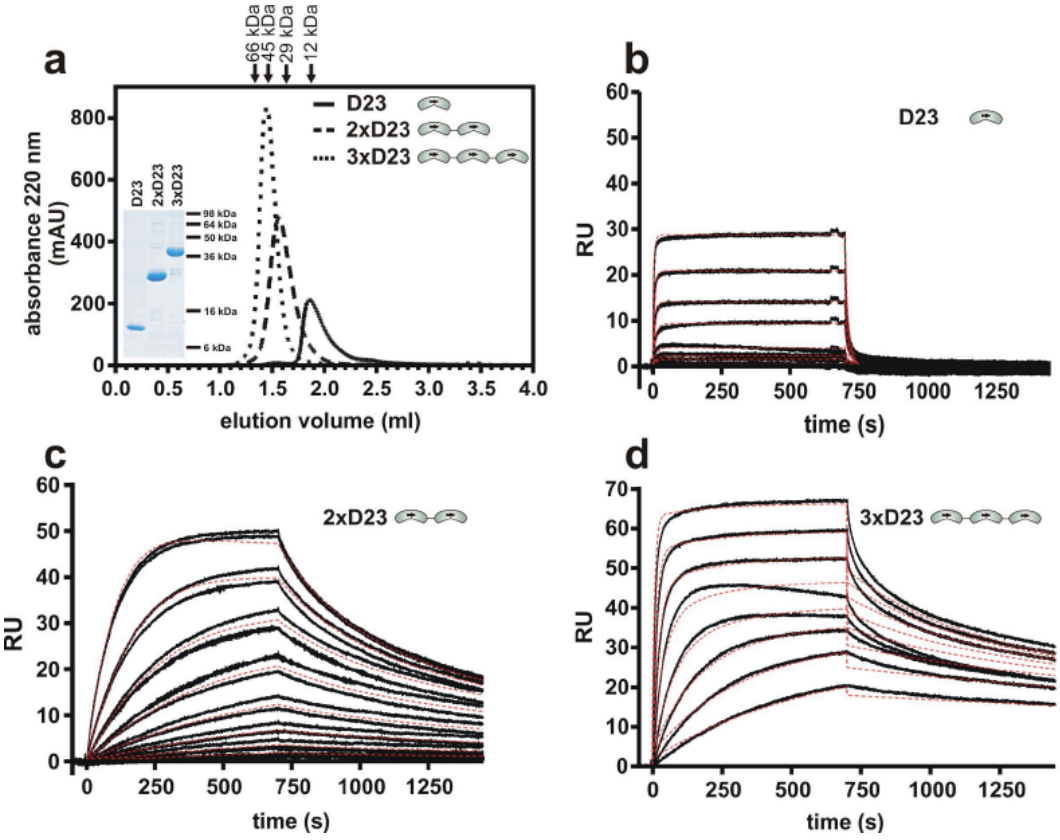

Figure 4**.** Multivalent DARPin constructs are stable and show improved binding to immobilized Aβ1-42. (a) Multivalent DARPin variants of D23 were constructed by fusing monovalent units by 10 AA long linkers. These constructs were well expressed and eluted as monomeric peaks from size exclusion chromatography with apparent molecular weights of 12 kDa (V_E=1.86 mL, D23), 30.4 kDa (V_E= 1.57 mL, 2xD23) and 44.3 kDa (V_E=1.45 mL, 3xD23). (b), (c) and (d) Surface plasmon resonance kinetics of mono-, bi- and trivalent DARPins on surface-immobilized Aβ1-42. (b) The C-terminally biotinylated peptide Aβ1-42 was immobilized on a streptavidin sensor chip and monovalent DARPin D23 was injected in duplicates at increasing concentrations of 1 to 128 nM. Association and dissociation phases were recorded and the kinetic rate constants k_{on} and k_{off} obtained by global fitting (red dotted lines) of the sensorgrams to a 1:1 binding model. The monovalent construct showed very fast on- and off-rates. Monovalent D23: k_{on} = 1.26 x 10^6 M^{-1} s^{-1}, k_{off} = 7.3 x 10^{-2} s^{-1}, K_D = 5.81 x 10^{-6} M. (c) Binding kinetics were similarly recorded 2xD23, but fitted to a bivalent binding model. Both on- and off-rates were decreased as compared to the monovalent construct. Bivalent 2xD23: k_{on1} = 3.72 x 10^4 M^{-1} s^{-1}, k_{on2} = 4.19 x 10^{-5}, k_{off1} = 2.8 x 10^{-3} s^{-1}, k_{off2} = 6.3 x 10^{-4} s^{-1}. (d) The trivalent construct 3xD23 displayed a comparable on-rate to D23 and a decreased off-rate. Trivalent 3xD23: k_{on1} = 4.03 x 10^5 M^{-1} s^{-1}, k_{on2} = 8.02 x 10^{-4}, k_{off1} = 1.3 x 10^{-3} s^{-1}, k_{off2} = 2.0 x 10^{-3} s^{-1}.

3.3.5 DARPin therapy improves cognition and lowers amyloid pathology

Two weeks after surgery, all mice underwent behavioral-testing. No differences in general health measures or any treatment-induced side effects were observed across all experimental groups (Supplementary Figures 6 and 7). Cognitive assessment in the Y-maze revealed a significant improvement in memory function upon treatment with both mono- and trivalent anti-Aβ DARPins, as compared to E2_5 and PBS treated control mice ($p<0.05$, Figure 5 A). The increase in spatial alternations could not be attributed to an increase in exploration, as the number of total arm entries and distance travelled did not differ between groups (data not shown).

Thioflavin S immunohistochemical analysis of brain sections revealed a treatment-induced trend towards less plaque deposition and size in both D23 and 3xD23 mice, as compared to E2_5 and PBS treated mice (Figure 5 B). Since Tg2576 mice only begin to deposit plaques at 11 months of age, these results provided the first evidence to investigate biochemically the effects of DARPins on amyloid levels in both soluble and insoluble fractions.

As a next step, we used MSD analysis to determine Aβ levels in two sequentially extracted protein fractions from hemi brain tissue (Figure 5 C-H). In agreement with our histological findings, D23 and 3xD23 treated mice showed a significant reduction of Aβ in the detergent soluble (RIPA soluble, Figure 5 C-E) protein fraction, as compared to E2_5 and PBS control mice. This trend was mirrored in the detergent insoluble (formic acid soluble, Figure 5 F-H) Aβ pool, though the effect was less pronounced.

These findings provide the first *in vivo* evidence that DARPins may successfully reverse Aβ-mediated cognitive deficits in a transgenic mouse model of brain amyloidosis and that the continuous infusion of DARPins can have a modulatory effect on brain Aβ levels.

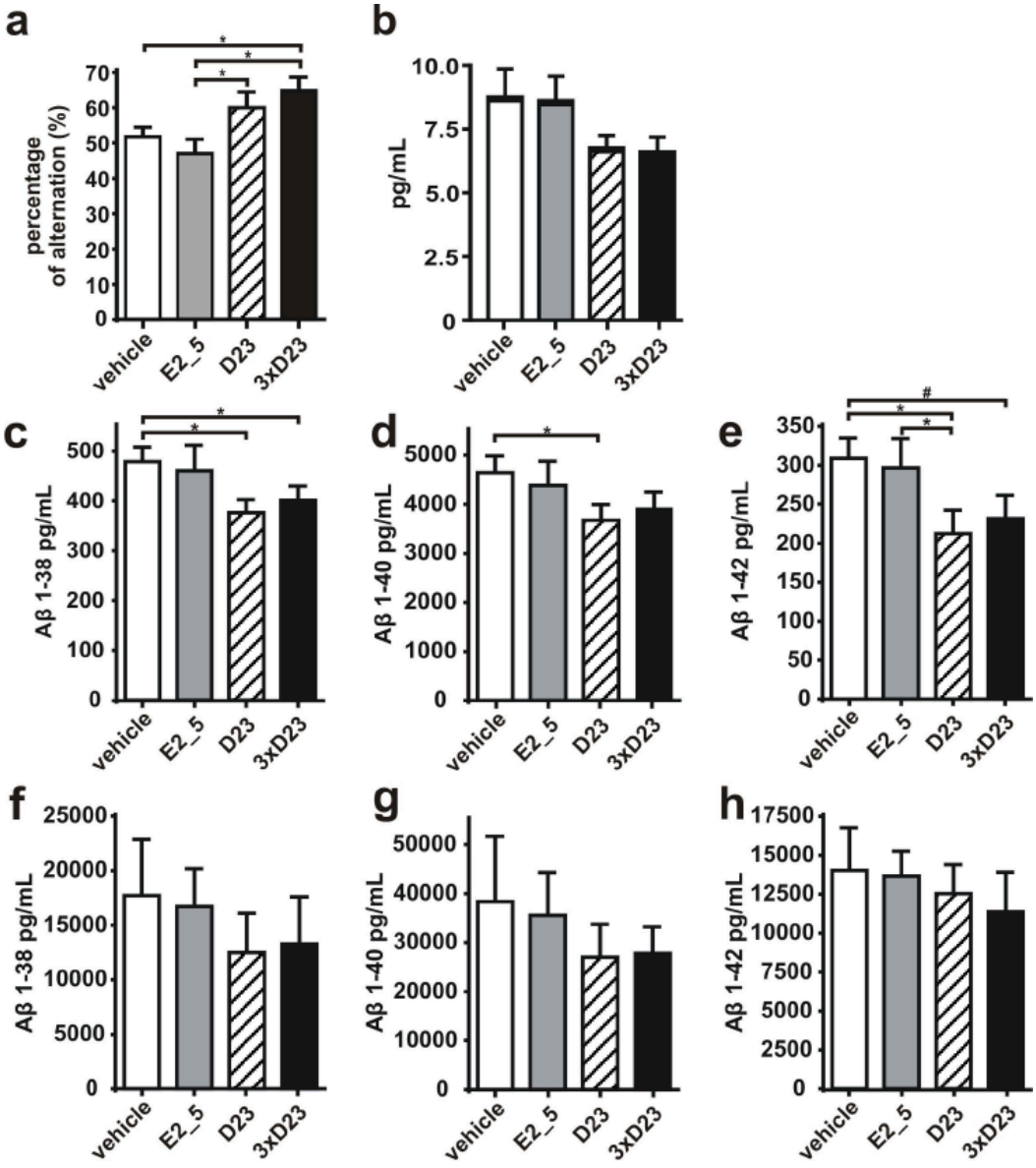

Figure 5. DARPin treatment restores memory deficits in APPSwe transgenic mice and influences soluble brain Aβ levels. (a) Two weeks after continuous intracerebroventricular infusion of mono- (fasciated) and trivalent (black) DARPins Tg2576 mice were cognitively assessed in a Y-maze experiment. Animals receiving anti-Aβ therapy performed significantly better than those animals receiving a non-specific DARPin (E2_5, grey) or PBS (white). (b) After four weeks of anti-Aβ therapy, animals were sacrificed and the brain cortical area covered by amyloid deposits determined. DARPin treatment appears to influence amyloid deposition, but does not reach significance. (c)-(h) Total levels of both soluble (RIPA, c-e) and insoluble (formic acid, f-h) brain Aβ1-38, Aβ1-40 and Aβ1-42 levels were measured. Levels of soluble Aβ1-38 in the CNS are significantly decreased for both the mono- and the trivalent DARPin and for Aβ1-40 and Aβ1-42 in case of the monovalent variant. Animals per group n = 10-12. Data shown as mean ± SEM. Statistical analysis by Mann Whitney U test; * $p<0.05$; # trend $p<0.10$.

3.4 Discussion

Ribosome display of combinatorial DARPin cDNA libraries have been utilized to select for DARPin binders against a diverse set of target proteins with characteristic three-dimensional folds, but not against peptide antigens (Baumann et al., 2010; Milovnik et al., 2009; Zahnd et al., 2007; DeMattos et al., 2001). In this study we were able to select, for the first time, a DARPin binder, termed D23, with nanomolar affinities for the Aβ peptide that showed superior binding characteristics in both direct and competition ELISA assays. D23 was, therefore, identified as the lead candidate for further characterization and to demonstrate the therapeutic potential of DARPins administered *in vivo* for the treatment of brain amyloidosis in APP transgenic mice.

Although the binding of D23 to surface-immobilized Aβ1-28 and Aβ1-42 was shown to be in the low nanomolar range, the physiologically more relevant specific binding to Aβ in solution needed to be clarified. Indeed, it has been shown that Aβ-binding macromolecules can display varying specificities for the quaternary structure of the peptide, ranging from soluble monomers (DeMattos et al, 2001), oligomeric intermediates (Kayed et al., 2003) to fibrillar states (O'Nuallain et al., 2002). A competition assay using freshly dissolved monomeric Aβ1-42 as competitor confirmed the observations made with surface-immobilized Aβ and suggested a K_I value of approximately 50 nM. This inhibition was specific, as the use of scrambled Aβ1-42 did not significantly reduce D23 binding to the surface-immobilized target (Figure 2 B). We had noticed that C-terminal amino acid extensions (longer than the 28 residues used for selection) resulted in slightly decreased affinities, but had no major influences on the binding properties of D23 to Aβ (Supplementary Figure 2). However, modifications at the peptide's N-terminus, such as the attachment of a biotin moiety, resulted in abrogation of the binding. Although we could not entirely exclude that this N-terminal modification had any influence on the structure of the Aβ monomer, the results likely indicate that the free N-terminus of the peptide must be involved in D23 binding. This was confirmed by an epitope mapping approach in which three monoclonal antibodies with distinct Aβ specificities were used to compete with D23 binding for Aβ. The strongest inhibition was demonstrated for 6E10, a monoclonal IgG recognizing Aβ residues 1-16, with less interference shown for 4G8, an antibody directed against the central domain of Aβ, thus suggesting D23 binding involves the N-terminus, as well as, parts of the central domain. These

findings were directly comparable as both the antibody concentrations and their affinities for the Aβ peptide were in similar order of magnitude (Ramakrishnan et al., 2009). More precise epitope mapping for D23 was investigated using a peptide scanning approach, which confirmed the N-terminus binding. However, not all fragments with a functional N-terminus displayed equal inhibition, with the highest inhibition observed when longer peptide variants were used such as Aβ1-16, Aβ1-28 and Aβ1-38, suggesting the recognition of a discontinuous rather than linear epitope. This observation is in accordance with previous findings that DARPins preferentially recognize three-dimensional, structural epitopes due to their intrinsic rigid scaffold that displays a relatively shallow and elongated binding interface (Binz et al., 2004; Schweizer et al., 2007; Stumpp et al., 2007).

To determine the binding characteristics of D23 *ex vivo*, we performed GFP-fused DARPin immunohistochemical analyses on brain tissue from a mouse model of AD (ArcAβ, Figure 2 C). The staining of amyloid deposits by D23 indicates that the missense mutation in the Arctic Aβ sequence did not markedly influence D23 binding. Moreover, when compared to anti-Aβ antibody stainings, D23 was found to bind preferentially the cross-β pleated dense central cores of the amyloid deposits. Such findings underscore D23's recognition of discontinuous amino acid stretches on both the N-terminal and central domain of the Aβ peptide that still exist in both the monomeric and aggregated form. Non-specific adherence of the hydrophobic internal DARPin scaffold to the 'sticky' amyloid plaques could be excluded as no tissue reactivity was observed with the non-specific E2_5 control DARPin. These findings suggest that the binding mode of D23 is fundamentally different from most monoclonal antibodies that recognize a linear stretch of both the Aβ peptide and APP. The absence of cross-reactivity to APP (data not shown) thus might prove advantageous for DARPin-based therapeutic purposes, as peripheral APP would be a scavenger that captures the majority of exogenously applied anti-Aβ DARPins.

As a first proof-of-principle, we were able to demonstrate *in vitro* using Thioflavin T (ThT) aggregation assays that D23 could delay Aβ aggregation in both a stirred cuvette-based (Figure 3 A) and quiescent microtiter plate assay (data not shown). As Thioflavin T only has limited affinity for β-sheets (Hudson et al., 2009; LeVine, 1993), we excluded that the addition of other exogenous compounds with higher affinities,

such as the DARPin scaffold, leads to a dissociation of the fibril-bound dye. The addition of D23 during log phase or after complete fibrillization did not lead to any decrease in ThT signal. We did however observe a dose-dependent inhibition of the aggregation process, when D23 was added during the lag phase of the ThT assay before a seeding of the aggregation process had occurred. This likely indicates that D23 binds to and stabilizes monomeric Aβ, thus excluding it from the aggregation process. As a further proof-of-principle, we were able to demonstrate that D23, but not E2_5 control DARPin, when administered into the medium of rat primary cortical neuron cultures could reduce Aβ-mediated neurotoxicity and preserve neuronal morphology (Figure 3 B). To optimize D23 binding behavior for potential therapeutic use, bi- and trivalent D23 DARPins were engineered by fusing two and three monovalent units of D23 into one continuous open reading frame. While these multivalent D23 DARPins showed similar structural integrity and binding to the Aβ peptide (Figure 4 A, Supplementary Figure 4), surface plasmon resonance kinetic analysis revealed differences in on- and off-rates for each individual construct. In particular, these findings suggest that the association kinetics of multivalent DARPins might be influenced by the sterical accessibility to the Aβ peptide rather than by their increased molecular weight and therefore limited diffusion. This is in contrast to previous publications where multivalent DARPin constructs did not show altered on-rates, presumably due to the use of a bulkier protein target that better enabled multi-unit DARPin recruitment (Eggel et al., 2009).The high off-rates of D23 indicate that the DARPin dissociates from its target in proportion to its association velocity limiting its affinity to a two-digit nanomolar range (Figure 4 B). An apparent increase of 2xD23 and 3xD23 in overall affinity is due to their built-in avidity allowing frequent re-binding to the sensor-surface. Overall, 3xD23 with its slightly decreased on-rate and strongly improved off-rate kinetics was identified as a lead candidate for targeting polymeric Aβ species such as oligomers or fibrils.

Finally, as a direct proof of therapeutic benefit, we were able to demonstrate the *in vivo* therapeutic potential of D23 and 3xD23 in Tg2576 mice. Following the direct intracerebroventricular infusion of mono- and trivalent DARPin constructs over 28 days treatment, D23 and 3xD23 treated mice showed improved cognitive performance, compared to E2_5 non-specific DARPin and PBS treated mice. These results were supported by immunohistochemical analyses with trends towards less

plaque deposition in both D23 and 3xD23 mice (Figure 5 B). However, as we infused anti-Aβ DARPins in Tg2576 mice at 11 months of age, the majority of the amyloid burden is still present in soluble Aβ forms explaining the limited number of amyloid deposits in the cortices of treated animals. This secondary preventative treatment paradigm was underscored by a biochemical analysis that showed further reductions of brain Aβ levels for both D23 and 3xD23 treated mice with the most pronounced modulatory effects on the soluble Aβ pool (Figure 5 C-E).

Our findings demonstrate the therapeutic potential of Aβ-specific DARPins for the treatment of Alzheimer's disease. With the advent of recombinant protein expression and efficient *in vitro* selection technologies, this novel class of engineered protein scaffolds present attractive opportunities for both diagnostic and therapeutic use.

3.5 Acknowledgements

We thank Wiebke Buck, Nadine Lucke and Anna Jeske for excellent technical support. This study was supported in parts by the Swiss National Science Foundation and the Forschungskredit grant of the University of Zurich.

3.6 Supplementary Material

General health, sensory-motor and mini-neurological examination. Mice were weighed and their coat appearance, handling responses and home cage social behavior registered. More specifically, coat appearance was assessed for matted, discolored fur, bald patches, missing whiskers, scarring, or wounds, which might otherwise indicate poor health, insufficient grooming, overgrooming and fighting. Unusual responses to handling including, extreme jumping, vocalizations, and attempts to bite the human handler may indicate poor health and were regarded as poor handling responses. Nesting patterns, sleeping in a huddle, allogrooming and normal social interaction behaviors were considered as good home cage social behaviors, whereas, social withdrawal or isolation, excessive fighting, over grooming was regarded as inappropriate home cage social behaviors. Any deviations from good coat appearance and appropriate handling responses and home cage social behavior would be regarded as poor health and scored as a fail, thus excluding the mouse from cognitive-behavioral testing. Successful righting reflex was recorded if the mouse was able to right itself when placed on its back and/or since mice able to right themselves often can't be placed on their backs, the inability to place the mouse on its back was considered successful righting as well. Grip strength was determined by placing the mouse on a grid and gently inverting the grid and observing whether or not the mouse was able to hold on will suspended upside down. The visual forepaw test involved holding the mouse by its tail at a height of about 15cm above a flat surface and noting the limbs held close to the body. As the mouse was gradually lowered to the surface, successful visual forepaw response was considered if the mouse extended its forepaws for a “soft landing” on the horizontal surface before or without the whiskers or nose touching. Acoustic startle reflex provides a good measure of gross hearing ability and was considered successful if the mouse displayed a flinch response to a loud hand clap. All abovementioned assessments were measured as a pass-or-fail or yes-or-no response by the human observer.

Supplementary figures

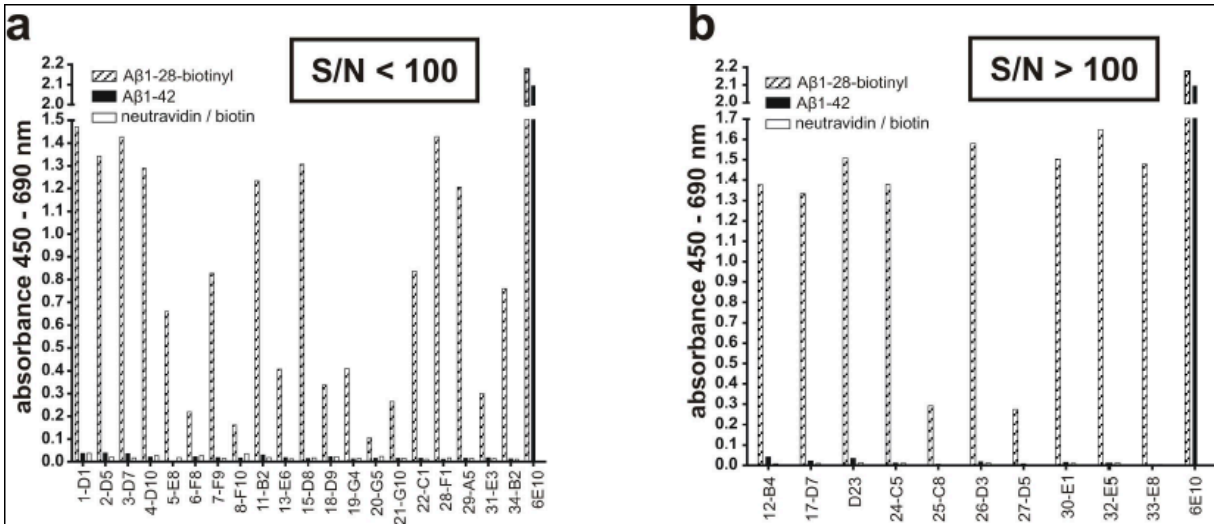

Supplementary figure 1 Results of post-selection screening ELISA. Lysates from several hundred clones were probed against Aβ peptides that either were directly immobilized on a microtiter plate (Aβ1-42) or bound on a previously coated neutravidin-layer (Aβ1-28-biotin). The thirty best binding signals are depicted. Bound DARPins were detected via an anti-RGS-hexahistidine antibody. Clones were subdivided into groups that showed a signal-to-noise ratio (S/N)<100 **(a)** or >100 **(b)**. Conformationally-insensitive Aβ1-42 immobilization (black bars) resulted in absence of DARPin binding to the plates. The monoclonal anti-Aβ antibody 6E10, used as positive control, does not differentiate between the immobilized Aβ species.

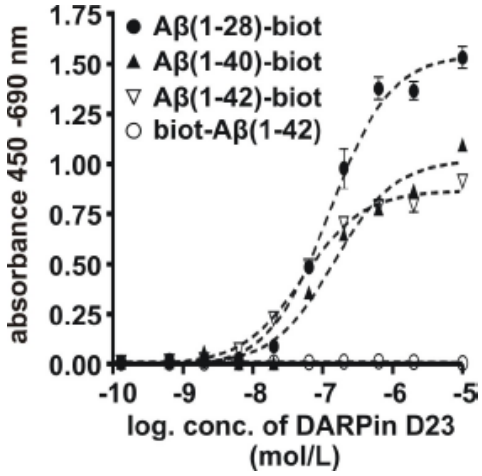

Supplementary figure 2 Influence of tag positions on the DARPin-Aβ interaction. Different Aβ species with biotin moieties at the N- or C-terminus of the peptide were immobilized via neutravidin on microtiter wells. D23 binding was probed at increasing concentrations on the different peptide coats. Bound DARPin was detected via an antibody directed against the N-terminal hexahistidine tag. The selected DARPin D23 binds longer peptide variants with slightly decreased affinity and shows total abrogation of the binding reaction if the biotin moiety is attached to the N-terminus of the peptide.

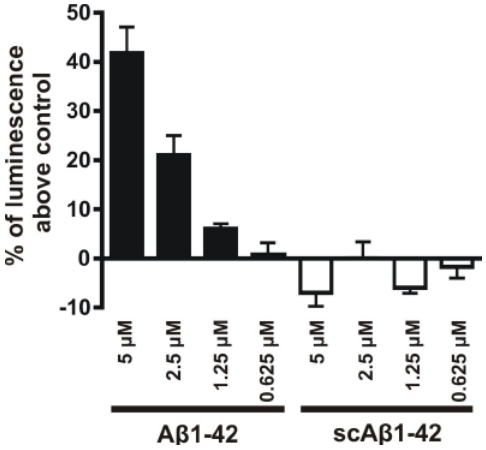

Supplementary figure 3 Determination of neurotoxic Aβ concentrations on primary neuronal cultures. Primary cortical neurons from rat embryos were taken into culture and incubated with increasing concentrations of recombinant Aβ1-42 or recombinant scrambled Aβ1-42 at DIV5 for 48 hours. The toxic effect of the peptides was determined by detecting protease activity released from damaged cells. Released proteases cleave a substrate that is subsequently used by a luciferase enzyme to emit light. Luminescence from vehicle-treated wells was subtracted as background correction. A dose-dependent neurotoxic effect for recombinant Aβ1-42 is observed, whereas the same concentration of scrambled Aβ1-42 does not produce any toxic effect above background.

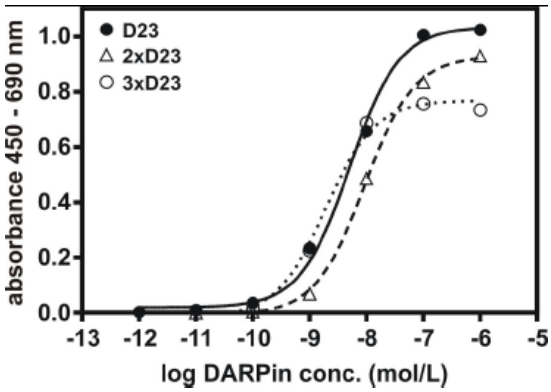

Supplementary figure 4 Multivalent DARPin constructs show minor improvements in anti-Aβ ELISA. The mono-, bi-, and trivalent variants of D23 were serially diluted and assessed for Aβ-binding affinity via ELISA. All D23 variants show activity in the nanomolar range as determined by a sigmoid dose-response curve fit (solid and dotted lines). The multivalent variants show a slightly decreased (2xD23) and a slightly increased (3xD23) affinity for immobilized Aβ, respectively, but a decreased maximal plateau.

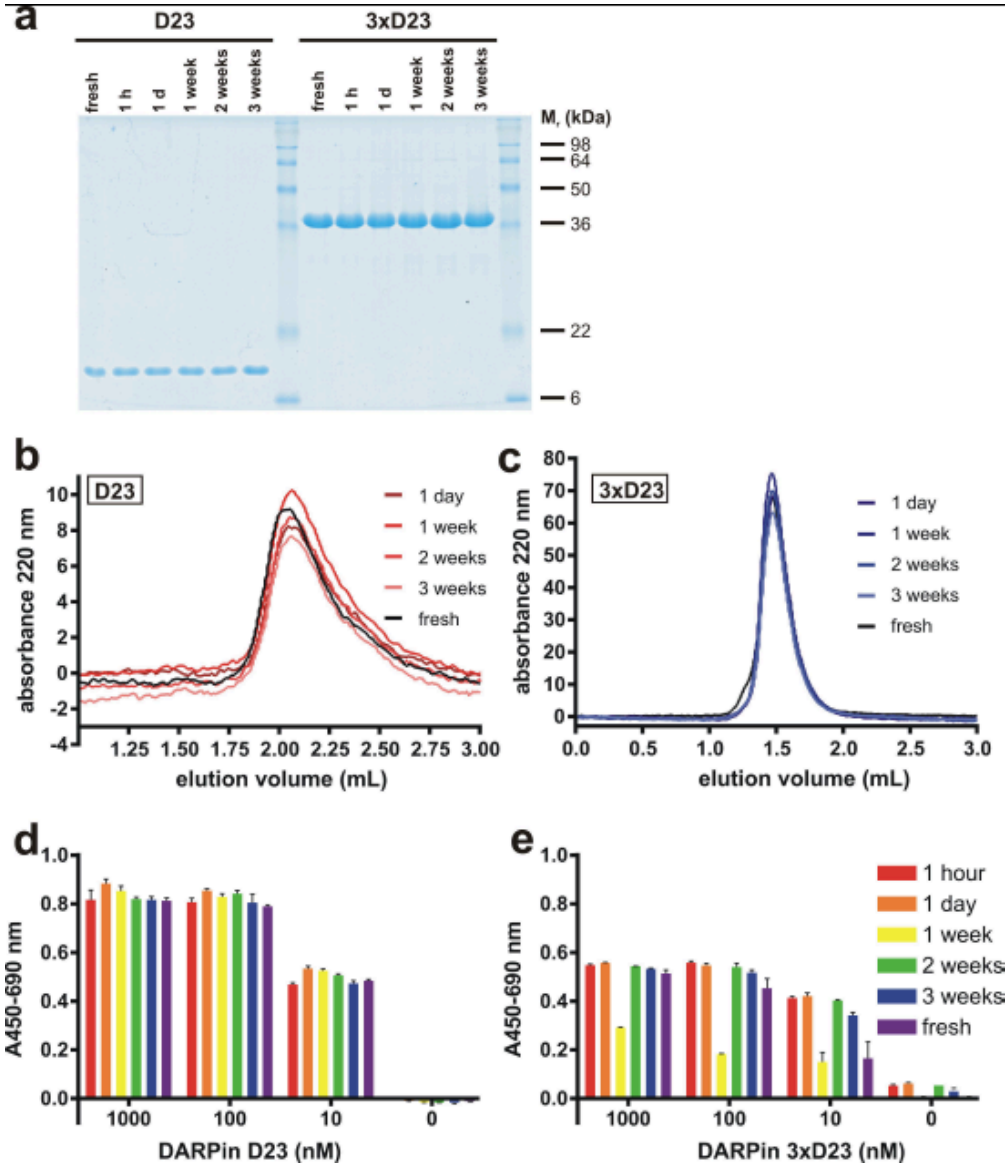

Supplementary figure 5 Long-term stability of selected DARPins in human serum and saline solution. **(a)** DARPins D23 and 3xD23 were incubated at 25 µM in PBS150 at 37°C and 5% CO_2 for 3 weeks. Samples were drawn at 1 hour, 1 day, 1 week, 2 weeks, and 3 weeks after incubation start and compared to freshly prepared samples. After mixing equivolumetric amounts of DARPin with loading buffer, the samples were subjected to SDS-PAGE and subsequently stained with Commassie Brilliant Blue. The molecular weight standard is shown in kDa. No degradation products can be detected. **(b)** Stability analysis of the DARPin D23 under native conditions using size exclusion chromatography. The samples were diluted to 2.5 µM in PBS and injected onto a gel filtration column. The respective peak heights and AUCs were compared to chromatograms of freshly prepared samples and showed less than 10% degradation during the observation time of three weeks. **(c)** Identical stability testing for the trimeric version 3xD23. **(d)** Functional analysis of D23 after stability challenge in human serum. The DARPin was diluted to 25 µM in 50 % human serum/PBS150 and incubated as described before. At each timepoint, the remaining DARPin activity, as measured in an anti-Aβ-binding ELISA, was quantified by performing a dilution series (1000, 100 and 10 nM) of the DARPin in triplicates. No significant loss of activity was observed even after 3 weeks serum incubation. **(e)** Same analysis as in **d** for the trimeric version 3xD23.

Supplementary Figure 6. General health, sensory-motor and mini-neurological examination. All experimental groups had normal coat appearances, appropriate handling responses and home cage behavior, intact visual-auditory function and normal basic reflexes, including visual forepaw response, acoustic startle and righting reflexes.

Experimental group	Aministration	Coat appearance	Handling response	Home cage behavior	Visual forepaw	Acoustic startle	Extension reflex	Righting reflex	Grip test
3xD23	ICV	good (20/20)	good (20/20)	good (20/20)	pass (20/20)	pass (20/20)	good (20/20)	pass (20/20)	pass (20/20)
D23	ICV	good (20/20)	good (20/20)	good (20/20)	pass (20/20)	pass (20/20)	good (20/20)	pass (20/20)	pass (20/20)
E2_5	ICV	good (23/23)	good (23/23)	good (23/23)	pass (23/23)	pass (23/23)	good (23/23)	pass (23/23)	pass (23/23)
vehicle	ICV	good (19/19)	good (19/19)	good (19/19)	pass (19/19)	pass (19/19)	good (19/19)	pass (19/19)	pass (19/19)

Supplementary Figure 7. Drop-outs and technical failures including, cannula misplacement or dislodgement or wrongful genotyping.

Experimental group	Aministration	Start (n)	Drop out	Technical failures	Finished
3xD23	ICV	20	2	6	12
D23	ICV	20	1	4	15
E2_5	ICV	23	5	4	14
vehicle	ICV	19	4	2	13

4

Intracellular fibrillar oligomers and late congophilic amyloid angiopathy in mice overexpressing the Osaka intra-Aß APP mutation

Luka Kulic, Jordan McAfoose, Tobias Welt, Christian Tackenberg, Claudia Späni, Fabian Wirth, Verena Finder, Uwe Konietzko, Maria Giese, Anne Eckert, Kinoshita Noriaki, Takahiko Shimizu, Kazuhiro Irie, Suhail Rasool, Charles Glabe, Christoph Hock & Roger M. Nitsch

Abstract

Pathogenic APP mutations clustered around position 693 of APP – position 22 of the Aß sequence – are commonly associated with congophilic amyloid angiopathy (CAA) and intracerebral hemorrhages. In contrast, the “Osaka” (E693Δ) intra-Aß APP mutation shows a recessive pattern of inheritance that leads to AD-like dementia despite low brain amyloid on *in vivo* PET imaging. Here, we investigated the effects of the “Osaka” APP mutation on Aß accumulation and deposition *in vivo* using a newly generated APP transgenic mouse model (E22ΔAβ) expressing the “Osaka” mutation together with the “Swedish” (K670N/M671L) double mutation. E22ΔAβ mice exhibited reduced α-processing of APP and early accumulation of intraneuronal fibrillar Aβ oligomers associated with cognitive deficits. In line with our *in vitro* findings, aged E22ΔAβ mice showed extracellular CAA deposits in leptomeningeal cerebellar and cortical vessels. *In vitro* results from Thioflavin T aggregation assays with recombinant Aβ peptides revealed a yet unknown anti-amyloidogenic property of the E693Δ mutation in the heterozygous state and an inhibitory effect of E22Δ Aβ42 on E22Δ Aβ40 fibrillogenesis. Moreover, E22Δ Aβ42 showed a unique aggregation kinetics lacking exponential fibril growth and poor seeding effects on wildtype Aβ aggregation. These results provide a possible explanation for the recessive trait of inheritance of the “Osaka” APP mutation and the apparent lack of amyloid deposition in E693Δ mutation carriers.

4.1 Introduction

Extracellular deposition of fibrillar amyloid-beta (Aβ) peptide as amyloid plaques and congophilic amyloid angiopathy (CAA) is considered a cardinal neuropathological feature of Alzheimer's disease (AD) (Thal et al., 2004; Thal et al., 2008). According to the "amyloid cascade hypothesis" soluble and fibrillar Aβ species play a central role in the pathogenesis of AD and start to accumulate in brain years before cognitive decline and dementia symptoms are observed (Hardy et al., 2002). Evidence supporting the "amyloid cascade hypothesis" comes from several sources including genetic studies of familial AD cases carrying mutations in the amyloid-beta peptide precursor (APP) gene and the presenilin genes (Hardy et al., 2002; Tanzi et al., 2005). Pathogenic mutations in the APP gene have been shown to influence the metabolism of the Aβ peptide in various ways. The "Swedish" double mutation (K670N/M671L), for example, located upstream of the Aβ N-terminus adjacent to the β-cleavage site, results in an increased production of both Aβ40 and Aβ42 species (Citron et al., 1992; Haass et al., 1995; Mullan et al., 1992), whereas mutations located at the γ-cleavage site of APP cause an increase of the Aβ42/Aβ40 ratio and, as a consequence of this, result in increased Aβ aggregation and deposition (Bugiani et al., 2010; Chartier-Harlin et al., 1991; Eckman et al., 1997; Goate et al., 1991; Murrell et al., 1991). The recently discovered E693Δ "Osaka" mutation in a Japanese pedigree (Tomiyama et al., 2008) is one of the six so-called "intra-Aβ" mutations clustered around the hydrophobic core of the Aβ sequence. Position 693 seems to be a critical site involved in pathogenic aggregate formation since mutations at or (±1) around this site including the "Dutch" (E693Q) (Levy et al., 1990), "Flemish" (E692G) (Hendriks et al., 1992), "Italian" (E693K) (Bugiani et al., 2010), "Iowa" (D694N) (Grabowski et al., 2001) and "Arctic" (E693G) (Nilsberth et al., 2001) mutations have been reported to result in an increase in total Aβ production (Haass et al., 1994) and – with the exception of the "Flemish" mutation – enhance Aβ aggregation and toxicity (Fraser et al., 1992; Murakami et al., 2003). Interestingly, all currently known intra-Aβ APP mutations – with the exception of E693Δ – have previously been shown to be "vasculotropic" and are characterized neuropathologically by prominent vascular amyloid deposition (Kumar-Singh et al., 2009).

Although neuropathological data have not been reported to date, homozygous carriers of the recessive “Osaka” APP mutation are believed to develop an AD-like clinical phenotype in the absence of relevant extracellular amyloid deposition as revealed by a very low signal on amyloid PET imaging (Tomiyama et al., 2008). *In vitro* experiments demonstrated enhanced oligomerization but no fibrillization of synthetic E22Δ Aβ40 and E22Δ Aβ42 preparations, suggesting that AD-like symptoms may be caused by the presence of synaptotoxic Aβ oligomers, rather than fibrillar Aβ, in the affected patients (Tomiyama et al., 2008). Consistent with these findings, synthetic E22Δ Aβ42 potently inhibited hippocampal long-term potentiation (LTP) (Tomiyama et al., 2008; Takuma et al., 2008) and induced synapse loss in mouse hippocampal slices (Suzuki et al., 2010). Further cell culture experiments and results from the recently reported E693Δ transgenic mouse model revealed enhanced accumulation of intraneuronal Aβ oligomers as a prominent feature of the “Osaka” APP mutation (Nishitsuji et al., 2009; Tomiyama et al., 2010; Umeda et al., 2011). E693Δ transgenic mice start to accumulate intraneuronal Aβ aggregates at an age of eight months and are completely devoid of extracellular amyloid deposits up to an age of 24 months (Tomiyama et al., 2010). The apparent lack of extracellular amyloid deposition in these mice has been suggested to be in line with the initial *in vitro* findings with synthetic Aβ preparations that E22Δ-mutated Aβ peptides do not form amyloid fibrils (Tomiyama et al., 2008).

Follow-up studies, however, revealed with recombinant Aβ preparations that both E22Δ Aβ40 and E22Δ Aβ42 readily formed amyloid fibrils *in vitro* (Suzuki et al., 2010; Inayathullah et al., 2011; Ovchinnikova et al., 2011). Based on these findings, we hypothesized that E22Δ-mutated Aβ may, in principle, also form amyloid fibrils *in vivo* and generated a novel APP transgenic mouse line (E22ΔAβ) to investigate the effects of the E693Δ mutation on amyloid accumulation and deposition *in vivo*. In line with our recent *in vitro* findings (Ovchinnikova et al., 2011), E22ΔAβ mice were characterized by a late but prominent extracellular amyloid deposition in the leptomeningeal vasculature at 24 months of age, which was preceded by an early accumulation of intracellular oligomeric Aβ species already at an age of three months. The results of this study provide strong evidence that E22Δ-mutated Aβ species are fibrillogenic, thus placing the E693Δ “Osaka” mutation on the list of other “vasculotropic” intra-Aβ APP mutations.

4.2 Materials and Methods

4.2.1 Animals

The newly generated E22ΔAβ mice express the human APP695 isoform containing the “Swedish” (K670N+M671L) and “Osaka” (E693Δ) mutations. The mutations were generated by site directed mutagenesis of pGEM-9zf(-)-huAPP695. The cDNA was inserted into pMoPrP-Xho (Borchelt et al., 1996), and the construct was sequenced. After removal of the vector sequence, the linear construct was injected into pronuclei of fertilized zygotes of B6D2F1 mice. Founders were screened for transgene expression by tail PCR and Western blot analysis, and the line used in this project was expanded on the hybrid background of C57Bl/6 and DBA/2 (B6D2). For all behavioral, biochemical and histological analyses offspring from the B6D2 generation backcrossed once with pure C57Bl/6 was used. Mice were kept on a 12 hour light/dark cycle at 22°C. Food pellets and water were available *ad libitum*.

For histological and Western blot analyses, mice at different ages were anesthetized and transcardially perfused with ice-cold PBS. One hemibrain was dissected into cortex and hippocampus, frozen in liquid nitrogen, and stored at –80°C. The other hemibrain was postfixed in 4 % (w/v) paraformaldehyde in PBS overnight at 4°C and embedded in paraffin.

All animal experiments were performed in compliance with Swiss national guidelines and were approved by the veterinarian authorities of the Canton of Zurich.

4.2.2 Protein extracts and Western blotting

Brain tissues were homogenized with a glass teflon homogenizer in a sixfold wet weight amount of “buffer A” containing 100 mM Tris-HCl, 150 mM NaCl, Complete Protease Inhibitor Cocktail (Roche Diagnostics) and Phosphatase Inhibitor Cocktails 1 + 2 (Sigma-Aldrich). After centrifugation at 100’000 g for 1 h supernatants were collected (=”Tris fraction”) and pellets were rehomogenized in buffer A containing 1 % Triton X-100. Centrifugation at 100’000 g was repeated and supernatants were again collected (=”Triton fraction”). The remaining pellets were rehomogenized in buffer A containing 2 % SDS. After an additional centrifugation step and collection of the supernatants (=“SDS fraction”) the resulting pellets were eventually dissolved in 70% formic acid (FA), sonicated for 30 sec at 30 % power, ultracentrifuged, supernatants extracted, lyophilized and reconstituted in buffer A containing 2 % SDS

for further analysis. Total protein concentrations were measured with the DC protein assay (BioRad Labs). Extracts were separated by SDS–PAGE, blotted onto nitrocellulose, boiled for 5 min in PBS, and blocked in TBS containing 5 % milk for one hour at room temperature. Primary antibodies were incubated overnight at 4°C (6E10 1:500; anti-C-terminal APP (Sigma) 1:2000) and visualized by peroxidase-conjugated antibodies and ECL reactions (Amersham Biosciences). Monoclonal anti-β-actin antibody (Abcam, 1:2000) was used as internal loading control and for normalization of densitometric analyses of the immunoreactive bands. Quantification of the immunoreactive bands was carried out by densitometry of the scanned films under conditions of non-saturated signal using the Image J software.

4.2.3 MSD analysis

Aβ fragments were measured in above mentioned brain homogenate fractions using an MSD 3plex multi-SPOT Aβ human kit (MesoScale Discovery, USA) for $Aβ_{38}$, $Aβ_{40}$ and $Aβ_{42}$, in accordance to manufacturer's instructions. Human sAPPα levels were determined using an MSD 2plex kit, and human Swedish sAPPβ levels were determined using an MSD 1plex kit, in accordance to manufacturer's instructions. MSD SECTOR Imager 6000 reader was used for analysis and the MSD DISCOVERY WORKBENCH software (Version 3.0.17) with Data Analysis Toolbox was used to calculate sample concentrations by comparing them against a standard curve (five-parameter logistic curve).

4.2.4 Histological analysis

Histological stainings were done on 5 µm paraffin brain sections by using standard published procedures. For the immunohistochemical detection of intraneuronal Aβ deposits, sections were boiled in 10 mM Sodium Citrate Buffer pH 6.0, followed by antigen retrieval with 95 % formic acid for five minutes. The following antibodies were used for immunohistochemistry: 6E10 (Signet, 1:500 dilution) and β-Amyloid Antibody (Cell Signaling, 1:200 dilution) were used for the detection of pan-Aβ. Anti-β-Amyloid Protein (1-40) antibody (Sigma, 1:100) and BA27 (Wako, Amyloid β-Protein Immunohistostain Kit) were used to specifically detect Aβ40. Beta Amyloid 42 Polyclonal Antibody (Signet, 1:100) and BC05 (Wako, Amyloid β-Protein Immunohistostain Kit) were used to specifically detect Aβ42. Polyclonal antibodies

A11 and OC (C. Glabe, both 1:100) were used for the detection of prefibrillar and fibrillar Aβ oligomers, respectively. 11A1 (IBL Japan, 1:100) was used to detect Aβ with a conformational turn epitope between positions 22 and 23 of the Aβ sequence (Murakami et al., 2010). Anti-Amyloid Precursor Protein, C-Terminal antibody (Sigma, 1:200) was used for the detection of full length APP and APP C-terminal fragments. Secondary antibodies were obtained from Vector Laboratories (Vectastain ABC kits PK-6101 and PK-6102) for peroxidase-diaminobenzidine stainings, and from Jackson Immunoresearch Laboratories (West Grove, PA) for immunofluorescence.

Thioflavin S staining and Congo red stainings were performed according to standard protocols as previously described (Knobloch et al., 2007).

4.2.5 Recombinant Aβ production

Production of recombinant Aβ peptides (wildtype Aβ40 and Aβ42, E22Δ Aβ40 and Aβ42, and E22G Aβ40 and Aβ42) was performed as previously described (Finder et al., 2010). In brief, recombinant Aβ peptides were expressed under the control of the T7 promoter/lac operator in *E. coli* BL21 (DE3) as fusion proteins to the peptide sequence $(NANP)_{19}$ with an N-terminal hexahistidine tag. Mutagenesis at codon 22 in both Aβ1–40 and Aβ1–42 was performed with the QuikChange site directed mutagenesis kit (Stratagene). The correct genetic sequences of the constructs were verified by DNA sequencing. Cleavage of the fusion proteins (100 μM) with 7.5 μM tobacco etch virus protease (TEV) was performed in 10 mM Tris–HCl (pH 8.0), 0.5 mM ethylenediaminetetraacetic acid, and 1 mM DTT for 1 h at room temperature, followed by incubation at 4 °C overnight. The cleaved Aβ peptides precipitated during the cleavage reactions and were pelleted by centrifugation (4500 g, 20 min, 4 °C), dissolved in 6M guanidinium chloride–HCl (pH 2.0), and purified via reversed-phase high-performance liquid chromatography. Peptides were eluted with CAN, aliquoted in Protein LoBind Eppendorf tubes (Vaudaux-Eppendorf), lyophilized, and stored at −80 °C. The high purity and identity of the peptides were verified by matrix-assisted laser desorption/ionization time-of-flight mass spectrometry using sinapinic acid as matrix.

4.2.6 Thioflavin T aggregation assays

Preparation of Aβ solutions and Thioflavin T aggregation assays were performed as described earlier (Finder et al., 2010; Ovchinnikova et al., 2011). In brief, Aβ variants were dissolved in 10 mM NaOH to concentrations of 100–150 µM. Aβ concentrations were determined via the absorbance of Aβ at 280 nm in 10 mM NaOH (extinction coefficient at 280 nm and pH 12 corresponding to a single tyrosine residue: 1730 M^{-1} cm^{-1}). Stock solutions were kept on ice and were used for aggregation experiments within 6 h. Aggregation reactions were performed at 37 °C with 2.5 or 5 µM Aβ (final concentration) in 10 mM H_3PO_4–NaOH (pH 7.4), 100 mM NaCl, and 35 µM Thioflavin T in a volume of 1000 µl in stirred quartz fluorescence cuvettes (1 cm—0.4 cm). The Thioflavin T concentration was determined via its extinction coefficient of 36,000 $M^{-1}cm^{-1}$ at 412 nm. Aggregation reactions were started by a dilution of the Aβ stock solution in 10 mM NaOH (prepared and ultracentrifuged immediately before use) with an aggregation buffer mix, resulting in pH 7.4 and the final concentrations indicated above. Thioflavin T fluorescence emission at 482 nm (excitation at 440 nm; excitation and emission slit: 1.6 nm) was monitored on a Quantamaster (QM-7/2003) fluorescence spectrometer (Photon Technology International).

4.2.7 Cognitive-behavioral testing

A battery of well-validated and carefully controlled tests was used to behaviorally assess mice for motoric and cognitive performance (Crawley, 2007). At the time of testing, mice were weighed and examined for general health measures to ensure that the mice were physically able to conduct the cognitive-behavioral test.

Locomotor activity in the Open Field Test

According to published procedures mice were placed in the center of a brightly lit white Plexiglas box (50x50cm), and their movements (distance traveled and average speed) were tracked using ANY-maze video tracking software (Stoelting Co., USA) for 5 min.

Y-Maze

Spatial working memory was assessed in mice using the Y-Maze (Y-shaped plastic maze, with 40 cm x 20 cm x 10 cm arm sizes). During a five-minute trial, the

sequence of arm entries was recorded using the ANY-maze Video Tracking System (Stoelting Co., USA). The percentage alternation was calculated as the ratio of actual to possible alternations (defined as the total number of arm entries -2) x 100%.

Barnes Maze

The Barnes Maze was used to assess hippocampus-dependent spatial learning and memory (Paul et al., 2009). The Barnes Maze consists of a grey, acrylic, circular disk 91 cm in diameter with 20 equally spaced holes (5-cm diameter) located 1.5 cm from the edge, and elevated 90 cm above the floor. The platform was illuminated by a 100 W electric bulb located 110 cm above the center of the maze (150 Lux), thus providing motivation for the animals to avoid the open surface and escape into a small dark recessed chamber (escape box) located under the platform. The inclusion of false boxes that look the same as the target escape box but are too small to be entered, were used to remove visual cues that might allow the mouse to discriminate the location of the escape hole from the other holes. A cylindrical plastic start chamber (10.5 cm diameter, 9.5cm height) was used to hold mice in the middle of the maze at the start of each trial. A web camera (Logitech) was placed 1.2 m above the center of the maze to record trials using the ANY-maze Video Tracking System (Stoelting Co., USA). Distinct spatial cues placed in a constant location around the maze served as a reference point to learn the position of the escape hole.

Mice completed four days of acquisition training with four trials per day with an inter-trial interval of 10-15 minutes. For each trial, mice were placed in the start chamber in the middle of the maze and after 10 seconds, the start chamber was raised to start the trial and the mouse was allowed to explore the maze for three minutes. During these three minutes the latency to enter the escape box, distance travelled, speed, time spent immobile and search strategy used was measured, among other parameters. The trial ended when the mouse successfully entered the escape box or after the three minutes had elapsed. If a mouse did not successfully enter the escape box during the three minutes it was placed back at the start position and gently guided to the escape hole, where the mouse remained in the escape box for one minute. At the end of each trial, mice were returned to their holding cage until the next trial. To reduce intra-maze odor cues, the maze surface and escape box were cleaned with 70% ethanol after each trial. Search strategies were determined

by examining individual track plots for each mouse per day and classifying their ability to find the escape location as either; 1) random search strategy – search patterns that cross through the center of the maze in a completely random fashion, 2) serial search strategy – in which mice search every hole or every other hole in a clockwise or counterclockwise systematic fashion, or 3) spatial search strategy – in which the mice were able to locate the escape box directly plus or minus two adjacent holes within the target quadrant only.

4.2.8 Statistical analysis

Data analysis was performed using the Statistica 10.0 and SPSS 19.0 statistical software. Tests for normal distribution were performed before statistical testing, according to the results of the Shapiro-Wilk and the Kolmogorov-Smirnov Test for normality, either Student's t Test or Mann-Whitney U Test for 2 sample groups or ANOVA was performed (followed by post-hoc Fischer LSD analysis). A p-value < 0.05 was considered statistically significant. Error bars are SEM.

4.3 Results

4.3.1 Transgene expression and APP processing

The newly generated E22ΔAβ mice overexpress the human APP695 isoform containing the "Swedish" (K670N + M671L) and "Osaka" (E693Δ) mutations. The "Swedish" double mutation was introduced to increase the amount of total secreted Aβ without affecting the Aβ42/Aβ40 ratio. Several transgenic founder lines were analyzed for brain expression of the full length human APP transgene, and a line expressing comparable transgene levels to our APP transgenic arcAβ mouse model (overexpression of the "Swedish" and "Arctic" (E693G) mutations) and the widely established Tg2576 AD mouse model (overexpression of the "Swedish" mutation alone) was chosen for further analysis (Figure 1 A). Western blot analysis of SDS extracts revealed similar full length APP and β-stub (C99) levels in the E22ΔAβ, arcAβ and Tg2576 mice (Figure 1 A). α-stub (C83) levels, however, were significantly reduced in both E22ΔAβ and arcAβ mice as compared to Tg2576 mice (Figure 1 A). MSD analysis of soluble APP levels from SDS brain extracts revealed a two- to threefold reduction in sAPPα levels in the E22ΔAβ and arcAβ mice. In

contrast, sAPPβ levels were comparable to the Tg2576 mice (Figure 1 B). These findings indicate that both intra-Aβ APP mutations at position 22 of the Aβ sequence specifically interfere with the α-secretase processing of APP *in vivo*.

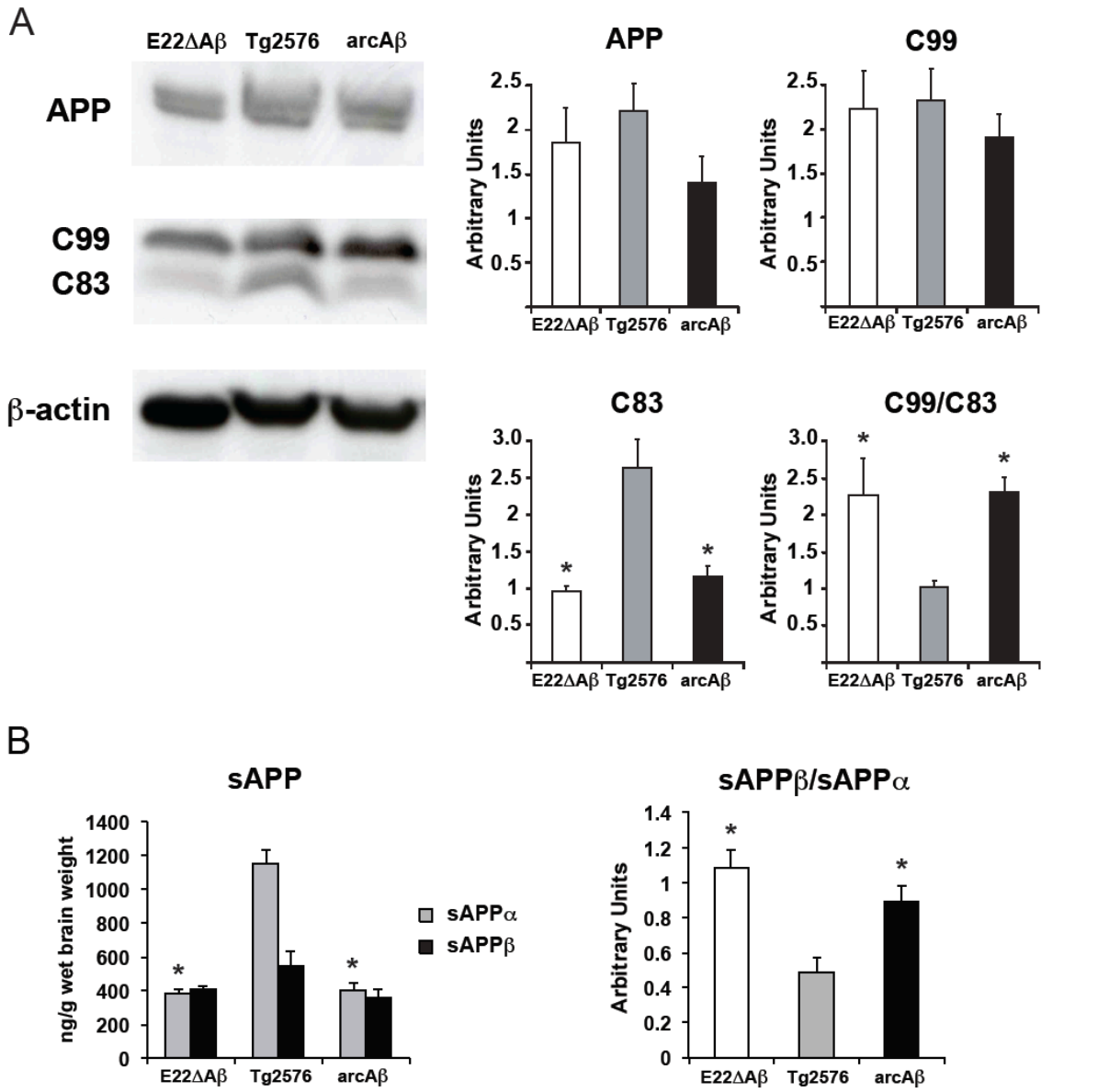

Figure 1. Transgene expression and APP processing. A, Western blot analysis of cortical SDS extracts from three month-old E22ΔAβ mice in comparison with age-matched Tg2576 and arcAβ mice. A C-terminal specific APP antibody (Sigma) was used for the detection of full length APP and APP C-terminal fragments (C99 and C83). Values were quantified and normalized to the loading control (β-actin). Quantification reveals no significant differences in full length APP and β-stub (C99) levels among the three mouse lines. α-stub (C83) levels, however, are significantly reduced and the C99/C83 ratio is increased in the E22ΔAβ and arcAβ mice as compared to the Tg2576 mice. * $p < 0.05$ E22ΔAβ and arcAβ versus Tg2576 (Mann-Whitney U Test). n = 4 per group. B, MSD analysis of sAPPα and sAPPβ levels in cortical samples extracted with Tris buffer containing 2 % SDS. In accordance with the results of the APP CTF analysis, sAPPβ levels were not significantly different among the three APP transgenic mouse lines, whereas sAPPα was reduced almost threefold in the E22ΔAβ and arcAβ mice as compared to the Tg2576 mice. * $p = 0.001$ E22ΔAβ and arcAβ versus Tg2576 (Mann-Whitney U Test). n = 6-8 per group.

4.3.2 Age-dependent changes in Aβ levels

As a next step, we used MSD and Western blot analysis to determine Aβ levels in four sequentially extracted protein fractions from cortical brain tissue (Figure 2). In agreement with previous findings (Hsiao et al., 1996; Kawarabayashi et al., 2001; Knobloch et al., 2007), Tg2576 and arcAβ mice showed an age-dependent exponential accumulation of Aβ in detergent insoluble (formic acid soluble) protein fractions (Figure 2 E-K) that accompanied the occurrence of parenchymal amyloid deposits in these mouse models (data not shown). Aβ accumulation occurred earlier and was more pronounced in the arcAβ mice as compared to age-matched Tg2576 mice (Figure 2 E-K), as previously reported in immunohistological findings (Hsiao et al., 1996; Knobloch et al., 2007). In contrast, most of the Aβ in the E22ΔAβ mice accumulated in the SDS (detergent-soluble) protein fraction up to the age of 15 months (Figure 2 A-C). MSD analysis of Tris buffer and Triton X-100 (mild detergent) extracts in the E22ΔAβ mice revealed only very low Aβ levels as compared to the Tg2576 mice (Figure 2 A-C). In addition, E22ΔAβ mice (similar to the arcAβ mice) showed four- to fivefold lower plasma Aβ levels than the Tg2576 mice (Supplementary Figure 1). These results indicate that the lack of accumulation of detergent insoluble (formic acid soluble) Aβ in the E22ΔAβ mice up to the age of 15 months was not accompanied by a relative increase in “soluble” brain or peripheral (plasma) Aβ levels. Western blot analysis of the four protein fractions at 15 months further confirmed the MSD findings (Supplementary Figure 2). At 24 months of age, however, a substantial increase in detergent insoluble (formic acid soluble) Aβ was observed in the E22ΔAβ mice (Figure 2 D). This change in Aβ solubility provided the first biochemical evidence for a substantial accumulation of fibrillar amyloid deposits in aged E22ΔAβ mice.

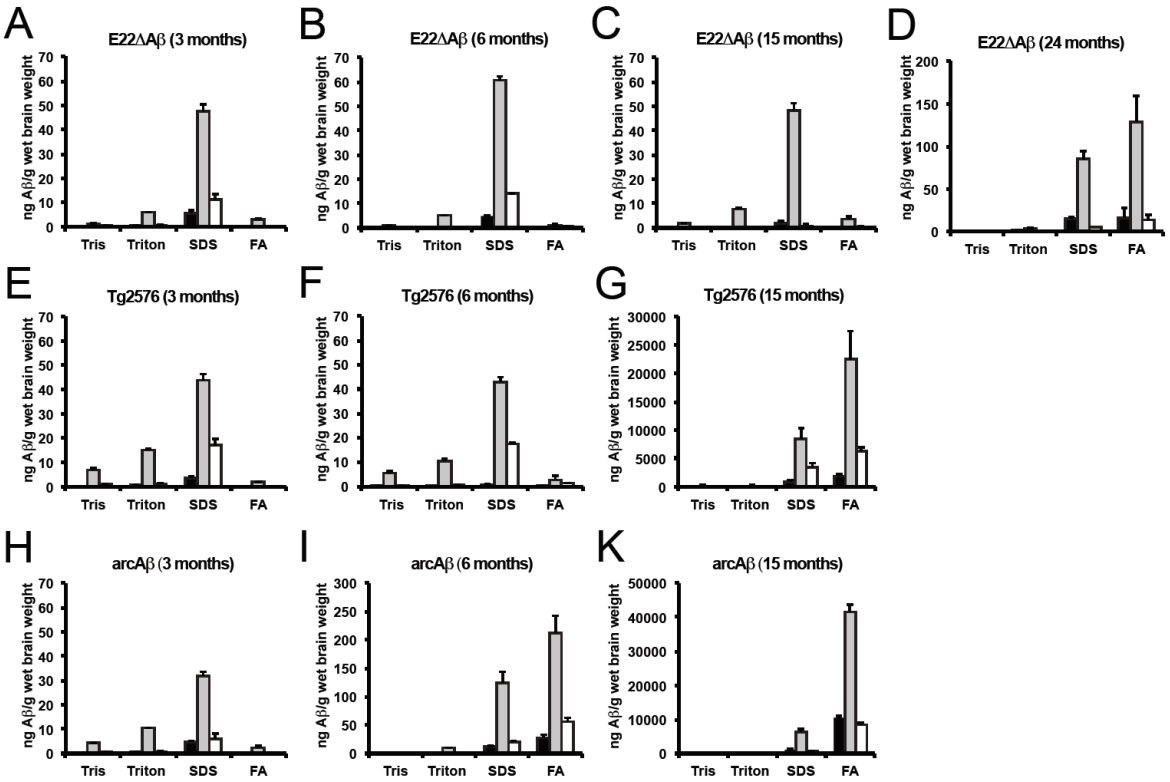

Figure 2. MSD analysis of Aβ38 (black column), Aβ40 (grey column) and Aβ42 (white column) in cortical samples serially extracted with Tris buffer, Tris buffer containing 1 % Triton, Tris buffer containing 2 % SDS and formic acid (FA). A-D, In E22ΔAβ mice most of the Aβ can be detected in the SDS soluble protein fraction up to the age of 15 months whereas Tris buffer soluble, Triton soluble and FA soluble Aβ levels are comparatively low. In 24 month-old E22ΔAβ mice, however, detergent insoluble FA Aβ D-F, In contrast, Tg2576 mice show higher (Tris and Triton) soluble Aβ levels and a prominent age-dependent Aβ accumulation in the detergent insoluble FA fraction at 15 months. **G-I**, Three month-old arcAβ mice show intermediate Tris and Triton soluble Aβ levels (as compared to age-matched E22ΔAβ and Tg2576 mice) and early accumulation of FA Aβ (already at the age of six months). n = 6-9 per group.

4.3.3 Absence of amyloid plaque deposition and late congophilic amyloid angiopathy (CAA)

Immunostainings of paraffin-embedded brain sections from aged E22ΔAβ mice with Aβ-specific antibodies showed no evidence of extracellular parenchymal amyloid deposition up to an age of 15 months (Figure 3 A,B). At 24 months of age, however, prominent vascular amyloid deposits were observed in cortical and – more pronounced – cerebellar leptomeningeal vessels (Figure 4). Vascular amyloid deposits were Thioflavin S (Figure 4 C-E) and Congo red positive (Figure 4 F,G) and were immunostained with several Aβ-specific antibodies (Figure 4 A,B,H,I). Immunostainings with Aβ40- and Aβ42-specific monoclonal antibodies revealed that

Aβ40 was the dominant Aβ species deposited in the vessel walls of the E22ΔAβ mice (Figure 4 H,I).

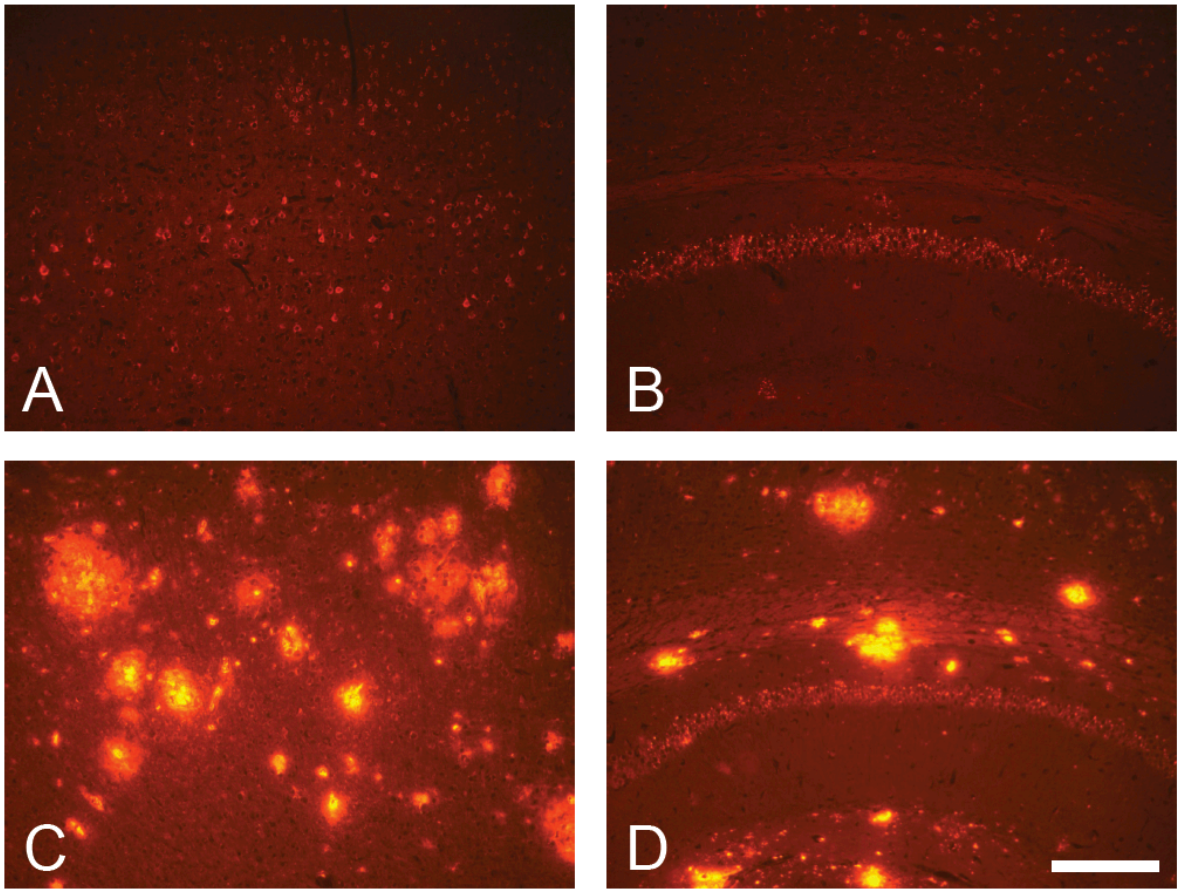

Figure 3. Lack of amyloid deposition in 15 month-old E22ΔAβ mice. A-D, Immunostaining with antibody 6E10 reveals a complete absence of extracellular amyloid deposits in 15 month-old E22ΔAβ mice (A: cortex; B: hippocampus). In contrast, arcAβ mice show a massive extracellular amyloid deposition at that age (C: cortex; D: hippocampus). Scale bars: 250 mm (A-D).

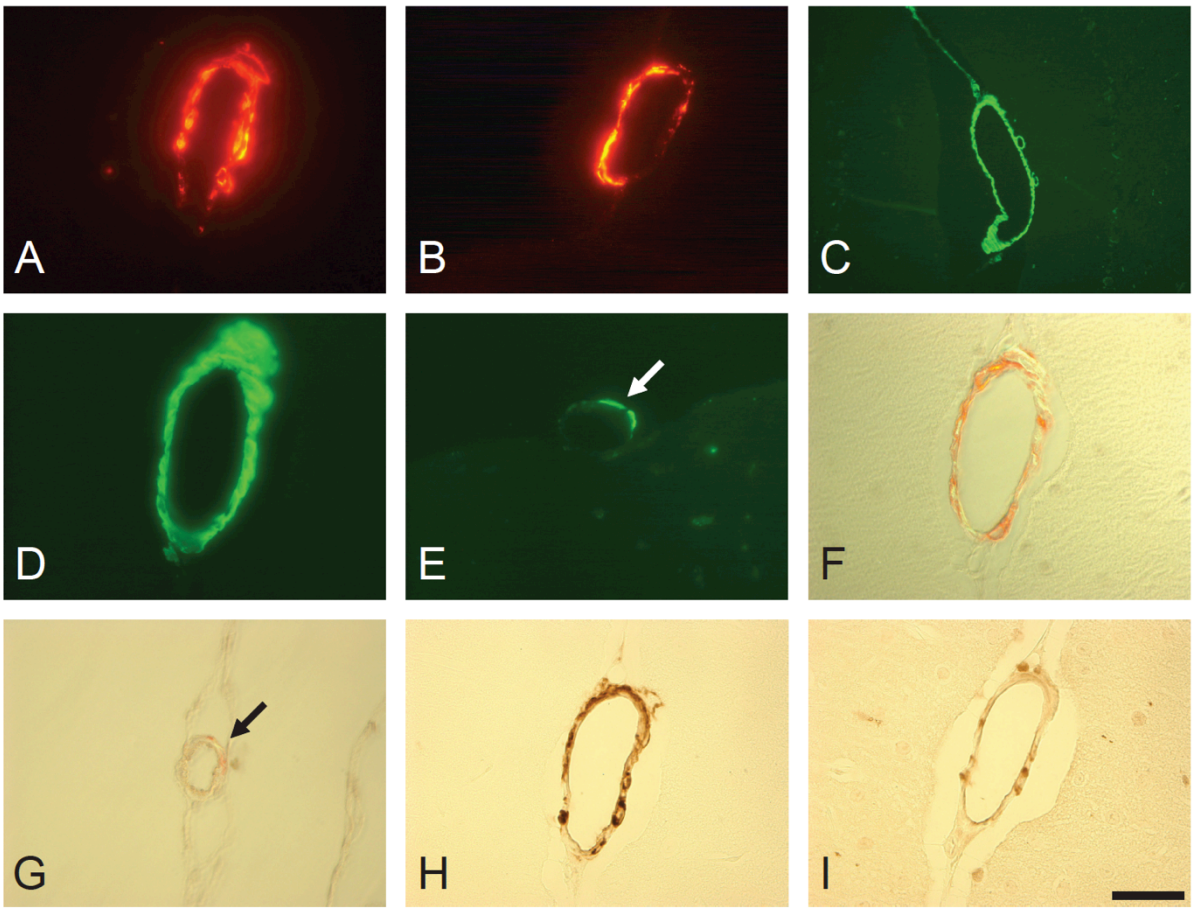

Figure 4. Aged E22ΔAβ mice develop congophilic amyloid angiopathy (CAA) at 24 months. A+B, Immunostaining of amyloid-laden leptomeningeal vessels with polyclonal anti-amyloid antibody directed against human pan-Aβ in the cortex (A) and cerebellum (B) of a 24 month-old E22ΔAβ mouse. C+D, Vascular amyloid deposits are Thioflavin S (C) and Congo red positive (D). Note the classical apple-green birefringence of Congo red stained vessels under polarized light (D). E+F, Immunostainings with Aβ40-specific monoclonal antibody BA27 (E) and Aβ42-specific monoclonal antibody BC05 (F) reveal that Aβ40 is the dominant Aβ species deposited in the vessel walls. Scale bars: 125 mm (A+B), 40 mm (C-F).

4.3.4 Early accumulation of intracellular Aβ oligomers

Although extracellular (vascular) amyloid deposits were detectable in the E22ΔAβ mice only as late as at the age of 24 months, immunostaining of paraffin-embedded brain sections with the monoclonal antibody 6E10 revealed prominent intraneuronal accumulation of dot-like aggregates mainly in hippocampal CA1 (Supplementary Figure 3 A) and cortical (Supplementary Figure 3 B) neurons that were observed already at the age of three months (data not shown). Double immunostaining with a polyclonal antibody directed against the APP C-terminus (Supplementary Figure 3 C,D) showed little colocalization of 6E10 and APP immunoreactivity in the cortex and hippocampus (Supplementary Figure 3 E,F) thus excluding 6E10-positive aggregates as full length APP or APP C-terminal fragments. Immunostaining with

Aβ-specific antibodies directed against the C-terminus of Aβ40 and Aβ42 confirmed that the intraneuronal deposits indeed corresponded to Aβ aggregates (Supplementary Figure 3 G-K). Interestingly, immunostaining with the Aβ40-specific antibody led to a more diffuse staining of both dot-like aggregates and neuronal cell bodies and processes (Supplementary Figure 3 G,H) whereas the Aβ42-specific specifically stained compact intraneuronal aggregates (Supplementary Figure 3 I,K).

Further characterization of the intraneuronal Aβ aggregates in the E22ΔAβ mice with several oligomer-specific (conformation-dependent) antibodies revealed that the dot-like Aβ deposits were strongly stained by the polyclonal OC antibody directed against fibrillar Aβ oligomers (Kayed et al., 2007) (Figure 5 A-D), but not the A11 antibody directed against prefibrillar oligomers (Kayed et al., 2003) (data not shown). OC-immunoreactive intraneuronal deposits were observed in CA1 hippocampal and cortical neurons as early as three months of age and appeared to grow and become more compact as the mice aged (Figure 5 A-D). Strikingly, the intraneuronal oligomeric Aβ deposits were also recognized by 11A1 (Figure 5 E,F), a novel conformation-dependent monoclonal antibody specifically designed against the turn between positions 22 and 23 of the Aβ sequence. 11A1 has recently been shown to stain intraneuronal Aβ aggregates in brains of AD patients but not APP transgenic mice (Murakami et al., 2010).

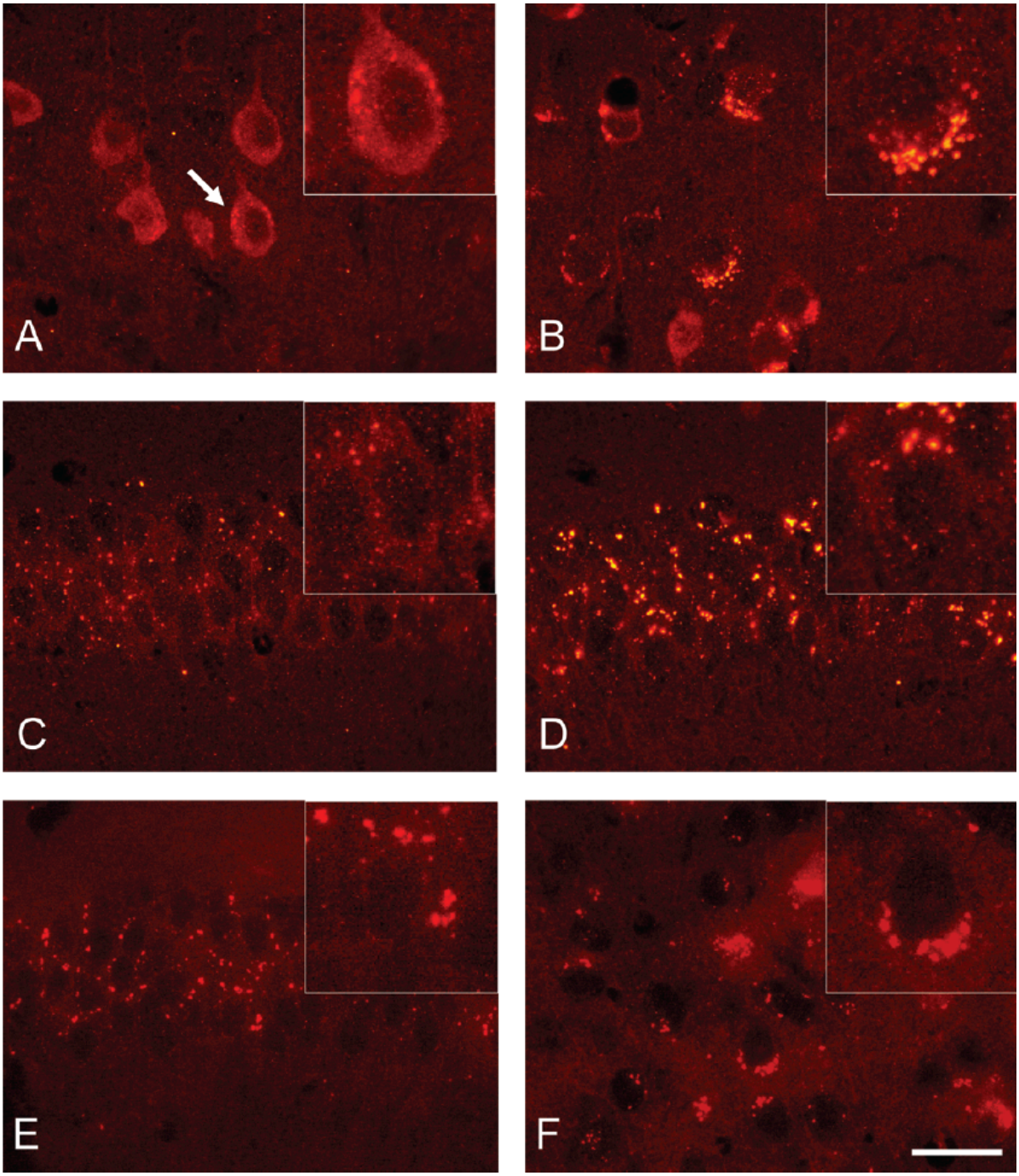

Figure 5. Intraneuronal Aβ consists of fibrillar oligomers bearing a “toxic turn” conformation. A-D, Immunostaining with polyclonal OC antibody directed against fibrillar Aβ oligomers reveals age-dependent accumulation of intracellular oligomeric deposits in cortical (A,B) and CA1 hippocampal neurons (C,D). Note the temporal change of intraneuronal oligomers from rather diffuse and smaller dot-like aggregates at three months of age (A,C) to bigger and more compact deposits at 15 months of age (B,D). E,F, Conformation-dependent monoclonal antibody 11A1 directed against the turn between positions 22 and 23 of the Aβ sequence stains hippocampal (E) and cortical (F) intraneuronal aggregates (representative immunostaining in a 15 month-old E22ΔAβ mouse). Scale bar: 40 mm (A-F).

4.3.5 Early cognitive deficits in transgenic E22ΔAβ mice

Based on our previous findings in the arcAβ mouse model in which intracellular Aβ deposits occurred concomitantly with robust cognitive deficits, we hypothesized that the early accumulation of intraneuronal oligomeric Aβ deposits particularly in hippocampal brain regions of the E22ΔAβ mice would also be accompanied by significant impairments on several cognitive tasks. Both E22ΔAβ mice and wildtype littermates displayed, across all age groups, similar general health measures, auditory-visual sensory integrity, comparable grip strength, intact righting and extension reflexes (data not shown). Assessment of body weight, demonstrated equivalent body weights across all experimental groups, for both males and females (data not shown*).* Locomotor and anxiety examination using the open field test demonstrated, the widely published phenotype, that transgenic mice, in comparison to wildtype littermates, showed increased locomotor activity and exploratory behavior, including increased total distance travelled, less time immobile and more time spent in the center zone (data not shown). Cognitive assessment in the Y-maze demonstrated a significant decrease in the percentage spatial alternation rate for E22ΔAβ mice at three months of age ($t_{(55)}$=-3.16, $p<0.005$), six months of age ($t_{(28)}$=-1.727, $p<0.05$) and nine months of age ($t_{(16)}$=-1.772, $p<0.05$), as compared to their wildtype littermates (Figure 6 A). The Barnes maze was also used at 3 months of age as a second hippocampus-dependent cognitive task to assess spatial learning and memory. Results demonstrated that both wildtype and transgenic E22ΔAβ mice showed successful learning, with significantly lower latencies to escape over the four days of training (all p's<0.05, Figure 6 B). Between genotypes, a significant main effect was shown for E22ΔAβ mice ($f_{(1,340)}$=16.656, $p<0.001$). Fischer LSD post-hoc analysis demonstrated a significantly longer latency to escape for E22ΔAβ mice, as compared to wildtype littermates on day three ($p=0.01$) and day four ($p=0.03$), with similar but non-significant trends on day one ($p=0.096$) and day two ($p=0.095$) (Figure 6 B). Qualitative assessment of Barnes Maze search strategies revealed a decrease in spatial search strategies in three month-old E22ΔAβ mice (Figure 6 D), as compared to wildtype control mice (Figure 6 C).

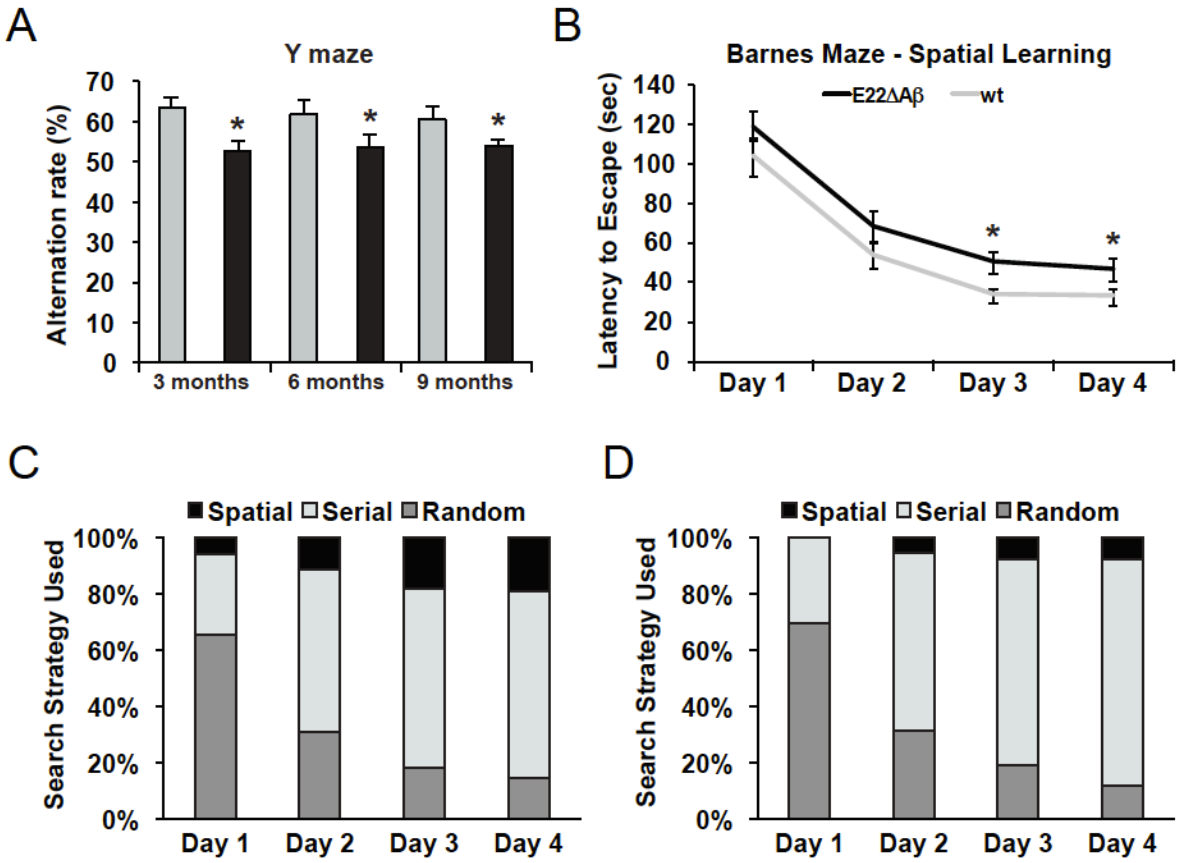

Figure 6. Early cognitive deficits in E22ΔAβ mice. A, Cognitive assessment in the Y-maze demonstrates a significant decrease in the percentage spatial alternation rate for E22ΔAβ mice as compared to their wildtype littermates at three, six and nine months of age. (all p's<0.05; Student's t Test). B, Assessment of Barnes Maze spatial learning at the age of three months reveals that both wildtype and E22ΔAβ transgenic mice show successful learning over the four days of training. However, E22ΔAβ mice, as compared to wildtype littermates, show significantly higher latencies to escape on day 3 (p=0.01) and day 4 (p=0.03), with similar but non-significant trends on day 1 (p=0.096) and day 2 (p=0.095) (ANOVA, followed by post-hoc Fisher LSD analysis). C,D, Qualitative assessment of Barnes Maze search strategies reveals a decrease in spatial and relative increase in serial search strategies in three month-old E22ΔAβ mice (D) in comparison with wildtype control mice (C). n = 22-24 per group.

4.3.6 Unique aggregation properties of recombinant E22Δ-mutated Aβ peptides

In agreement with our previous findings that both E22Δ Aβ40 and E22Δ Aβ42 readily formed amyloid fibrils *in vitro*, we observed fibrillar (congophilic) amyloid deposits *in vivo* in aged APP transgenic E22ΔAβ mice. Extracellular amyloid deposition in the E22ΔAβ mice, however, only occurred as leptomeningeal CAA at an advanced age of 24 months (Figure 4), whereas wildtype Aβ producing Tg2576 mice and E22G ("Arctic") Aβ producing arcAβ mice accumulated fibrillar amyloid deposits at a much

earlier age (Figure 2, Figure 3). To further investigate the biophysical basis of the E22Δ intra-Aβ mutation leading to early intracellular and very late extracellular amyloid deposition *in vivo*, we conducted *in vitro* Thioflavin T aggregation assays of recombinant E22Δ Aβ40 and E22Δ Aβ42 peptides. E22ΔAβ aggregation curves were compared to the aggregation curves of wildtype Aβ40 and Aβ42 and E22G ("Arctic") Aβ40 and Aβ42 (Figure 7). Results demonstrated typical aggregation kinetics of wildtype Aβ42 and E22G ("Arctic") Aβ42 peptides involving a lag phase, an exponential growth phase and a plateau phase of saturated fibril growth (Figure 7 A,B). In contrast, no obvious lag phase and no exponential growth phase were observed for E22Δ Aβ42 at 2.5 µM (Figure 7 A) and – more obvious – at 5 µM (Figure 7 B). Instead, E22Δ Aβ42 showed a constant non-exponential increase in Thioflavin T fluorescence from time point 0' on and – in contrast to E22G Aβ42 and wildtype Aβ42 – formed detergent insoluble high molecular weight (HMW) aggregates immediately after reconstitution at pH 7.4 as revealed by Western blotting of the recombinant peptide preparations that were used for the Thioflavin T analysis (Figure 7 C). Thioflavin T analysis of recombinant Aβ40 peptide variants revealed a dramatically accelerated fibril formation for both E22Δ and E22G ("Arctic") Aβ40 in comparison with wildtype Aβ40 (Figure 7 D). In contrast to E22Δ Aβ42, E22Δ Aβ40 aggregation was characterized by a lag phase, an exponential growth phase and a plateau phase with unusually high absolute Thioflavin T fluorescence values indicating increased Thioflavin T binding capacity of the E22Δ Aβ40 peptide as previously reported (Ovchinnikova et al., 2011). In summary, Thioflavin T analysis of recombinant E22Δ Aβ42 and E22Δ Aβ40 aggregation kinetics confirmed our previous findings of a highly increased fibrillogenic property of single preparations of the two peptide variants (Ovchinnikova et al., 2011).

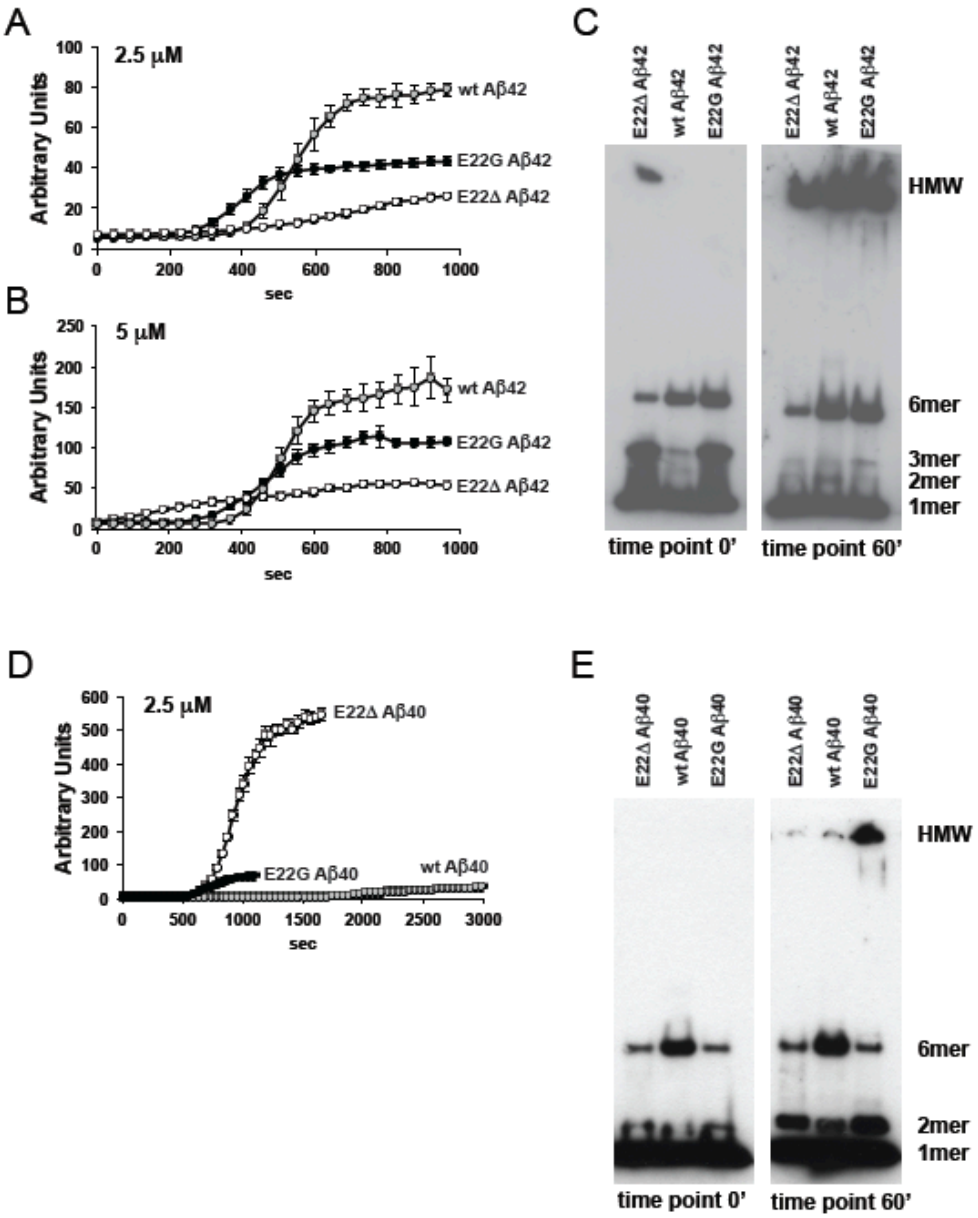

Figure 7. Unique aggregation kinetics of recombinant E22Δ Aβ peptides *in vitro*. Fibril formation is measured via the absolute increase in Thioflavin T fluorescence at 482 nm during aggregation. Aggregation of Aβ peptides (identical total monomer concentrations: 2.5 µM in A+C, 5 µM in B) at pH 7.4 and 37 °C is initiated by a 10-fold dilution of Aβ stock solutions in 10 mM NaOH with buffer. Average curves of three independent experiments are shown (±SEM). A,B, Thioflavin T analysis of E22G ("Arctic") Aβ42 and wildtype Aβ42 reveals typical aggregation kinetics of the two Aβ peptide variants: a lag phase, which is shorter for E22G Aβ42 than wildtype Aβ42, is followed by an exponential growth phase that eventually reaches a plateau of saturated beta-sheet formation. In contrast, no obvious lag phase and no exponential growth phase are observed for E22Δ Aβ42 at 2.5 µM (A) and – more obvious – at 5 µM (B). Instead, E22Δ Aβ42 is characterized by slow non-exponential fibril growth, however, forms detergent insoluble high molecular weight (HMW) aggregates immediately after reconstitution at pH 7.4 as revealed by Western blotting of the recombinant peptide preparations that were used for the Thioflavin T analysis at time point 0' and time point 60' of the assay (C). D, In contrast to E22Δ Aβ42, E22Δ Aβ40 – similar to E22G ("Arctic") Aβ40 – shows an aggregation kinetics characterized by a lag phase, an exponential growth phase and a plateau phase. Note the unusually high Thioflavin T fluorescence values for E22Δ Aβ40 in contrast to E22G and wildtype Aβ40 and the remarkably shorter lag phases of the E22 mutated Aβ40 variants in comparison with the wildtype peptide. E, In contrast to the Aβ42 analysis, Western blot analysis of Aβ40 peptide variants reveals no formation of detergent insoluble HMW aggregates at time point 0'.

4.3.7 Inhibition of E22Δ Aβ aggregation in the presence of wildtype Aβ

The E693Δ APP mutation is one of the two currently known familial AD mutations in the APP gene with a recessive Mendelian trait of inheritance (Di Fede et al., 2009; Tomiyama et al., 2008). The second recessive mutation, A673V, has recently been shown to be highly amyloidogenic in the homozygous state, but anti-amyloidogenic in the heterozygous state as revealed by an inhibition of Aβ aggregation when mutated and wildtype peptides were co-incubated (Di Fede et al., 2009). We hypothesized similar effects of wildtype Aβ peptides on the aggregation kinetics of the E22Δ mutated Aβ peptides for both co-incubated E22Δ Aβ42 with wildtype Aβ42 (Figure 8 A) and E22Δ Aβ40 with wildtype Aβ40 (Figure 8 B). Strikingly, co-aggregation of the E22Δ mutated peptides with the respective wildtype peptides led to a significant extension of the lag phase and a delay of the growth phase in comparison with the aggregation of the respective Aβ peptide variants alone (Figure 8 A,B). In contrast, co-aggregation of E22G ("Arctic") Aβ42 with wildtype Aβ42 revealed a similar aggregation kinetics as aggregation of E22G Aβ42 alone (see Figure 8 A), and co-aggregation of E22G Aβ40 with wildtype Aβ40 only slightly delayed fibril formation in comparison with E22G Aβ40 alone (Figure 8 B).

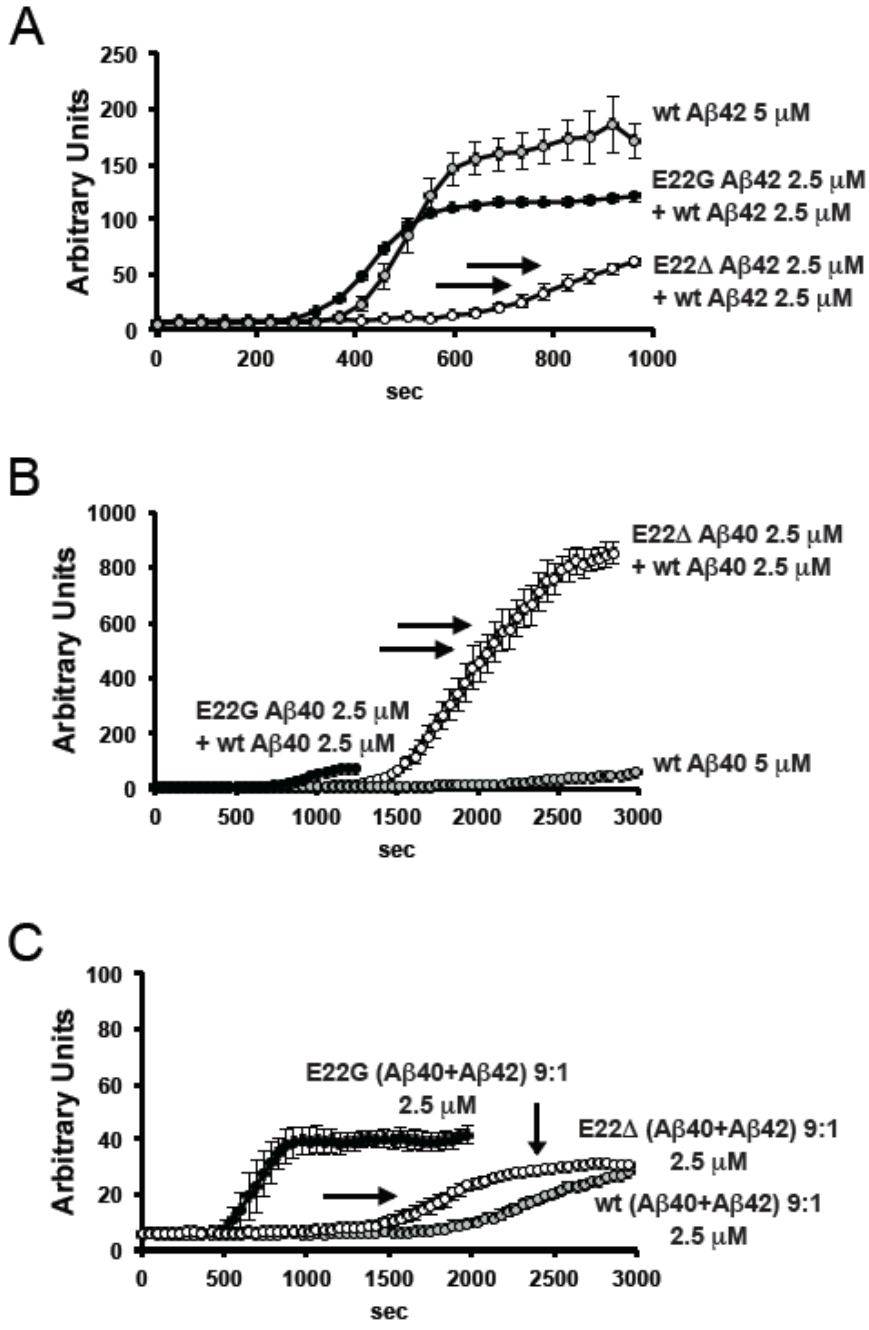

Figure 8. Anti-amyloidogenic property of E22Δ Aβ peptides in mixtures of different Aβ peptide variants. A,B, Co-aggregation of E22Δ Aβ42 with wildtype Aβ42 (A) or E22Δ Aβ40 with wildtype Aβ40 (B) leads to a significant extension of the lag phase and a delay of the growth phase in comparison with the aggregation of the respective Aβ peptide variants alone (see Figure 7) (total monomer concentrations for each peptide variant: 2.5 μM). In contrast, co-aggregation of 2.5 μM E22G (Arctic) Aβ42 with 2.5 μM wildtype Aβ42 (A) results in a similar aggregation curve as with 2.5 or 5 μM E22G Aβ42 alone (see Figure 7). Co-aggregation of E22G Aβ40 with wildtype Aβ40 (B) only slightly delays beta-sheet formation in comparison with E22G Aβ40 alone. C, Co-aggregation of E22Δ Aβ40 with E22Δ Aβ42 in a physiological 9:1 ratio (total monomer end concentration in solution: 2.5 μM) leads to a strong inhibition of E22Δ Aβ40 aggregation. Note the dramatic delay of the growth phase and remarkable loss of absolute Thioflavin T fluorescence in comparison with E22Δ Aβ40 alone (Figure 7). In contrast, 9:1 mixtures of E22G Aβ40 and E22G Aβ42 result in an aggregation curve very similar to E22G Aβ40 alone. Average curves of three independent experiments are shown (±SEM).

4.3.8 Inhibition of E22Δ Aβ40 aggregation in the presence of E22Δ Aβ42

Based on our results that co-incubation of wildtype Aβ with E22Δ Aβ significantly delayed amyloid fibril formation we hypothesized that co-incubation of E22Δ Aβ40 with E22Δ Aβ42 may have similar anti-fibrillogenic effects. Therefore, recombinant E22Δ Aβ40 and E22Δ Aβ42 peptides were co-incubated in a physiological 9:1 ratio at 2.5 µM, and the increase in Thioflavin T fluorescence was monitored over time (Figure 8 C). We found a dramatic delay of the growth phase and a remarkable loss of absolute Thioflavin T fluorescence when we compared the aggregation curve with the aggregation curve of E22Δ Aβ40 alone (Figure 7 D, Figure 8 C). Again in contrast, 9:1 mixtures of E22G Aβ40 and E22G Aβ42 resulted in an aggregation curve very similar to E22G Aβ40 alone (Figure 7 D, Figure 8 C).

4.3.9 Poor seeding of wildtype Aβ42 aggregation by E22Δ Aβ42 fibrils

Based on the assumption that amyloid formation can be seeded by preformed amyloid fibrils we finally addressed the question whether preaggregated E22Δ Aβ42 fibrils were capable of (a) seeding their own growth and (b) seeding the growth of wildtype Aβ42 fibrils. As control experiments, wildtype Aβ42 and E22G (“Arctic”) Aβ42 fibrils were incubated with preparations of their respective monomeric peptides which resulted in an immediate increase in Thioflavin T fluorescence without a lag phase thus indicating good seeding properties (Supplementary Figure 4 A,B). Incubation of preaggregated E22Δ Aβ42 fibrils with fresh preparations of E22Δ Aβ42 peptide also resulted in an immediate increase in Thioflavin T fluorescence that was steeper as compared to the aggregation curve of E22Δ Aβ42 in the absence of fibrillar seeds (Figure 7 A, Supplementary Figure 4 C). However, when E22Δ Aβ42 fibrils were used for the seeding of wildtype Aβ42, a significant delay of fibril formation was observed which indicated poor seeding properties (Supplementary Figure 4 E). In contrast, E22G Aβ42 fibrils appeared only slightly inferior to wildtype Aβ42 fibrils in seeding wildtype Aβ42 aggregation (Supplementary Figure 4 D).

4.4 Discussion

Homozygous E693Δ APP mutation carriers develop an AD-like clinical phenotype characterized by early memory disturbances, visuospatial deficits and executive dysfunction, followed by atypical neurological signs including cerebellar ataxia and gait difficulties during later stages of the disease (Shimada et al., 2011; Tomiyama et al., 2008). Brain amyloid imaging by PIB PET revealed a very weak signal in E693Δ APP mutation carriers with advanced dementia suggesting that AD-like clinical symptoms occurred in the absence of relevant amyloid deposition in these patients (Shimada et al., 2011; Tomiyama et al., 2008). *In vitro* experiments with synthetic E22Δ Aβ40 and E22Δ Aβ42 peptide preparations demonstrated an enhanced oligomerization propensity, but no fibril formation and led to the hypothesis that AD-like dementia can be caused by the sole presence of synaptotoxic Aβ oligomers (Tomiyama et al., 2008). In contrast to these initial *in vitro* findings, subsequent work, including our own recent study with highly pure recombinant peptide preparations, demonstrated that both E22Δ Aβ40 and E22Δ Aβ42 readily formed amyloid fibrils *in vitro* (Inayathullah et al., 2011; Ovchinnikova et al., 2011; Suzuki et al., 2010). Based on these *in vitro* findings, we hypothesized that E22Δ Aβ40 and E22Δ Aβ42 would, at least in principle, also form amyloid fibrils *in vivo*. Indeed, aged E22ΔAβ mice accumulated detergent insoluble (formic acid soluble) Aβ and showed Thioflavin S and Congo red positive amyloid deposits in leptomeningeal cortical and – more pronounced – cerebellar vessels; in contrast to the recently published E693Δ mouse model, which completely lacked extracellular amyloid deposition even at a very advanced age (Tomiyama et al., 2010). E22ΔAβ mice highly overexpress human APP at levels comparable to those in the Tg2576 mouse line. Moreover, the introduction of the “Swedish” (K670N+M671L) double mutation in the E22ΔAβ mice results in an additional increase in total Aβ levels (Haass et al., 1995), which might explain the differences between our model and the E693Δ mice. Interestingly, CAA deposits in the E22ΔAβ mice were more pronounced in the leptomeningeal vasculature of the cerebellum than in cortical vessels (data not shown), which is in agreement with recent amyloid PET findings in E693Δ mutation carriers showing a relative increase in PIB retention in cerebellar brain regions (Shimada et al., 2011). The identification of CAA as a key neuropathological feature of aged E22ΔAβ mice adds the “Osaka” E693Δ mutation to the list of vasculotropic intra-Aβ APP mutations essentially comprising all of the currently known mutations at or around position 22

of the Aβ sequence (for a review Kumar-Singh et al., 2009). Our immunohistological analysis of CAA deposits identified Aβ40 as the major E22Δ Aβ species depositing in the vessel walls of the E22ΔAβ mice which is in in line with previous findings in sporadic and familial AD cases (Kumar-Singh et al., 2008; Kumar-Singh et al., 2002) including the "Dutch" E693Q APP mutation (Herzig et al., 2004). Further experiments are needed to elucidate the mechanisms underlying the "vasculotropism" of E22Δ-mutated Aβ and whether similar mechanisms as previously reported for the "Dutch" mutation (i.e. a reduced receptor-mediated clearance across the blood brain barrier) play a role (Deane et al., 2004; Monro et al., 2002).

E22ΔAβ mice – similar to our previously reported arcAβ mice (Knobloch et al., 2007) – develop intraneuronal Aβ aggregates that coincides the cognitive deficits as early as three months of age. Intraneuronal Aβ accumulation is generally believed to be an early event in AD pathogenesis although it's relevance and role in the disease process remain a controversial topic (Gouras et al., 2010; Tampellini et al., 2010). This may partly be due to technical considerations including the use of non-specific antibodies for the detection of intraneuronal Aβ. The intraneuronal Aβ aggregates in our E22ΔAβ mouse model only partially colocalized with APP/APP C-terminal fragments and were stained by different Aβ C-terminus-specific antibodies, which do not cross-react with APP or APP fragments, including BC05 and BA27 (data not shown) (Winton et al., 2011). These results therefore indicate that the intraneuronal aggregates in the E22ΔAβ mice indeed correspond to Aβ and not accumulating APP/APP fragments. Further immunohistological characterization of the deposits revealed that the intraneuronal aggregates are strongly stained by OC antibody, directed against fibrillar oligomers, but not A11 antibody (data not shown), which recognizes prefibrillar oligomers (Kayed et al., 2003; Kayed et al., 2007). Interestingly, soluble fibrillar oligomers detected by OC antibody (but not prefibrillar oligomers) have recently been shown to be elevated in multiple brain regions of AD patients and to correlate with cognitive dysfunction (Tomic et al., 2009). Building on the hypothesis that intra-Aβ mutations at or around position 22 of the Aβ increase Aβ fibrillogenesis through a facilitation of a "toxic turn" conformation between positions 22 and 23 of the Aβ sequence, Murakami et al. (2010) developed a novel monoclonal antibody (11A1) directed against this specific conformational epitope of Aβ42 (Murakami et al., 2010). In human AD brains, 11A1 stained both extracellular

and intracellular Aβ deposits, whereas, in APP transgenic Tg2576 mice only extracellular deposits were labeled (Murakami et al., 2010). Interestingly, 11A1 stained intraneuronal Aβ aggregates in the brains of the E22ΔAβ mice, suggesting that the oligomeric E22Δ-mutated Aβ deposits contained the abovementioned “toxic turn” conformation.

Western blot and MSD analysis of APP cleavage products from cortical brain extracts revealed a relative increase in amyloidogenic (beta-secretase-mediated) APP processing in the two mouse models bearing the E22 intra-Aβ APP mutations, which is in accordance with previous *in vitro* findings (Nishitsuji et al., 2009; Sahlin et al., 2007; Stenh et al., 2002). Since both E22ΔAβ and arcAβ mice overexpress similar full length APP, sAPPß and C99 levels, but significantly reduced sAPPα and C83 levels, as compared the Tg2576 mice, we concluded that the two intra-Aβ mutations specifically interfered with the α-secretase cleavage of APP *in vivo*. Previous *in vitro* reports in the “Arctic” mutation revealed that E693G APP was not a poor substrate to α-secretase, but instead reduced APP levels at the cell surface making “Arctic” APP less available for α-secretase cleavage, and increasing Aβ levels, especially at intracellular locations (Sahlin et al., 2007). Similar to the “Arctic” APP mutation, E693Δ APP overexpression in cell culture was also associated with reduced extracellular Aβ levels *in vitro* (Nishitsuji et al., 2009; Sahlin et al., 2007; Stenh et al., 2002). Although these results may imply similar effects of the two intra-Aβ mutations on APP processing, we currently cannot exclude E693Δ APP as an inferior substrate to α-secretase-mediated cleavage thus leading to the relative increase in amyloidogenic APP processing; as shown previously for other intra-Aβ APP mutations, including the “Flemish” E692G APP mutation (Lammich et al., 1999).

MSD analysis revealed a marked reduction of buffer and Triton buffer soluble brain Aβ as well as peripheral plasma Aβ levels, in particular when E22ΔAβ mice were compared to age-matched Tg2576 mice expressing wildtype Aβ. This indicated that the absence of extracellular amyloid deposition up to an age of 15 months was not associated with a relative increase in soluble or peripheral (plasma) Aβ levels. Instead, most of the Aβ accumulated in the SDS soluble protein fraction likely corresponding to intraneuronal Aβ pools. These results are in agreement with recent *in vitro* results from cell culture experiments showing increased intracellular Aβ

accumulation, but markedly reduced secreted Aβ levels in E693Δ APP-transfected cell lines (Tomiyama et al., 2008; Nishitsuji et al., 2009; Umeda et al., 2011). The early accumulation of intracellular fibrillar oligomeric Aβ deposits in brains of the E22ΔAβ mice is in line with the unique aggregation profiles of the recombinant E22Δ Aβ40 and E22Δ Aβ42 peptides showing accelerated beta-sheet formation in Thioflavin T aggregation assays as compared to the respective wildtype Aβ peptides (this study and Inayathullah et al., 2011; Ovchinnikova et al., 2011; Suzuki et al., 2011). When aggregation curves of E22Δ, E22G and wildtype Aβ40 and Aβ42 were compared, E22Δ Aβ42 showed the highest fibrillogenesis propensity as it aggregated without a lag phase and formed SDS-resistant amyloid fibrils immediately after reconstitution in solution at pH 7.4. However, E22Δ Aβ42 fibril growth after reconstitution in solution occurred only in a slow non-exponential fashion in contrast to the other peptides, including E22Δ Aβ40, whose aggregation was characterized by an exponential growth phase following lag phase. This slow fibril growth and lack of exponential growth in E22Δ Aβ42 may be a crucial factor in the prevention of extracellular amyloid deposition in the E22ΔAβ mice.

Apart from A673V, a recently described familial AD APP mutation in an Italian pedigree, E693Δ is the second currently known recessive APP mutation that is pathogenic only in the homozygous state (Di Fede et al., 2009; Tomiyama et al., 2008). Similar to the A673V mutation, which is anti-amyloidogenic in the heterozygous state (Di Fede et al., 2009), our co-aggregation experiments with recombinant E22Δ Aβ peptides variants also revealed an inhibition of Aβ aggregation when mutated and wildtype peptides were co-incubated. In contrast, co-aggregation of E22G (“Arctic”) Aβ peptides with the respective wildtype Aβ peptides resulted in aggregation curves very similar to those of the E22G Aβ peptides alone. Moreover, E22Δ Aβ42 fibrils, in contrast to wildtype Aβ42 and E22G Aβ42 fibrils, only very inefficiently seeded wildtype Aβ42 fibrillogenesis. These results provide a possible explanation why heterozygous carriers of the E693Δ mutation do not develop the disease whereas heterozygous carriers of the autosomal dominant “Arctic” mutation develop dementia.

Hence, we propose the following hypothetical model to explain the phenotype of the ”Osaka” E693Δ mutation, in which E22Δ Aβ aggregation occurs primarily

intracellularly where peptide concentrations are high enough to allow for aggregate formation (Supplementary Figure 5). Outside the cell, E22Δ Aβ peptide variants may interact with each other – and possibly also other peptides – in a way that results in an inhibition of aggregation and amyloid seed formation. Moreover, the E22Δ Aβ42 peptide shows specific aggregation properties (slow non-exponential growth, lack of exponential growth phase) that likely further prevent parenchymal amyloid plaque deposition (Supplementary Figure 5). However, late vascular amyloid deposition occurs, possibly due to the “vasculotropism” of the E22 mutated Aβ peptide variant and age-related changes along perivascular clearing pathways (Supplementary Figure 5).

4.5 Acknowledgements

We thank Anna Jeske for technical support. This study was supported in parts by the Swiss National Science Foundation grant no. 33CM30-124111/1 and the Forschungskredit grant of the University of Zurich.

4.6 Supplementary material

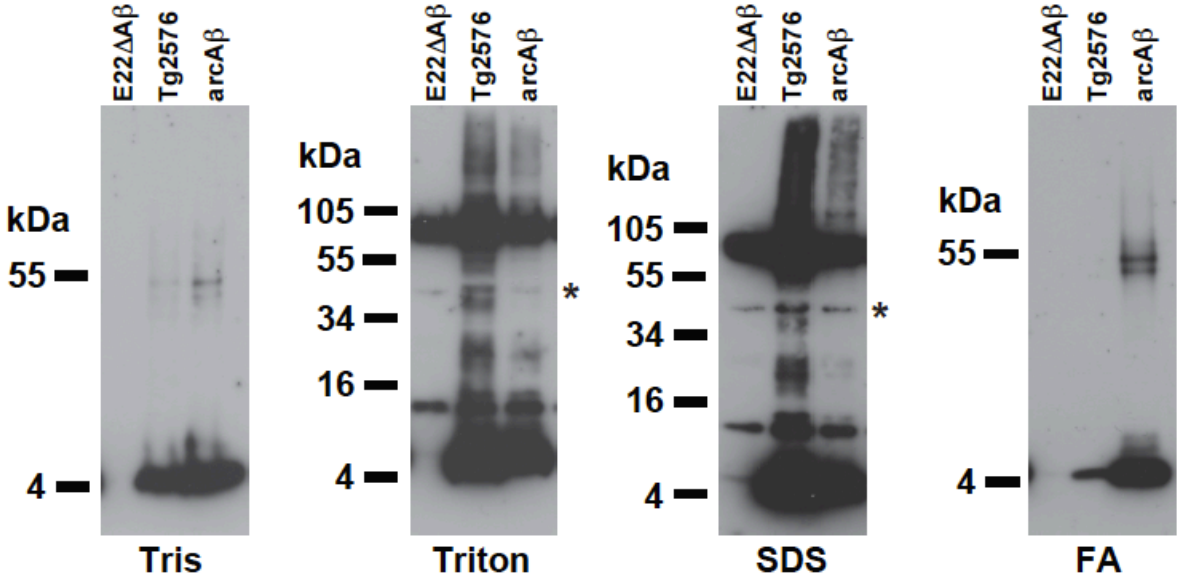

Supplementary Figure 1. Representative western blot analysis of serially extracted cortical samples from a 15 month-old E22ΔAβ mouse and age-matched Tg2576 and arcAβ mice. Immunoblotting with monoclonal antibody 6E10 reveals only a very faint monomeric Aβ band in the E22ΔAβ mouse, which is most readily detectable in the SDS fraction. In contrast, 15 month-old Tg2576 and arcAβ mice show a massive accumulation of both monomeric and oligomeric Aβ species throughout the fractions. The prominent band at around 100 kDa corresponds to APP. * corresponds to an unspecific protein band.

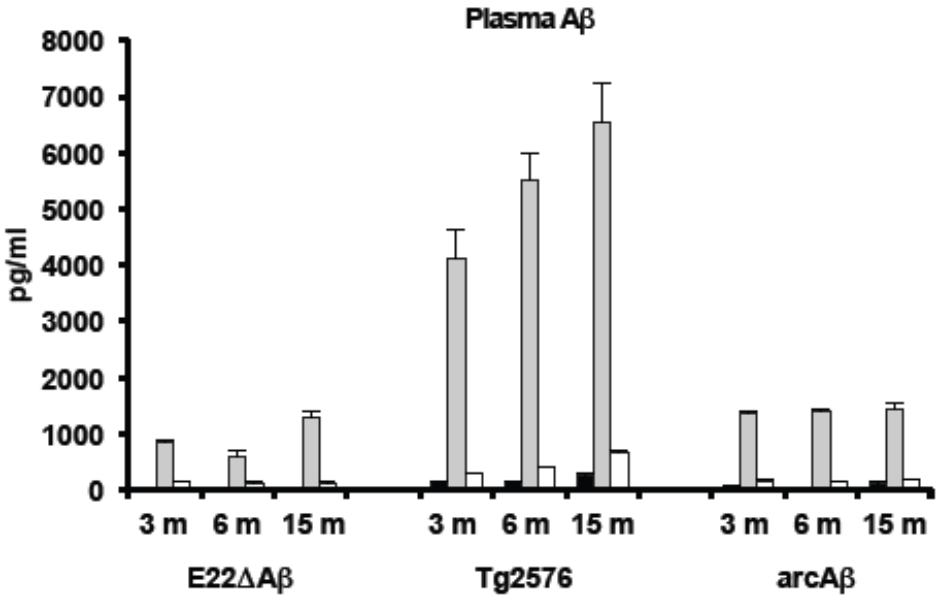

Supplementary Figure 2. MSD analysis of Aβ38 (black column), Aβ40 (grey column) and Aβ42 (white column) in plasma samples of E22ΔAβ, arcAβ and Tg2576 mice at three different ages (three, six and 15 months). Plasma Aβ levels are up to four- to fivefold lower in the E22ΔAβ and arcAβ mice as compared to the Tg2576 mice. Lowest plasma Aβ levels are detected in the E22ΔAβ mice. n = 6-9 per group.

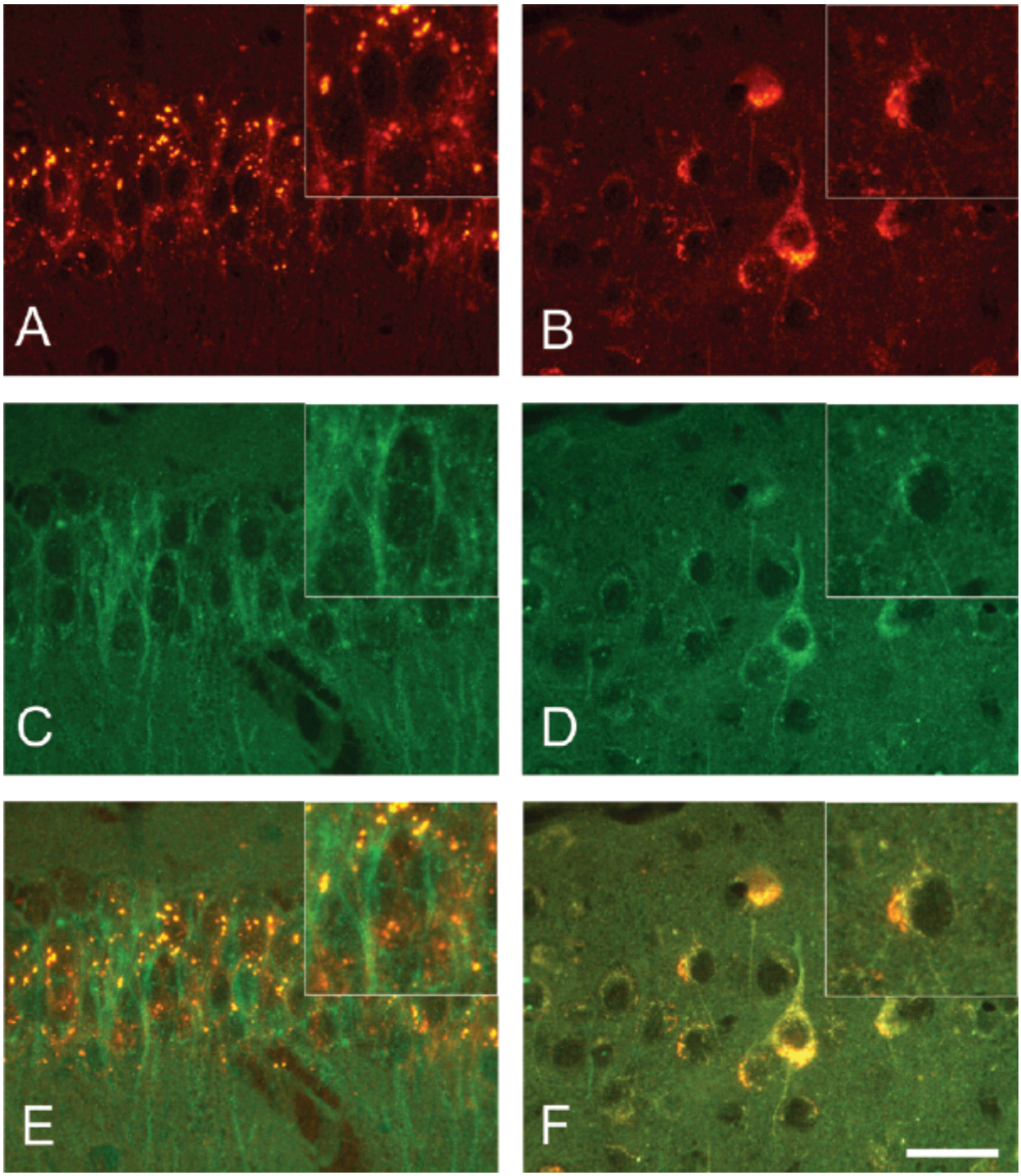

Supplementary Figure 3. Intraneuronal Aβ deposits and APP. A,B: 6E10 immunoreactive dot like deposits are readily detectable within hippocampal CA1 (A) and cortical (B) neurons of a 15 month-old E22ΔAβ mouse. Double immunostaining with a polyclonal antibody directed against the APP C-terminus (C,D) reveals only partial colocalization of 6E10 and APP immunoreactivity in the cortex (F) and virtually no colocalization in the CA1 region of the hippocampus (E). Scale bar: 40 mm (A-F).

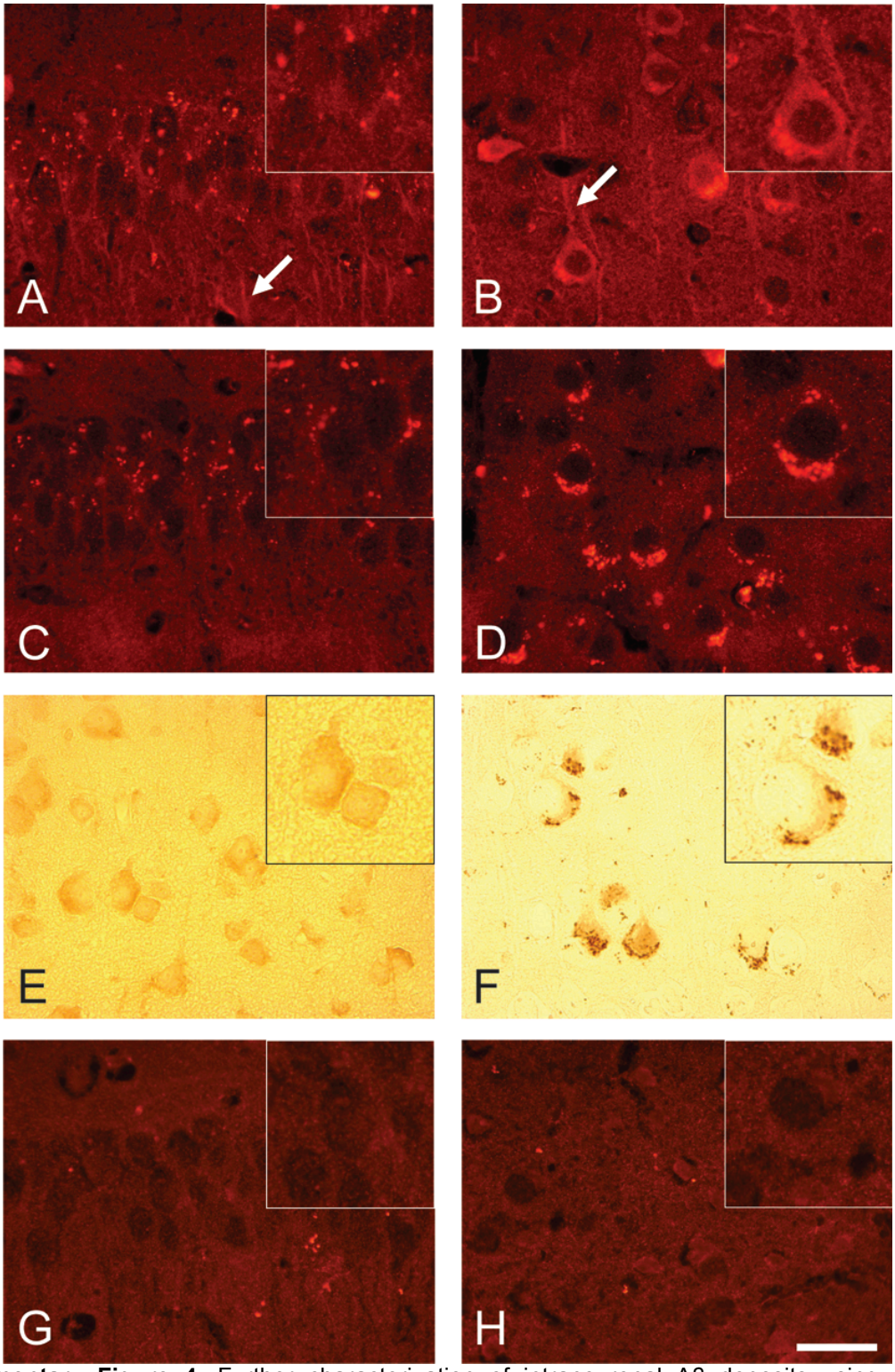

Supplementary Figure 4. Further characterization of intraneuronal Aβ deposits using Aβ- and oligomer-specific antibodies. A,B, Immunostaining with Aβ40-specific polyclonal antibody (Sigma) reveals both dot-like and diffuse (arrow) Aβ immunoreactivity in CA1 hippocampal (A) and cortical (B) neurons of a 15 month-old E22ΔAβ mouse. C,D, In contrast, an Aβ42-specific polyclonal antibody (Signet) exclusively stains compact (dot-like) intracellular deposits in hippocampal CA1 (C) and cortical neurons (D) of the same mouse. E,F, Similar results are obtained using Aβ40-specific BA27 (E) and Aβ42-specific BC05 (F) monoclonal antibodies (representative immunostainings of cortical brain sections from a 15 month-old E22ΔAβ mouse are shown). G,H, Immunostaining with A11 antibody directed against prefibrillar oligomers reveals no significant immunoreactivity in CA1 hippocampal (G) and cortical (H) neurons of a 15 month-old E22ΔAβ mouse. Scale bar: 40 mm.

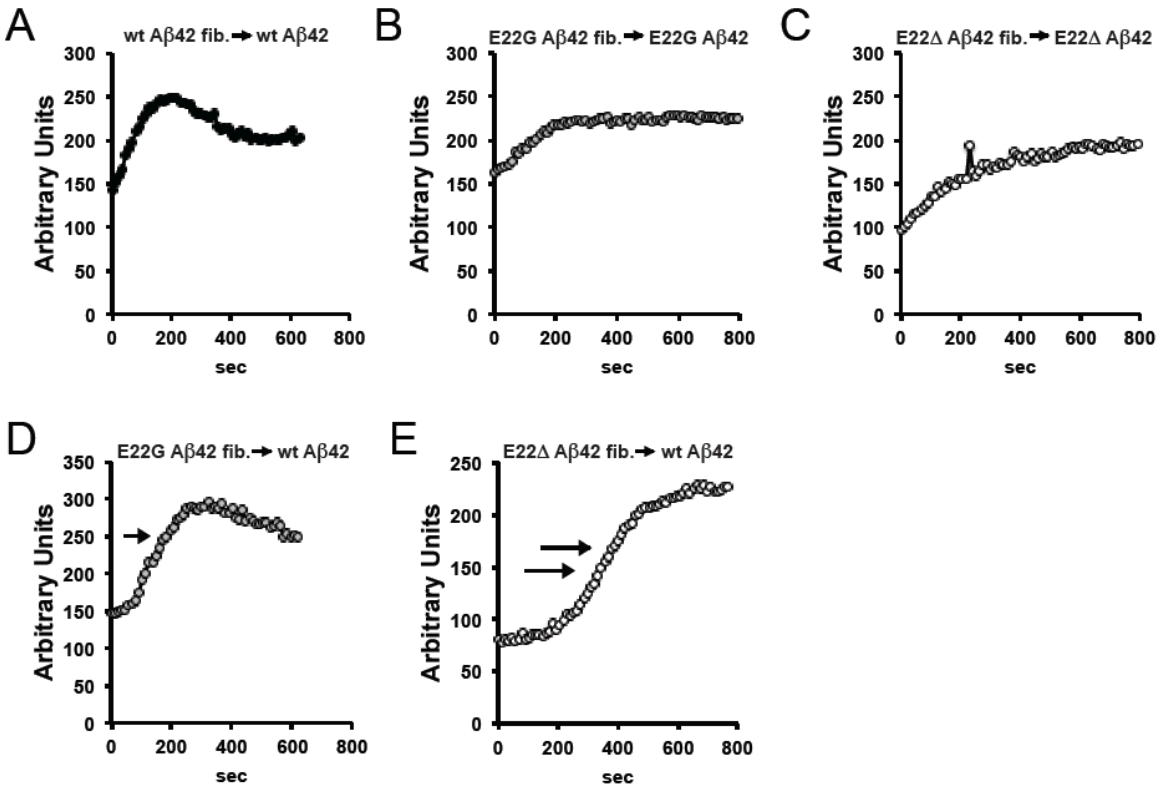

Supplementary Figure 5. Seeding experiments. Recombinant E22Δ, E22G ("Arctic") and wildtype Aβ42 peptides were reconstituted at 2.5 µM (1 ml buffer solution, pH 7.4) and were incubated at 37 ºC under continuous stirring to allow for amyloid fibril formation. After 1000 sec (when all aggregation curves had reached the plateau phase) 500 µl of the fibril solution were incubated with an identical volume of a solution that contained fresh (monomeric) Aβ42 peptides (total monomer concentration of fresh peptide: 2.5 µM). Representative figures of at least three independent experiments are shown. A-C, Incubation of wildtype Aβ42 (A), E22G Aβ42 (B) or E22Δ Aβ42 fibrils (C) with preparations of their respective monomeric peptides results in an immediate increase in Thioflavin T fluorescence without a lag phase which indicates good seeding. D, E22G Aβ42 fibrils are slightly inferior to wildtype Aβ42 fibrils in seeding wildtype Aβ42 aggregation (note the slight delay of the increase in Thioflavin T fluorescence), whereas E, seeding of wildtype Aβ42 aggregation is relatively delayed when wildtype Aβ42 monomers are incubated with E22Δ Aβ42 fibrils.

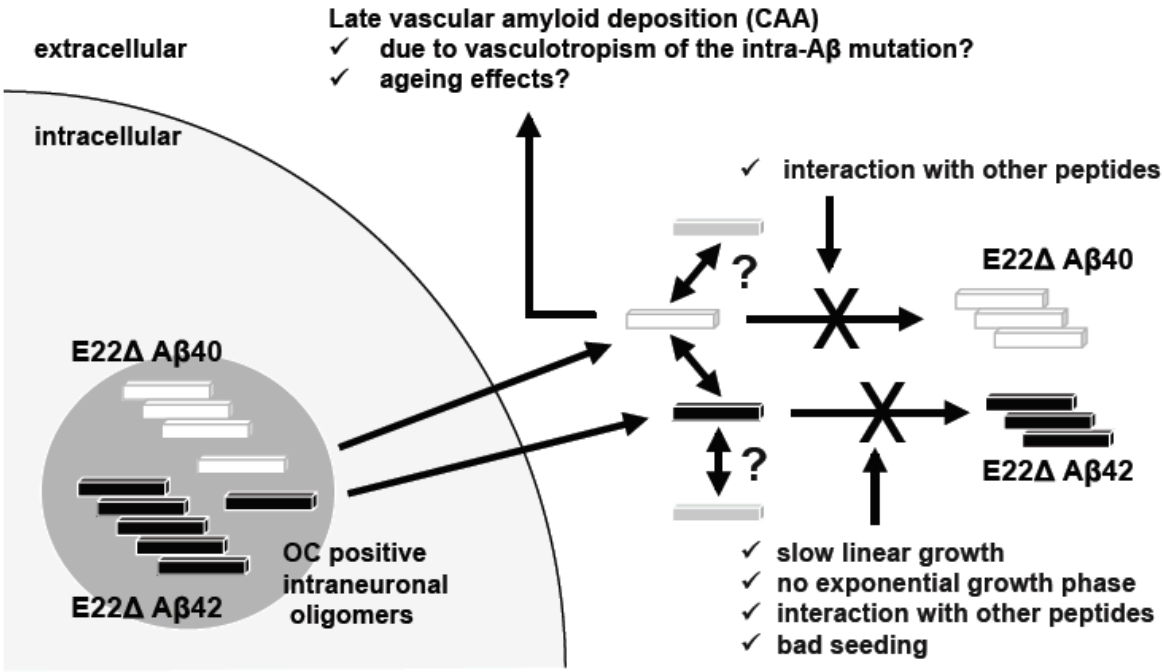

Supplementary Figure 6. Hypothetical model to explain the phenotype of the "Osaka" E693Δ APP mutation.

5 Conclusion and Outlook

5.1 Anti-TNF project

Tobinick and colleagues (2006), demonstrated, in a Phase I clinical trial, that weekly perispinal injections of etanercept anti-TNF therapy for six months could ameliorate the cognitive deficits in AD patients, as compared to baseline measurement. Subsequently, Tobinick and colleagues (2008) later described the rapid cognitive improvement in an AD case study following weekly perispinal injections of etanercept. These tantalizing effects raised many questions and lead to the suggestion that etanercept anti-TNF therapy might inhibit neuroinflammatory responses, stabilize TNF-mediated synaptic dysregulation, or possibly through TNF- or Fc-mediated mechanisms lower amyloid pathology. Not surprisingly, etanercept anti-TNF therapy has now entered Phase II clinical trail investigations, albeit, the underlying therapeutic mechanisms remain to be fully resolved. In **Chapter 2**, we sought to investigate in an AD mouse model the underlying therapeutic mechanisms, with particular emphasis on determining if anti-TNF therapy could rescue cognitive deficits, lower amyloid pathology and inhibit neuroinflammation.

Our findings demonstrated that anti-TNF etanercept therapy, administered intracerebroventricularly (28 days infusion) or intraperitoneally (4 weekly ip injections) could rescue cognitive deficits, as well as, reduce amyloid plaque deposition in 12 month old arcAβ mice. Here we choose to use to modes of administration (icv infusion and ip injections) in order to differentiate between the therapeutic effects of directly modulating TNF-mediated responses within the central nervous system, versus systemic TNF-mediated immune/inflammatory processes and/or its important role in brain-immune signaling. Our findings showed that similar to icv-treated mice with wide distrubtion of the etanercept, ip-treated mice also showed diffusion of the biologic within the brain at sites of impaired blood-brain-barrier (BBB). Indeed, impaired BBB integrity and other vascular changes have been widely described in the ArcAβ mice (Knobloch et al., 2007; Merlini et al., 2011), and future experiments using an alternative AD mouse model, such as tg2576 mice, which lack pronounced vascular pathology might be better able to differentiate

between central and peripheral modes of action of anti-TNF therapy. Here, however, in our study, the entry of peripherally administered etanercept within the brain excludes any restricted systemic effect of anti-TNF treatment and lends support towards a CNS-delivered therapeutic approach. However, with Phase II clinical trials underway to investigate the therapeutic potential of subcutaneously administered etanercept in Alzheimer's disease patients, it will be possible to determine, in human subjects, if systemic anti-TNF therapy may have beneficial effects as well. To investigate transient versus long-term effects of TNF inhibition, we also included in this study ArcAβ mice backcrossed with TNF knockout mice. These mice allowed us to investigate the development of amyloid pathology in the absence of TNF expression. The histological and biochemical results from these experiments were in line with acute anti-TNF therapy in which we could demonstrate that ArcAβ mice on a TNF deficient background showed improved cognitive performance, lower amyloid pathology, reduced astrocytosis and increased microglia activation.

As mentioned above, cognitive assessment in both the Ymaze and NORT demonstrated improvements in cognitive performance for both icv- and ip-treated mice, as compared to controls. Importantly, the improvement seen in cognitive performance was comparable to wildtype mice, suggesting a full rescue in cognitive deficits. Moreover, given the short duration of treatment (1 month), our findings support the rapid cognitive rescue observed in humans following etanercept anti-TNF treatment (Tobinick et al., 2008). These behavioral findings were supported by histological reductions in the number of plaques, as well as, lower percentage area covered by plaques in icv- and ip-treated mice, as compared to controls. Upon further histological investigations, etanercept icv-treated mice were shown to display increased CAA as compared to controls, suggesting a redistribution of parenchymal plaques towards the vasculature. As a potential consequence of this redistribution we investigated for a possible increase in micro-bleeds, but found no correlation between treatment and the frequency of micro-bleeds. Indeed, our results demonstrated that many areas of heavy CAA deposition in etanercept icv-treated mice did not show signs of micro-bleeds, suggesting an amyloid-induced risk for micro-bleeds and not a treatment-induced risk for micro-bleeds, per se. However, one possible explanation for these findings could be that these micro-bleed free areas of heavy CAA deposition might reflect newly formed CAA pathology following

anti-TNF treatment induced redistribution of amyloid towards the vasculature and that with time, if not cleared efficiently, these vessels might deteriorate, lose their integrity and begin to bleed. Future experiments should therefore look to identify the temporal change in CAA pathology and how these changes over time may or may not lead to micro-bleeds.

We were also able to demonstrate biochemically, using MSD multi-SPOT elctrochemiluminesces to measure Aβ levels, that icv- and ip-treated etanercept mice showed significant reductions in detergent insoluble formic acid fraction Aβ levels, as compared to control mice. Together, these findings provide evidence that anti-TNF etanercept treatment may successfully reverse Aβ-mediated cognitive deficits in an AD mouse model and that the continuous infusion of etanercept may have a modulatory effect on brain Aβ levels, as well as, amyloid deposition. Indeed, it has been widely shown that TNF over-expression may promote amyloid plaque deposition, as well as, mediate amyloid induced cognitive dysfunction (He et al., 2007; Rowan et al., 2007; Wang et al., 2005). Medeiros and colleagues (2007) demonstrated that TNF signaling pathways and iNOS act as central mediators of Aβ with both pharmacological and genetic blockage of TNF and iNOS improving cognitive deficits evoked by Aβ. Other evidence supports the role of TNF-mediated synaptic dysfunction in the progression of AD following prolonged Aβ-induced neuronal inactivity (Small, 2008).

Histological findings demonstrated in icv-treated mice that anti-TNF treatment resulted in the lowering of reactive astrocytosis. Such findings suggest a normalization of reactive astrocytes towards physiological conditions and lend support for an anti-TNF therapy mediated reversal of TNF-mediated synaptic dysfunction. In pilot study (data not shown) we were able to show that acute administration of anti-TNF therapy resulted in a partial rescue of LTP deficits in ArcAβ transgenic mouse hippocampal slices. Future experiments are planned to look at both the genetic and pharmacological inhibition of TNF in ArcAβ transgenic hippocampal slices and synaptic activity. Such studies could determine for the first time if anti-TNF therapy can restore altered synaptic activity. Similarly, it is possible with such experimental methods to decipher the exact cellular mechanisms involved, with speculations that astrocytic release of TNF during prolonged neuronal inactivity

(synaptic scaling) maybe an early compensatory response in Alzheimer's disease pathogenesis that later leads to synaptic dysregulation.

Lastly, in this study we were able to show in icv-treated mice and ArcAβ TNF knockout mice an increase level of actived microgliosis. It is hypothesized that during normal disease progression the overexpression of TNF may interfere with microglia activation and that following anti-TNF therapy microglia resume a more activated state that promotes effective amyloid plaque clearance. Here, future studies, using two-photon microscopy might be able to determine the time dependent activation state of microglia before and after anti-TNF treatment and if following treatment these activated microglia become more efficient in phagocytizing amyloid plaques.

Combined, our results indicate that anti-TNF therapy may restore physiological astrocyte functions, promote microglia activation, reduce amyloid burden and successfully reverse abeta-induced cognitive deficits in 12 month old arcAβ transgenic mice.

5.2 DARPin project

In the last decade numerous amyloid-lowering therapeutic approaches have been developed and brought into clinical trial investigations. As an alternative, we described in **Chapter 3**, the selection of a novel class of Aβ-specific DARPins, their affinity determination and binding kinetics, as well as, their ability to prevent Aβ aggregation, reduce Aβ-mediated neurotoxicity and *in vivo* therapeutic potential in Swedish (Tg2576) transgenic mice. At one-tenth the molecular weight of IgGs, DARPins are likely to exhibit a higher degree of tissue penetration and increased ability to cross the blood brain barrier (BBB) upon peripheral administration, with lower risk for immunogenicity, potential aversive immune reactions and the production of neutralizing antibodies following repeated administration. In this study we were able to select, for the first time, a DARPin binder, termed D23, with nanomolar affinities for the Aβ peptide that showed superior binding characteristics in both direct and competition ELISA assays.

Epitope mapping confirmed that D23 binding involves the N-terminus, as well as, parts of the central domain, with evidence to suggest D23's recognition of a

discontinuous rather than linear epitope. This observation is in accordance with previous findings that DARPins preferentially recognize three-dimensional, structural epitopes due to their intrinsic rigid scaffold that displays a relatively shallow and elongated binding interface (Binz et al., 2004; Schweizer et al., 2007; Stumpp et al., 2007). To determine the binding characteristics of D23 *ex vivo*, we performed GFP-fused DARPin immunohistochemical analyses on brain tissue from a mouse model of AD. The staining of amyloid deposits by D23 indicates that the missense mutation in the Arctic Aβ sequence did not markedly influence D23 binding and that when compared to anti-Aβ antibody stainings, D23 was found to bind preferentially the cross-β pleated dense central cores of the amyloid deposits. Together these findings suggest that the binding mode of D23 is fundamentally different from most monoclonal antibodies that recognize a linear stretch of both the Aβ peptide and APP. The absence of cross-reactivity to APP might be considered advantageous for DARPin-based therapeutic purposes, as peripheral APP would be a scavenger that captures the majority of exogenously applied anti-Aβ DARPins.

Subsequently, we were able to demonstrate *in vitro* using Thioflavin T (ThT) aggregation assays that D23 could delay Aβ aggregation. As a further proof-of-principle, we were able to demonstrate that D23, but not E2_5 control DARPin, when administered into the medium of rat primary cortical neuron cultures could reduce Aβ-mediated neurotoxicity and preserve neuronal morphology. To optimize D23 binding behavior for potential therapeutic use, bi- and trivalent D23 DARPins were engineered by fusing two and three monovalent units of D23 into one continuous open reading frame. While these multivalent D23 DARPins showed similar structural integrity and binding to the Aβ peptide, surface plasmon resonance kinetic analysis revealed differences in on- and off-rates for each individual construct.

Finally, as a direct proof of therapeutic benefit, we were able to demonstrate the *in vivo* therapeutic potential of D23 and 3xD23 in Tg2576 mice. Here we directly infused mono- and trivalent DARPin constructs intracerebroventricularly over 28 days. Following infusion D23 and 3xD23 treated mice demonstrated improved cognitive performance, compared to E2_5 non-specific DARPin and PBS treated mice. These findings were supported by histological and biochemical analyses with trends towards less plaque deposition and significant reductions of brain Aβ levels

for both D23 and 3xD23 treated mice; with the most pronounced modulatory effects on the soluble Aβ pool.

5.3 Delta project

In 2008, it was described by Tomiyama and colleagues that a rare mutation in APP at site 693 (E693Δ) lead to the development of AD-like dementia in homozygous carriers. Interestingly, these patients demonstrated very weak PET PIB signaling, suggesting the absence of relevant amyloid deposition in these patients (Shimada et al., 2011; Tomiyama et al., 2008). *In vitro* experiments with synthetic E22Δ Aβ40 and E22Δ Aβ42 peptide preparations demonstrated an enhanced oligomerization propensity, but no fibril formation and led to the hypothesis that AD-like dementia can be caused by the sole presence of synaptotoxic Aβ oligomers (Tomiyama et al., 2008). In contrast to these initial *in vitro* findings, subsequent work, including our own recent study with highly pure recombinant peptide preparations, demonstrated that both E22Δ Aβ40 and E22Δ Aβ42 readily formed amyloid fibrils *in vitro* (Inayathullah et al., 2011; Ovchinnikova et al., 2011; Suzuki et al., 2010). Based on these findings, we hypothesized that E22Δ Aβ peptides could indeed form amyloid fibrils *in vivo*. As shown in **Chapter 4**, E22ΔAβ mice displayed increased levels detergent insoluble (formic acid soluble) Aβ in brain homogenates at 24 months of age. Moreover, these aged mice demonstrated Thioflavin S and Congo red positive amyloid deposits in leptomeningeal cortical and – more pronounced – cerebellar vessels. The identification of CAA as a key neuropathological feature of aged E22ΔAβ mice adds the E693Δ mutation to the list of vasculotropic intra-Aβ APP mutations essentially comprising all of the currently known mutations at or around position 22 of the Aβ sequence (for a review Kumar-Singh et al., 2009). However, further experiments are needed to elucidate the mechanisms underlying the "vasculotropism" of E22Δ-mutated Aβ and whether similar mechanisms as previously reported for the "Dutch" mutation (i.e. a reduced receptor-mediated clearance across the blood brain barrier) play a role (Deane et al., 2004; Monro et al., 2002).

We were also able to demonstrate in this study that E22ΔAβ mice – similar to our previously reported arcAβ mice (Knobloch et al., 2007) – develop intraneuronal Aβ aggregates at a very young age and that these intraneuronal aggregates correlate

with cognitive deficits. Immunohistological characterization of the deposits revealed that the intraneuronal aggregates were strongly stained by OC antibody, directed against fibrillar oligomers, but not A11 antibody, which recognizes prefibrillar oligomers (Kayed et al., 2003; Kayed et al., 2007). Building on the hypothesis that intra-Aβ mutations at or around position 22 of the Aβ increase Aβ fibrillogenesis through a facilitation of a “toxic turn” conformation between positions 22 and 23 of the Aβ sequence, Murakami et al. (2010) developed a novel monoclonal antibody (11A1) directed against this specific conformational epitope of Aβ42 (Murakami et al., 2010). Interestingly, 11A1 stained intraneuronal Aβ aggregates in the brains of the E22ΔAβ mice, suggesting that the oligomeric E22Δ-mutated Aβ deposits contained the abovementioned “toxic turn” conformation.

Apart from A673V, a recently described familial AD APP mutation in an Italian pedigree, E693Δ is the second currently known recessive APP mutation that is pathogenic only in the homozygous state (Di Fede et al., 2009; Tomiyama et al., 2008). Similar to the A673V mutation, which is anti-amyloidogenic in the heterozygous state, our co-aggregation experiments with recombinant E22Δ Aβ peptides variants also revealed an inhibition of Aβ aggregation when mutated and wildtype peptides were co-incubated. In contrast, co-aggregation of E22G (Arctic) Aβ peptides with the respective wildtype Aβ peptides resulted in aggregation curves very similar to those of the E22G Aβ peptides alone. Moreover, E22Δ Aβ42 fibrils, in contrast to wildtype Aβ42 and E22G Aβ42 fibrils, inefficiently seeded wildtype Aβ42 fibrillogenesis. These results provide a possible explanation why heterozygous carriers of the E693Δ mutation do not develop the disease whereas heterozygous carriers of the autosomal dominant Arctic mutation develop dementia.

Future research is planned to determine the pathological mechanisms of E693Δ mutation on tau pathology. For these experiments, we have crossed our E693Δ mouse model with Tau P301L transgenic mice. Preliminary findings suggest that, unlike arcAβ/Tau P301L double transgenic mice, E693Δ/Tau P301L mice do not develop pronounced tau pathology. These findings raise interesting questions as to how E22Δ Aβ fibrils exert their toxic effects.

6 References

Aguzzi, A. and O'Connor, T. (2010). Protein aggregation diseases: pathogenicity and therapeutic prespectives. *Nature Reviews Drug Discovery*, 9, 237-248.

Aguzzi, A. and Rajendran, L. (2009). The transcellular spread of cytosolic amyloids, prions, and prionoids. *Neuron*, 64, 783-790.

Albensi BC, Mattson MP (2000). Evidence for the involvement of TNF and NF-kappaB in hippocampal synaptic plasticity. *Synapse*, 35,151-159.

Allen, N.J., and Barres, B.A. (2009). Neuroscience: Glia - more than just brain glue. *Nature,* 457, 675-677.

Alkam, T., A. Nitta, et al. (2008). Restraining tumor necrosis factor-alpha by thalidomide prevents the amyloid beta-induced impairment of recognition memory in mice. *Behavioral Brain Research*, 189(1), 100-106.

Aloe L, et al. (1999). Learning abilities, NGF and BDNF brain levels in two lines of TNF-alpha transgenic mice, one characterized by neurological disorders, the other phenotypically normal. *Brain Research*, 840, 125-137.

Alvarez, A., et al. (2007). Serum TNF-alpha levels are increased and correlate negatively with free IGF-I in Alzheimer disease. *Neurobiology of Aging*, 28, 533-536.

Amstutz, P. et al. (2005). Intracellular kinase inhibitors selected from combinatorial libraries of designed ankyrin repeat proteins. *Journal of Biological Chemistry*, 280, 24715-24722.

Avital A, et al. (2003). Impaired interleukin-1 signaling is associated with deficits in hippocampal memory processes and neural plasticity. *Hippocampus*, 13, 826-834.

Bains, J.S., and Oliet, S.H. (2007). Glia: they make your memories stick! *Trends Neurosci*ence, 30, 417-424.

Banks, W. A., and Erickson, M. A. (2010). The blood-brain barrier and immune function and dysfunction. *Neurobiology of Disease*, 37(1), 26-32.

Bard, F., et al. (2000). Peripherally administered antibodies against amyloid beta-peptide enter the central nervous system and reduce pathology in a mouse model of Alzheimer disease. *Nature Medicine*, 6, 916-919.

Barres, B.A. (2008). The mystery and magic of glia: a perspective on their roles in health and disease. *Neuron*, 60, 430-440.

Bayer, A.J., et al. (2005). Evaluation of the safety and immunogenicity of synthetic Abeta42 (AN1792) in patients with AD. *Neurology*, 64, 94-101.

Balschun D, et al. (2004): Interleukin-6: a cytokine to forget. *Faseb J*, 18, 1788-1790.

Barnham, K., Masters, C. L., and Bush, A. I. (2004). Neurodegenerative diseases and oxidative stress. *Nature Reviews Drug Discovery*, 3, 205-214.

Baumann, M. J., et al. (2010). DARPins against a functional IgE epitope. *Immunology Letters*, 133, 78-84.

Baune B. T., et al. (2008a). Cognitive dysfunction in mice deficient for TNF- and its receptors. *American Journal of Medical Genetics Part B: Neuropsychiatric Genetics*, 147B(7), 1056-1064.

Baune B. T., et al. (2008b). Association between genetic variants of IL-1beta, IL-6 and TNF-alpha cytokines and cognitive performance in the elderly general population of the MEMO-study. *Psychoneuroendocrinology*, 33, 68-76.

Beattie E. C., et al. (2002). Control of synaptic strength by glial TNFalpha. *Science*, 295, 2282-2285.

Bermejo, P., et al. (2008). Differences of peripheral inflammatory markers between mild cognitive impairment and Alzheimer's disease. *Immunology Letters*, 117, 198-202.

Bertram, L. and Tanzi, R. E. (2008). Thirty years of Alzheimer's disease genetics: the implications of systematic meta-analyses. *Nature Reviews Neuroscience*, 9(10), 768-778.

Bertram, L. Lill, C. M., and Tanzi, R. E. (2010). The genetics of Alzheimer disease: Back to the Future. *Neuron*, 68, 270-281.

Bhat, R. and Steinman, L. (2009). Innate and adaptive autoimmunity directed to the central nervous system. *Neuron*, 64(1), 123-132.

Binz, H. K., et al. (2003). Designing repeat proteins: well-expressed, soluble and stable proteins from combinatorial libraries of consensus ankyrin repeat proteins. *Journal of Molecular Biology*, 332, 489-503.

Binz, H. K. et al. (2004). High-affinity binders selected from designed ankyrin repeat protein libraries. *Nature Biotechnology*, 22, 575-582.

Block, M.L., Zecca, L., and Hong, J.S. (2007). Microglia-mediated neurotoxicity: uncovering the molecular mechanisms. *Nature Reviews Neuroscience*, 8, 57-69.

Boche, D., and Nicoll, J.A. (2008). The role of the immune system in clearance of Abeta from the brain. *Brain Pathology*, 18, 267-278.

Borchelt, D.R., et al. (1996). A vector for expressing foreign genes in the brains and hearts of transgenic mice. *Genet Anal*, 13, 159-163.

Brennan F. X., Beck K. D., and Servatius R. J. (2003). Low doses of interleukin-1beta improve the leverpress avoidance performance of Sprague-Dawley rats. *Neurobiology of Learning and Memory*, 80, 168-171.

Britschigi, M., et al., (2009). Neuroprotective natural antibodies to assemblies of amyloidogenic peptides decrease with normal aging and advancing Alzheimer's disease. *Proceedings of the National Academy of Sciences*, 106(29), 12145-12150.

Brody, D.L., and Holtzman, D.M. (2008). Active and passive immunotherapy for neurodegenerative disorders. *Annul Reviews Neuroscience*, 31, 175-193.

Bruel-Jungerman, E., Davis, S., and Laroche, S. (2007a). Brain plasticity mechanisms and memory: a party of four. *Neuroscientist*, 13, 492-505.

Bruel-Jungerman, E., Rampon, C., and Laroche, S. (2007b). Adult hippocampal neurogenesis, synaptic plasticity and memory: facts and hypotheses. *Reviews Neuroscience*,18, 93-114.

Bugiani, O., et al. (2010). Hereditary cerebral hemorrhage with amyloidosis associated with the E693K mutation of APP. *Archives Neurology*, 67, 987-995.

Burrone J., and Murthy, V. N. (2003). Synaptic gain control and homeostasis. *Current Opinion Neurobiology*, 13, 560-567.

Bushati, N. and Cohen, S. M. (2008). MicroRNAs in neurodegeneration. Current Opinion Neurobiology, 18(3), 292-6.

Butler, M. P., et al. (2004). Dissection of tumor-necrosis factor-alpha inhibition of long-term potentiation (LTP) reveals a p38 mitogen-activated protein kinase-dependent mechanism which maps to early-but not late-phase LTP. *Neuroscience,* 124(2), 319-26.

Camacho, I. E., et al. (2004). Peroxisome-proliferator-activated receptor gamma induces a clearance mechanism for the amyloid-beta peptide. *Journal of Neuroscience,* 24(48), 10908-17.

Campbell I. L., et al. (1997). Transgenic models to assess the pathogenic actions of cytokines in the central nervous system. *Molecular Psychiatry*, 2, 125-129.

Chadwick, W., et. al. (2008) Targeting TNF-alpha receptors for neurotherapeutics. *Trends in Neuroscience*, 31, 504-511.

Chartier-Harlin, M.C., et al. (1991). Screening for the beta-amyloid precursor protein mutation (APP717) in extended pedigrees with early onset Alzheimer's disease. *Neuroscience Letters*, 129, 134-135.

Citron, M., et al. (1992). Mutation of the beta-amyloid precursor protein in familial Alzheimer's disease increases beta-protein production. *Nature*, 360, 672-674.

Citron, M. (2010). Alzheimer's disease: strategies for disease modification. *Nature Reviews Drug Discovery*, 9, 387-398.

Cleary, J.P., et al., (2005). Natural oligomers of the amyloid-beta protein specifically disrupt cogni-tive function. *Nature Neuroscience*, 8(1), 79-84.

Coogan, A. N., O'Neill, L. A., and O'Connor, J. J. (1999). The P38 mitogen-activated protein kinase inhibitor SB203580 antagonizes the inhibitory effects of interleukin-1beta on long-term potentiation in the rat dentate gyrus in vitro. *Neuroscience*, 93, 57-69.

Crawley, J.N., *What's wrong with my mouse? Behanioral phenotyping of transgenic and knockout mice*. 2nd ed. 2007, Hoboken, New Jersey: John Wiley & Sons, Inc.

Davoust, N., et al. (2008). From bone marrow to microglia: barriers and avenues. *Trends in Immunology*, 29(5), 227-234.

Deane, R., et al. (2004). LRP/amyloid beta-peptide interaction mediates differential brain efflux of Abeta isoforms. *Neuron*, 43, 333-344.

Delrieu, J., et al. (2012). 'Clinical trials in Alzheimer's disease': immunotherapy approaches. *Journal of Neurochemistry*, 120, 186-193.

DeMattos, R. B. et al. (2001). Peripheral anti-Aβ antibody alters CNS and plasma Aβ clearance and decreases brain Aβ burden in a mouse model of Alzheimer's disease. *Proceedings of the National Academy of Sciences of the United States of America,* 98, 8850 -8855.

Diamond, B., et al. (2009). Losing your nerves? Maybe it's the antibodies. *Nature Reviews Immunology*, 9, 449-456.

Di Fede, G., et al. (2009). A recessive mutation in the APP gene with dominant-negative effect on amyloidogenesis. *Science*, 323, 1473-1477.

Di Filippo, M., et al. (2008). Neuroinflammation and synaptic plasticity: theoretical basis for a novel, immune-centred, therapeutic approach to neurological disorders. *Trends in Pharmacological Sciences,* 29(8), 402-412.

DiMauro, S. and Schon, E. A. (2008). Mitochondrial disorders in the nervous system. *Annual Review of Neuroscience*, 31, 91-123.

Dorshkind, K., Montecino-Rodriguez, E., and Signer, R.A. (2009). The ageing immune system: is it ever too old to become young again? *Nature Review Immunology*, 9, 57-62.

Du, Y., et al. (2001). Reduced levels of amyloid beta-peptide antibody in Alzheimer disease. *Neurology*, 57, 801-805.

Eckman, C.B., et al. (1997). A new pathogenic mutation in the APP gene (I716V) increases the relative proportion of A beta 42(43). *Human Molecular Genetics*, 6, 2087-2089.

Edison, P., et al. (2008). Microglia, amyloid, and cognition in Alzheimer's disease: An [11C](R)PK11195-PET and [11C]PIB-PET study. *Neurobiology of Disease*, 32, 412-419.

Eggel, A., et al. (2009). DARPins as bispecific receptor antagonists analyzed for immunoglobulin E receptor blockage. *Journal Molecular Biology*, 393, 598-607.

Engelhardt, B. and Ransohoff, R. M. (2005). The ins and outs of T-lymphocyte trafficking to the CNS: anatomical sites and molecular mechanisms. *Trends in Immunology*, 26(9), 485-495.

Escribano, L., et al. (2009). Rosiglitazone reverses memory decline and hippocampal glucocorticoid receptor down-regulation in an Alzheimer's disease mouse model. *Biochemistry Biophysical Research Communication,* 379(2), 406-10.

Farina, C., Aloisi, F., and Meinl, E. (2007). Astrocytes are active players in cerebral innate immunity. *Trends in Immunology*, 28, 138-145.

Ferrer, I., et al. (2004). Neuropathology and pathogenesis of encephalitis following amyloid-beta immunization in Alzheimer's disease. *Brain Pathology*, 14, 11-20.

Fiala, M., et al. (2007). Phagocytosis of amyloid-beta and inflammation: two faces of innate immunity in Alzheimer's disease. *Journal of Alzheimer's Disease*, 11, 457-463.

Finder, V. H., et al. (2010). The Recombinant Amyloid-[beta] Peptide A[beta]1-42 Aggregates Faster and Is More Neurotoxic than Synthetic A[beta]1-42. *Journal of Molecular Biology*, 396, 9-18.

Forman, M. S., Trojanowski, J. Q. and Lee, V. M. (2004). Neurodegenerative diseases: A decade of discoveries paves the way for therapeutic breakthroughs. *Nature Medicine*, 10,1055-1063.

Fraser, P.E., et al. (1992). Fibril formation by primate, rodent, and Dutch-hemorrhagic analogues of Alzheimer amyloid beta-protein. *Biochemistry*, 31, 10716-10723.

Freshney, R. I. (2010). Culture of Animal Cells: A Manual of Basic Technique and Specialized Applications. John Wiley and Sons: New Jersey.

Friguet, B., et al. (1985). Measurements of the true affinity constant in solution of antigen-antibody complexes by enzyme-linked immunosorbent assay. *Journal of Immunological Methods*, 77, 305-319.

Geylis, V., et al. (2005). Human monoclonal antibodies against amyloid-beta from healthy adults. *Neurobiology of Aging*, 26, 597-606.

Gilman, S., et al. (2005). Clinical effects of Abeta immunization (AN1792) in patients with AD in an interrupted trial. *Neurology,* 64, 1553-1562.

Gimeno, D., Marmot, M.G., and Singh-Manoux, A. (2008). Inflammatory markers and cognitive function in middle-aged adults: the Whitehall II study. *Psychoneuroendocrinology,* 33, 1322-1334.

Goate, A., et al. (1991). Segregation of a missense mutation in the amyloid precursor protein gene with familial Alzheimer's disease. *Nature*, 349, 704-706.

Godbout JP, Johnson RW: Interleukin-6 in the aging brain. *Journal of Neuroimmunology*, 2004;147:141-144.

Goshen I, et al. (2007). A dual role for interleukin-1 in hippocampal-dependent memory processes. *Psychoneuroendocrinology*, 32, 1106-1115.

Graeber, M. B. (2010). Changing Face of Microglia. *Science*, 330, 783-788.

Goshen, I., et al. (2007). A dual role for interleukin-1 in hippocampal-dependent memory processes. *Psychoneuroendocrinology,* 32(8-10), 1106-15.

Gouras, G.K., et al. (2010). Intraneuronal beta-amyloid accumulation and synapse pathology in Alzheimer's disease. *Acta Neuropathologia*, 119, 523-541.

Grabowski, T.J., et al. (2001). Novel amyloid precursor protein mutation in an Iowa family with dementia and severe cerebral amyloid angiopathy. *Annuals Neurology*, 49, 697-705.

Griffin, W.S. (2008). Perispinal etanercept: Potential as an Alzheimer therapeutic. *Journal of Neuroinflammation*, 5, 3.

Haass, C., et al. (1995). The Swedish mutation causes early-onset Alzheimer's disease by beta-secretase cleavage within the secretory pathway. *Nature Medicine*, 1, 1291-1296.

Haass, C. and Selkoe, D. J. (2007). Soluble protein oligomers in neurodegeneration: lessons form the Alzheimer’s amyloid β-peptide. *Nature Reviews Molecular Cell Biology*, 8, 101-112.

Haass, C., et al. (1994). Mutations associated with a locus for familial Alzheimer's disease result in alternative processing of amyloid beta-protein precursor. *Journal of Biological Chemistry*, 269, 17741-17748.

Hager, K., et al. (2007). Alpha-lipoic acid as a new treatment option for Alzheimer's disease--a 48 months follow-up analysis. *Journal of Neural Transmission*, Suppl, 189-193.

Halassa, M.M., Fellin, T., and Haydon, P.G. (2007). The tripartite synapse: roles for gliotransmission in health and disease. *Trends in Molecular Medicine*, 13, 54-63.

Hanisch, U.K., and Kettenmann, H. (2007). Microglia: active sensor and versatile effector cells in the normal and pathologic brain. *Nature Neuroscience*, 10, 1387-1394.

Hardy, J. and Selkoe, D. J. (2002). The amyloid hypothesis of Alzheimer's disease: Progress and problems on the road to therapeutics. *Science*, 297(5580), 353-356.

He, P., et al. (2007). Deletion of tumor necrosis factor death receptor inhibits amyloid {beta} generation and prevents learning and memory deficits in Alzheimer's mice. *Journal of Cell Biology,* 178(5), 829-41.

Hendriks, L., et al. (1992). Presenile dementia and cerebral haemorrhage linked to a mutation at codon 692 of the beta-amyloid precursor protein gene. *Nature Genetics*, 1, 218-221.

Herzig, M.C., et al. (2004). Abeta is targeted to the vasculature in a mouse model of hereditary cerebral hemorrhage with amyloidosis. *Nature Neuroscience*, 7, 954-960.

Hock, C., et al. (2002). Generation of antibodies specific for beta-amyloid by vaccination of patients with Alzheimer disease. *Nature Medicine*, 8, 1270-1275.

Hock, C., et al. (2003). Antibodies against beta-amyloid slow cognitive decline in Alzheimer's disease. *Neuron*, 38, 547-554.

Holmes, C., et al. (2008). Long-term effects of Abeta42 immunisation in Alzheimer's disease: follow-up of a randomised, placebo-controlled phase I trial. *Lancet*, 372, 216-223.

Hryniewicz A, et al. (2007). Impairment of recognition memory in interleukin-6 knock-out mice. *European Journal of Pharmacology*, 577, 219-220.

Hsiao, K., et al. (1996). Correlative memory deficits, Abeta elevation, and amyloid plaques in transgenic mice. *Science*, 274, 99-102.

Huber, T., et al. (2007). In vitro selection and characterization of DARPins and Fab fragments for the co-crystallization of membrane proteins: The Na(+)-citrate symporter CitS as an example. *Journal of Structural Biology*, 159, 206-221.

Hudson, S. A., et al. (2009). The thioflavin T fluorescence assay for amyloid fibril detection can be biased by the presence of exogenous compounds. *FEBS Journal*, 276, 5960-5972.

Inayathullah, M. and Teplow, D.B. (2011). Structural dynamics of the DeltaE22 (Osaka) familial Alzheimer's disease-linked amyloid beta-protein. *Amyloid*, 18, 98-107.

Jankowsky JL, Derrick BE, Patterson PH: Cytokine responses to LTP induction in the rat hippocampus: a comparison of in vitro and in vivo techniques. Learn Mem 2000;7:400-412.

Jimenez, S., et al. (2008). Inflammatory response in the hippocampus of PS1M146L/APP751SL mouse model of Alzheimer's disease: age-dependent switch in the microglial phenotype from alternative to classic. *Journal of Neuroscience*, 28, 11650-11661.

Johnston, M., et al. (2004). Evidence of connections between cerebrospinal fluid and nasal lymphatic vessels in humans, non-human primates and other mammalian species. *Cerebrospinal Fluid Research*, 1, 2.

Kawarabayashi, T., et al. (2001). Age-dependent changes in brain, CSF, and plasma amyloid (beta) protein in the Tg2576 transgenic mouse model of Alzheimer's disease. *Journal of Neuroscience*, 21, 372-381.

Kayed, R. et al. (2003). Common Structure of Soluble Amyloid Oligomers Implies Common Mechanism of Pathogenesis. *Science*, 300, 486 -489.

Kayed, R., et al. (2007). Fibril specific, conformation dependent antibodies recognize a generic epitope common to amyloid fibrils and fibrillar oligomers that is absent in prefibrillar oligomers. *Molecular Neurodegeneration*, 2, 18.

Kellner, A., et al. (2009). Autoantibodies against beta-amyloid are common in Alzheimer's disease and help control plaque burden. *Annuals of Neurology*, 65, 24-31.

Kettenmann, H. (2007). Neuroscience: the brain's garbage men. *Nature*, 446, 987-989.

Kim et al. (1988). Production and characterization of monoclonal antibodies reactive to synthetic cerebrovascular amyloid peptide. *Neuroscience Research Commication,* 2, 121-130.

Knobloch, M., et al., (2007) Intracellular Aβ and cognitive deficits precede β-amyloid deposition in transgenic arcAβ mice. *Neurobiology of Aging*, 28, 1297-1306.

Koenigsknecht-Talboo, J., et al. (2008). Rapid microglial response around amyloid pathology after systemic anti-Abeta antibody administration in PDAPP mice. *Journal of Neuroscience*, 28, 14156-14164.

Kumar-Singh, S. (2009). Hereditary and sporadic forms of abeta-cerebrovascular amyloidosis and relevant transgenic mouse models. *International Journal of Molecular Science*, 10, 1872-1895.

Kumar-Singh, S. (2008). Cerebral amyloid angiopathy: pathogenetic mechanisms and link to dense amyloid plaques. *Genes Brain Behavior*, 7 Suppl 1, 67-82.

Kumar-Singh, S., et al. (2002). Dense-core senile plaques in the Flemish variant of Alzheimer's disease are vasocentric. *American Journal of Pathology*, 161, 507-520.

Lacor, P.N., et al., (2007). Abeta oligomer-induced aberrations in synapse composition, shape, and density provide a molecular basis for loss of connectivity in Alzheimer's disease. *Journal of Neuroscience*, 27(4), 796-807.

Lammich, S., et al. (1999). Constitutive and regulated alpha-secretase cleavage of Alzheimer's amyloid precursor protein by a disintegrin metalloprotease. *Proceedings of the National Academy of Sciences of the United States of America,* 96, 3922-3927.

Landreth, G., et al. (2008). PPARgamma agonists as therapeutics for the treatment of Alzheimer's disease. *Neurotherapeutics,* 5, 481-489.

Lee, S.-J., et al. (2010). Cell-to-cell transmission of non-prion protein aggregates. *Nature Review Neurology*, 6, 702-706.

Lemere, C. A., and Masliah, E. (2010). Can Alzheimer disease be prevented by amyloid-β immunotherapy? *Nature Reviews Neurology*, 6, 108-119.

Lesne, S., et al. (2006). A specific amyloid-beta protein assembly in the brain impairs memory. *Nature*, 440(7082), 352-357.

Leung, E., et al. (2009). Microglia activation mediates fibrillar amyloid-beta toxicity in the aged primate cortex. *Neurobiology of Aging*.

LeVine, H. (1993). Thioflavine T interaction with synthetic Alzheimer's disease beta-amyloid peptides: detection of amyloid aggregation in solution. *Protein Science*, 2, 404-410.

Levy, E., et al. (1990). Mutation of the Alzheimer's disease amyloid gene in hereditary cerebral hemorrhage, Dutch type. *Science*, 248, 1124-1126.

Li A. J., et al. (1997). Interleukin-6 inhibits long-term potentiation in rat hippocampal slices. *Brain Research*, 748, 30-38.

Li, S., et al., (2009). Soluble oligomers of amyloid Beta protein facilitate hippocampal long-term de-pression by disrupting neuronal glutamate uptake*. Neuron*, 62(6), 788-801.

Liao, Y. F., et al. (2004). Tumor necrosis factor-alpha, interleukin-1beta, and interferon-gamma stimulate gamma-secretase-mediated cleavage of amyloid precursor protein through a JNK-dependent MAPK pathway. *Journal of Biological Chemistry*, 279(47), 49523-32.

Lin, M. T. and Beal, F. M. (2006). Mitochondrial dysfunction and oxidative stress in neurodegenerative diseases. *Nature*, 443, 7887-795.

Loane, D. J., et al. (2007). Interleukin-4 mediates the neuroprotective effects of rosiglitazone in the aged brain. *Neurobiology of Aging*.

Lu, T., et al. (2004). Gene regulation and DNA damage in the ageing human brain. *Nature*, 429(6994): 883-91.

Malenka RC, Bear MF (2004). LTP and LTD: an embarrassment of riches. *Neuron*, 44, 5-21.

Mandel, S., et al. (2007). Iron dysregulation in Alzheimer's disease: multimodal brain permeable iron chelating drugs, possessing neuroprotective-neurorescue and amyloid precursor protein-processing regulatory activities as therapeutic agents. *Progress in Neurobiology*, 82, 348-360.

Marcello, A., et al. (2011). Reduced levels of IgM autoantibodies against N-truncated pyroglutamate Aβ in plasma of patients with Alzheimer's disase. *Neurobiology of Aging*, 32(8), 1379-1387.

Martinez-Vicente, M. and Cuervo, A. M. (2007). Autophagy and neurodegeneration: when the cleaning crew goes on strike. *The Lancet Neurology*, 6(4), 352-361.

Masliah, E., et al. (2005). Abeta vaccination effects on plaque pathology in the absence of encephalitis in Alzheimer disease. *Neurology*, 64, 129-131.

McAfoose, J., Koerner, H., and Baune, B. (2008). The effects of TNF deficiency on age-related cognitive performance. *Psychoneuroendocrinology*, 34(4), 615-619.

McAfoose, J. and Baune, B. (2009). Evidence for a cytokine model of cognitive function. *Neuroscience & Biobehavioral Reviews*, 33(3), 355-366)

McKinnon, P. J. (2009). DNA repair deficiency and neurological disease. *Nature Reviews Neuroscience*, 10(2): 100-12.

Medeiros, R., et al. (2007). Connecting TNF-alpha signaling pathways to iNOS expression in a mouse model of Alzheimer's disease: relevance for the behavioral and synaptic deficits induced by amyloid beta protein. *Journal of Neuroscience,* 27(20), 5394-404.

Merlini, M., et al. (2011). Vascular β-amyloid and early astrocyte alternations impair cerebrovascular function and cerebral metabolism in transgenic arcAβ mice. *Acta Neuropathologica*, 122(3), 293-311.

Meyer-Luehmann, M., et al. (2008). Rapid appearance and local toxicity of amyloid-beta plaques in a mouse model of Alzheimer's disease. *Nature,* 451, 720-724.

Milovnik, P., et al. (2009). Selection and characterization of DARPins specific for the neurotensin receptor 1. *Protein Engineering Design and Selection,* 22, 357 -366.

Mohajeri, M. H. et al. (2002). Passive Immunization against β-Amyloid Peptide Protects Central Nervous System (CNS) Neurons from Increased Vulnerability Associated with an Alzheimer's Disease-causing Mutation. *Journal of Biological Chemistry*, 277, 33012 -33017.

Monro, O.R., et al. (2002). Substitution at codon 22 reduces clearance of Alzheimer's amyloid-beta peptide from the cerebrospinal fluid and prevents its transport from the central nervous system into blood. *Neurobiology of Aging*, 23, 405-412.

Morgan, D. et al. (2000). A beta peptide vaccination prevents memory loss in an animal model of Alzheimer's disease. *Nature*, 408, 982-985.

Mullan, M., et al. (1992). A pathogenic mutation for probable Alzheimer's disease in the APP gene at the N-terminus of beta-amyloid. *Nature Genetics*, 1, 345-347.

Murakami, K., et al. (2003). Neurotoxicity and physicochemical properties of Abeta mutant peptides from cerebral amyloid angiopathy: implication for the pathogenesis of cerebral amyloid angiopathy and Alzheimer's disease. *Journal of Biological Chemistry*, 278, 46179-46187.

Murakami, A., et al. (2010). Monoclonal Antibody Against the Turn of the 42-Residue Amyloid β-Protein at Positions 22 and 23. *ACS Chemistry Neuroscience*, 1, 747-756.

Murakami, K., et al. (2010). The turn formation at positions 22 and 23 in the 42-mer amyloid beta peptide: the emerging role in the pathogenesis of Alzheimer's disease. *Geriatrics Gerontology International,* 10 Suppl 1, S169-179.

Murrell, J., et al. (1991). A mutation in the amyloid precursor protein associated with hereditary Alzheimer's disease. *Science*, 254, 97-99.

Neff, F., et al. (2008). Immunotherapy and naturally occurring autoantibodies in neurodegenerative disorders. *Autoimmunity Reviews*, 7, 501-507.

Nelson, P. T., et al. (2008). MicroRNAs (miRNAs) in neurodegenerative diseases. *Brain Pathology*, 18(1), 130-8.

Neumann, H., Kotter, M.R., and Franklin, R.J. (2009). Debris clearance by microglia: an essential link between degeneration and regeneration. *Brain*, 132, 288-295.

Neumann H, et al. (2002). Tumor necrosis factor inhibits neurite outgrowth and branching of hippocampal neurons by a rho-dependent mechanism. *Journal of Neuroscience*, 22, 854-862.

Nicoll, J.A., et al. (2003). Neuropathology of human Alzheimer disease after immunization with amyloid-beta peptide: a case report. *Nature Medicine*, 9, 448-452.

Nikolaev, A., et al. (2009). APP binds DR6 to trigger axon pruning and neuron death via distinct caspases. *Nature*, 457, 981-989.

Nikolich-Zugich, J. (2008). Ageing and life-long maintenance of T-cell subsets in the face of latent persistent infections. *Nature Review Immunology*, 8, 512-522.

Nilsberth, C., et al. (2001). The 'Arctic' APP mutation (E693G) causes Alzheimer's disease by enhanced Abeta protofibril formation. *Nature Neuroscience*, 4, 887-893.

Nishitsuji, K., et al. (2009). The E693Delta mutation in amyloid precursor protein increases intracellular accumulation of amyloid beta oligomers and causes endoplasmic reticulum stress-induced apoptosis in cultured cells. *American Journal of Pathology*, 174, 957-969.

Nizri E, et al. (2006) Anti-inflammatory properties of cholinergic up-regulation: A new role for acetylcholinesterase inhibitors. *Neuropharmacology*, 50, 540-547.

O'Nuallain, B. and Wetzel, R. (2002). Conformational Abs recognizing a generic amyloid fibril epitope. *Proceedings of the National Academy of Sciences of the United States of America*, 99, 1485-1490.

Orgogozo, J.M., et al. (2003). Subacute meningoencephalitis in a subset of patients with AD after Abeta42 immunization. *Neurology*, 61, 46-54.

Ovchinnikova, O.Y., et al. (2011). The Osaka FAD mutation E22Delta leads to the formation of a previously unknown type of amyloid beta fibrils and modulates Abeta neurotoxicity. *Journal of Molecular Biology*, 408, 780-791.

Papachroni, K. K., et al. (2007). Autoantibodies to alpha-synuclein in inherited Parkinson's disease. *Journal of Neurochemistry*, 101, 749-756.

Parrish W. R., et al. (2008) Modulation of TNF release by choline requires alpha7 subunit nicotinic acetylcholine receptor-mediated signaling. *Molecular Medicine*, 14, 567-574.

Paul, C.M., Magda, G. and Abel, S. (2009). Spatial memory: Theoretical basis and comparative review on experimental methods in rodents. *Behavioural Brain Research*, 203, 151-164.

Pavlov V. A., et al. (2009) Brain acetylcholinesterase activity controls systemic cytokine levels through the cholinergic anti-inflammatory pathway. *Brain Behavior and Immunity*, 23, 41-45.

Pedersen, W. A., et al. (2006). Rosiglitazone attenuates learning and memory deficits in Tg2576 Alzheimer mice. *Experimental Neurology,* 199(2), 265-73.

Perez-Otano I., and Ehlers M. D. (2005). Homeostatic plasticity and NMDA receptor trafficking. *Trends in Neuroscience*, 28, 229-238.

Perry, H. V., Cunningham, C. and Holmes, C. (2007). Systemic infections and inflammation affect chronic neurodegeneration. *Nature Reviews Immunology*, 7, 161-167.

Perry, H. V., Nicoll, J. A. R., and Holmes, C. (2010). Microglia in neurodegenerative diease. *Nature Reviews Neurology*, 6, 193-201.

Pickering, M., Cumiskey, D., and O'Connor, J. J. (2005). Actions of TNF-alpha on glutamatergic synaptic transmission in the central nervous system. *Experimental Physiology*, 90, 663-670.

Popovich, P.G., and Longbrake, E.E. (2008). Can the immune system be harnessed to repair the CNS? *Nature Reviews Neuroscience*, 9, 481-493.

Pride, M., et al. (2008). Progress in the active immunotherapeutic approach to Alzheimer's disease: clinical investigations into AN1792-associated meningoencephalitis. *Neurodegenerative Diseases*, 5, 194-196.

Pugh, C., et al. (2001). The immune system and memory consolidation: a role for the cytokine IL-1beta. *Neuroscience & Biobehavioral Reviews*, 25, 29-41.

Rademakers, R. and Rovelet-Lecrux, A. (2009). Recent insights into the molecular genetics of dementia. *Trends in Neurosciences*, 32(8), 451-461.

Ramakrishnan, M., et al. (2009). Surface Plasmon Resonance Binding Kinetics of Alzheimer's Disease Amyloid β Peptide-Capturing and Plaque-Binding Monoclonal Antibodies. *Biochemistry,* 48, 10405-10415.

Ransohoff, R. M. (2007). Microgliosis: the questions shape the answers. *Nature Neuroscience*. 10, 1507-1509.

Ransohoff, R.M., Kivisakk, P., and Kidd, G. (2003). Three or more routes for leukocyte migration into the central nervous system. *Nature Reviews Immunology*, 3, 569-581.

Ransohoff, R.M., and Perry, V.H. (2009). Microglial Physiology: Unique Stimuli, Specialized Responses. *Annual Review of Immunology*, 27, 119-145.

Reeve, A. K., Krishnan, K. J. and Turnbull, D. (2008). Mitochondrial DNA mutations in disease, aging, and neurodegeneration. *Annals of the New York Academy of Sciences,* 1147, 21-29.

Relkin, N. R. et al. (2009). 18-Month study of intravenous immunoglobulin for treatment of mild Alzheimer disease. *Neurobiology of Aging*, 30, 1728-1736.

Reuben, D.B., et al. (2002). Peripheral blood markers of inflammation predict mortality and functional decline in high-functioning community-dwelling older persons. *Journal American Geriatric Society*, 50, 638-644.

Richez, C., et al. (2005) Neuropathy resembling CIDP in patients receiving tumor necrosis factor-alpha blockers. *Neurology*, 64, 1468-1470.

Rinne, J. O. et al. (2010). 11C-PiB PET assessment of change in fibrillar amyloid-[beta] load in patients with Alzheimer's disease treated with bapineuzumab: a phase 2, double-blind, placebo-controlled, ascending-dose study. *The Lancet Neurology*, 9, 363-372.

Risner, M. E., et al. (2006). Efficacy of rosiglitazone in a genetically defined population with mild-to-moderate Alzheimer's disease. *Pharmacogenomics*, 6, 246-254.

Rodriguez, M., Warrington, A.E., and Pease, L.R. (2009). Invited Article: Human natural autoantibodies in the treatment of neurologic disease. *Neurology,* 72, 1269-1276.

Rojo, L.E., et al., (2008) Neuroinflammation: implications for the pathogenesis and molecular diagnosis of Alzheimer's disease. *Archives Medical Research*, 39(1), 1-16.

Ron-Harel, N. and Schwartz, M. (2009). Can rejuvenation of immunity reverse memory loss? *Trends in Neurosciences*, 32(7), 367-375.

Ross, F. M., et al., (2003). A dual role for interleukin-1 in LTP in mouse hippocampal slices. *Journal of Neuroimmunology*, 144, 61-67.

Rostene, W., Kitabgi, P. and Parsadaniantz, S. M. (2007). Chemokines: a new class of neuromodulator? *Nature Reviews Neuroscience*, 8, 895-903.

Rowan, M. J., et al. (2007). Synaptic memory mechanisms: Alzheimer's disease amyloid beta-peptide-induced dysfunction. *Biochemical Society Transactions,* 35(5), 1219-1223.

Rubinsztein, D. C. (2006). The roles of intracellular protein-degradation pathways in neurodegeneration. *Nature*, 443, 780-786.

Sahlin, C., et al. (2007). The Arctic Alzheimer mutation favors intracellular amyloid-beta production by making amyloid precursor protein less available to alpha-secretase. *Journal of Neurochemistry*, 101, 854-862.

Salminen, A., et al. (2009). Inflammation in Alzheimer's disease: Amyloid-beta oligomers tigger innate immunity defence via pattern recognition receptors. *Progress in Neurobiology*, 87, 181-194.

Sastre, M., J., et al. (2008). Interactions between APP secretases and inflammatory mediators. *Journal of Neuroinflammation*, 5: 25.

Schenk, D. et al. (1999). Immunization with amyloid-beta attenuates Alzheimer-disease-like pathology in the PDAPP mouse. *Nature*, 400, 173-177.

Schliebs, R. and Arendt, T. (2010). The cholinergic system in aging and neuronal degeneration. *Behavioural Brain Research*, 221(2), 555-563.

Schneider, H., et al. (1998). A neuromodulatory role of interleukin-1beta in the hippocampus. *Proceedings of the National Academy of Sciences of the United States of America,* 95, 7778-7783.

Schram, M.T., et al. (2007). Systemic markers of inflammation and cognitive decline in old age. *Journal American Geriatric Society*, 55, 708-716.

Schwartz, M., and Ziv, Y. (2008a). Immunity to self and self-maintenance: a unified theory of brain pathologies. *Trends in Immunology*, 29, 211-219.

Schwartz, M., and Ziv, Y. (2008b). Immunity to self and self-maintenance: what can tumor immunology teach us about ALS and Alzheimer's disease? *Trends in Pharmacological Sciences*, 29, 287-293.

Schwartz, M., and Shechter, R. (2010). Protective autoimmunity functions by intracranial immunosurveillance to support the mind: The missing link between health and disease. *Molecular Psychiatry*, 15, 342-554.

Schweizer, A. et al. (2007). Inhibition of caspase-2 by a designed ankyrin repeat protein: specificity, structure, and inhibition mechanism. *Structure*, 15, 625-636.

Shankar, G.M., et al., (2008). Amyloid-beta protein dimers isolated directly from Alzheimer's brains impair synaptic plasticity and memory. *Nature Medicine*, 14(8), 837-842.

Shaw, A. C., et al. (2010). Aging of the innate immune system. *Current Opinion in Immunology*, 22(4), 507-513.

Shie, F.S., et al. (2009). Modulation of Microglial Innate Immunity in Alzheimer's Disease by Activation of Peroxisome Proliferator-activated Receptor Gamma. *Current Medical Chemistry*, 16, 643-651.

Shimada, H., et al. (2011). Clinical course of patients with familial early-onset Alzheimer's disease potentially lacking senile plaques bearing the E693Delta mutation in amyloid precursor protein. *Dementia Geriatric Cognitive Disorders*, 32, 45-54.

Sicotte N. L., and Voskuhl R. R. (2001) Onset of multiple sclerosis associated with anti-TNF therapy. *Neurology*, 57, 1885-1888.

Siemers, E. R., et al. (2010). Safety and changes in plasma and cerebrospinal fluid amyloid beta after a single administration of an amyloid beta monoclonal antibody in subjects with Alzheimer disease. *Clinical Neuropharmacology*, 33, 67-73.

Small, D. H. (2008). Network dysfunction in Alzheimer's disease: does synaptic scaling drive disease progression? *Trends in Molecular Medicine,* 14(3), 103-108.

Solano, R.M., et al. (2008). Glial dysfunction in parkin null mice: effects of aging. *Journal of Neuroscience*, 28, 598-611.

Sorrells, S. F. and Sapolsky, R. M. (2007). An inflammatory review of glucocorticoid actions in the CNS. *Brain, Behavior, and Immunity*, 21(3), 259-272.

Sotiropoulos, I., et al. (2008). Stress and glucocorticoid footprints in the brain – The path from depression to Alzheimer's disease. *Neuroscience & Biobehavioral Reviews*, 32(6), 1161-1173.

Stellwagen, D., et al. (2005). Differential regulation of AMPA receptor and GABA receptor trafficking by tumor necrosis factor-alpha. *Journal of Neuroscience*, 25, 3219-3228.

Stellwagen, D., and Malenka, R. C. (2006). Synaptic scaling mediated by glial TNF-alpha. *Nature*, 440, 1054-1059.

Stenh, C., et al. (2002). The Arctic mutation interferes with processing of the amyloid precursor protein. *Neuroreport*, 13, 1857-1860.

Stine, W. B., et al. (2003). In vitro characterization of conditions for amyloid-beta peptide oligomerization and fibrillogenesis. *Journal Biological Chemistry*, 278, 11612-11622.

Streit, W.J. (2006). Microglial senescence: does the brain's immune system have an expiration date? *Trends in Neuroscience*, 29, 506-510.

Streit, W.J., et al. (2008). Microglial degeneration in the aging brain--bad news for neurons? *Frontiers in Bioscience*, 13, 3423-3438.

Stumpp, M. T., Binz, H. K., and Amstutz, P. (2008). DARPins: a new generation of protein therapeutics. *Drug Discovery Today*, 13, 695-701.

Stumpp, M. T., and Amstutz, P. (2007). DARPins: a true alternative to antibodies. *Current Opinion Drug Discovery Development*, 10, 153-159.

Suzuki, T., et al. (2010). E22Delta Mutation in Amyloid beta-Protein Promotes beta-Sheet Transformation, Radical Production, and Synaptotoxicity, But Not Neurotoxicity. *International Journal of Alzheimers Disease*, 431320.

Szabo, P., Relkin, N., and Weksler, M. E. (2008). Natural human antibodies to amyloid beta peptide. *Autoimmune Reviews*, 7, 415-420.

Szelenyi, J. (2001). Cytokines and the central nervous system. *Brain Research Bulletin*, 54, 329-338.

Takuma, H., et al. (2008). Amyloid-beta E22Delta variant induces synaptic alteration in mouse hippocampal slices. *Neuroreport*, 19, 615-619.

Tampellini, D. et al. (2007). Internalized Antibodies to the Aβ Domain of APP Reduce Neuronal Aβ and Protect against Synaptic Alterations. *Journal of Biological Chemistry,* 282, 18895 -18906.

Tampellini, D., and Gouras, G. K. (2010). Synapses, synaptic activity and intraneuronal abeta in Alzheimer's disease. *Frontiers in Aging Neuroscience*, 2.

Tancredi V., et al. (2000). The inhibitory effects of interleukin-6 on synaptic plasticity in the rat hippocampus are associated with an inhibition of mitogen-activated protein kinase ERK. *Journal of Neurochemistry*, 75, 634-643.

Tanzi, R.E., and Bertram, L. (2005). Twenty years of the Alzheimer's disease amyloid hypothesis: a genetic perspective. *Cell*, 120, 545-555.

Taoufik, E., et al. (2008). Positive and negative implications of tumor necrosis factor neutralization for the pathogenesis of multiple sclerosis. *Neurodegenerative Diseases*, 5, 32-37.

Thal, D.R., Del Tredici, K., and Braak, H. (2004). Neurodegeneration in normal brain aging and disease. *Science Aging Knowledge Environment*, 26.

Thal, D.R., Griffin, W.S., and Braak, H. (2008). Parenchymal and vascular Abeta-deposition and its effects on the degeneration of neurons and cognition in Alzheimer's disease. *Journal of Cell Molecular Medicine*, 12, 1848-1862.

Tobinick, E. (2008). Perispinal etanercept for neuroinflammatory disorders. *Drug Discovery Today*, 14(3-4), 168-177.

Tobinick, E. (2009). Tumor Necrosis Factor Modulation for Treatment of Alzheimer's Disease: Rationale and Current Evidence. *CNS Drugs*, 23(9), 713-725.

Tobinick, E., et al. (2006). TNF-alpha modulation for treatment of Alzheimer's disease: a 6-month pilot study. *MedGenMed*, 8(2), 25.

Tobinick, E.L., and Gross, H. (2008a). Rapid cognitive improvement in Alzheimer's disease following perispinal etanercept administration. *Journal of Neuroinflammation*, 5, 2.

Tomic, J.L., et al. (2009). Soluble fibrillar oligomer levels are elevated in Alzheimer's disease brain and correlate with cognitive dysfunction. *Neurobiology of Disease*, 35, 352-358.

Tomiyama, T., et al. (2008). A new amyloid beta variant favoring oligomerization in Alzheimer's-type dementia. *Annuals Neurology*, 63(3), 377-387.

Tomiyama, T., et al. (2010). A mouse model of amyloid beta oligomers: their contribution to synaptic alteration, abnormal tau phosphorylation, glial activation, and neuronal loss in vivo. *Journal of Neuroscience*, 30, 4845-4856.

Townsend, M., et al., (2006). Effects of secreted oligomers of amyloid beta-protein on hippocampal synaptic plasticity: a potent role for trimers. *Journal of Physiology*, 572(2), 477-492.

Turrigiano, G. G. (2006). More than a sidekick: glia and homeostatic synaptic plasticity. *Trends in Molecular Medicine*, 12, 458-460.

Turrigiano, G. (2007). Homeostatic signaling: the positive side of negative feedback. *Current Opinion Neurobiology*, 17, 318-324.

Tweedie, D., Sambamurti, K., and Greig N. H. (2007) TNF-alpha inhibition as a treatment strategy for neurodegenerative disorders: new drug candidates and targets. *Current Alzheimer Reseach*, 4, 378-385.

Umeda, T., et al. (2011). Intraneuronal amyloid beta oligomers cause cell death via endoplasmic reticulum stress, endosomal/lysosomal leakage, and mitochondrial dysfunction in vivo. *Journal of Neuroscience Research*, 89, 1031-1042.

Vellas, B., et al. (2009). Long-term follow-up of patients immunized with AN1792: reduced functional decline in antibody responders. *Current Alzheimer Research*, 6, 144-151.

Vitkovic, L., Bockaert, J., and Jacque, C. (2000a) Inflammatory cytokines: neuromodulators in normal brain? *Journal of Neurochemistry*, 74, 457-471.

Vitkovic, L., et al. (2000b) Cytokine signals propagate through the brain. *Molecular Psychiatry*, 5, 604-615.

Vogel, M., et al. (2007). Designed ankyrin repeat proteins as anti-idiotypic-binding molecules. *Ann. N. Y. Acad. Sci*, 1109, 9-18.

Wang, D.D., and Bordey, A. (2008). The astrocyte odyssey. *Progress in Neurobiology*, 86, 342-367.

Wang, Q., J., et al. (2005). Beta-amyloid inhibition of long-term potentiation is mediated via tumor necrosis factor. *European Journal of Neuroscience,* 22(11), 2827-2832.

Walsh, D.M., et al., (2002). Naturally secreted oligomers of amyloid beta protein potently inhibit hippocampal long-term potentiation in vivo. *Nature*, 416(6880), 535-539.

Watson, G. S., et al. (2005). Preserved cognition in patients with early Alzheimer disease and amnestic mild cognitive impairment during treatment with rosiglitazone: a preliminary study. *American Journal of Geriatric Psychiatry*, 13(11), 950-8.

Weksler, M. E., Pawelec, G., and Franceschi, C. (2009). Immune therapy for age-related diseases. *Trends in Immunology*, 30(7), 344-350.

Weksler, M.E., et al. (2002). Patients with Alzheimer disease have lower levels of serum anti-amyloid peptide antibodies than healthy elderly individuals. *Experimental Gerontology*, 37, 943-948.

Winters, B.D., Saksida, L. M. and Bussey, T. J., (2008). Object recognition memory: Neurobiological mechanisms of encoding, consolidation and retrieval. *Neuroscience & Biobehavioral Reviews*, 32, 1055-1070.

Winton, M.J., et al. (2011). Intraneuronal APP, not free Abeta peptides in 3xTg-AD mice: implications for tau versus Abeta-mediated Alzheimer neurodegeneration. *Journal of Neuroscience*, 31, 7691-7699.

Wisniewski, T., and Konietzko, U. (2008). Amyloid-beta immunisation for Alzheimer's disease. *Lancet Neurology*, 7, 805-811.

Wong E., and Cuervo, A. M. (2010). Autophagy gone awry in neurodegenerative diseases. *Nature Neuroscience*, 13(7), 805-811.

Wood, S. J., et al. (1996). Physical, morphological and functional differences between ph 5.8 and 7.4 aggregates of the Alzheimer's amyloid peptide Abeta. *Journal Molecular Biology*, 256, 870-877.

Wyss-Coray, T., et al., (2003). Adult mouse astrocytes degrade amyloid-β *in-vitro* and *in situ*. *Nature Medicine*, 9, 453-457.

Wyss-Coray, T. (2006). Inflammation in Alzheimer disease: driving force, bystander or beneficial response? *Nature Medicine*, 12(9): 1005-15.

Yamamoto, M., et al. (2007). Interferon-γ and Tumor Necrosis Factor-α Regulate Amyloid-β Plaque Deposition and β-Secretase Expression in Swedish Mutant APP Transgenic Mice. *The American Journal of Pathology,* 170, 680-692.

Yanamadala, V. and Friedlander, R. M. (2010). Complement in neuroprotection and neurodegeneration. *Trends in Molecular Medicine*, 16(2), 69-76.

Yanker, B. A., et al. (2008). The aging brain. *Annual Review of Pathology: Mechanisms of Disease*, 3: 41-66.

Yirmiya, R., Winocur, G., and Goshen, I. (2002). Brain interleukin-1 is involved in spatial memory and passive avoidance conditioning. *Neurobiology of Learning and Memory*, 78, 379-389.

Zahnd, C. et al. (2007). A designed ankyrin repeat protein evolved to picomolar affinity to Her2. *Journal Molecular Biology*, 369, 1015-1028.

Zahnd, C., Amstutz, P. and Plückthun, A. (2007). Ribosome display: selecting and evolving proteins in vitro that specifically bind to a target. *Nature Methods*, 4, 269-279.

Zahnd, C. et al. (2010). Efficient tumor targeting with high-affinity designed ankyrin repeat proteins: effects of affinity and molecular size. *Cancer Research*, 70, 1595-1605.

Zecca, L., et al. (2004). Iron, brain ageing and neurodegenerative disorders. *Nature Reviews Neuroscience*, 5, 863-873.

Zlokovic, B.V. (2008). The blood-brain barrier in health and chronic neurodegenerative disorders. *Neuron*, 57, 178-201.

7 Acknowledgements

First and foremost, I would like to thank Prof. Dr. Roger M. Nitsch for outstanding supervision, support and mentorship. I am particularly grateful for your consistent encouragement to participate in collaborative projects and freedom and support to pursue my own goals. I also owe a debt of gratitude to Prof. Dr. Christoph Hock for his continual support and mentorship. It has been a great honor and pleasure to work closely with two world-leading specialists, whose mentorship will have a lasting impact on my scientific, professional and personal life. I have and will continue to appreciate your scientific insight and business know-how and look forward to continuing both our friendship and professional work together.

Additionally, I would like to thank my steering committee (Prof. Dr. Roger M. Nitsch, Prof. Dr. Christoph Hock, Prof. Dr. Burkhard Becher, Prof. Dr. Adriano Fontana and Prof. Dr. Esther Stöckli) for helpful guidance and encouragement.

To my dear friends and colleagues, Dr. Uwe Konietzko, Dr. Tobias Welt and Dr. Luka Kulic, thanks for all the support, advice and collaborative work. It has truly been a pleasure to work the long hours, nights, weekends, holidays, basically 24/7, together with you guys as a team. It is rewarding to look back and see how much we have accomplished together over these few years! Of course, I would also like to thank Big DARPIN, Dr. Michael Hanenberg, for the opportunity to work on the exciting DARPin project. I hope our 'team-science' approach can serve as an example to other young scientists, that working together is far more productive and enjoyable. Especially in todays cut throat, clandestine, 'its-all-about-me' scientific environment, it is refreshing to be apart of a team that works hard to promote the success of each individual member! Furthermore, I will also remember all the great scientific discussions, laughs, good BBQs and fun we shared together. To my extended NBR family (Fabian Wirth, Benedetta Maimone, Claudia Späni, Rebecca Derungs, Anna Jeske, Maik Krüger, Armanda Prister, Salome Zeller, Daniel Preisig, Anika Simon and former members, Dr. Sarah Hoey and Mauela Hitz), I would also like to say thanks for all the support and great working environment. I have learned a great deal from each and every one of you and have enjoyed the few moments in which I could give something back. With such talented students, the future of neuroscience is looking bright! It has been a pleasure to be apart of your early careers! Keep up the great work!

To my clinical colleagues and friends (Dr. Anton Gietl, Andrea Kälin, Marie-Louise Lüthi, Noemi Ribaut, Esmeralda Gruber, Daniel Summermatter, Dr. Florian Riese, Dr. Ana Botosaneanu, Dr. Henrike Wolf, Dr. Husam Suliman, Dr. Mathias Laurig, Dr. Senol Apaydin, among others), thanks for always reminding me that dementia is a human disease with clinical symptoms and not a mouse or cell culture. It has been highly rewarding to work in such a translational research environment with one foot in clinical research and the other foot in basic science. Moreover, I would also like to thank the many lab members at the Division of Psychiatry Research for fruitful collaborations and a friendly work environment: Dr. Zoe Goodger, Dr. Mario Merlini,

Dr. Annapoorna Bhat, Dr. Verena Finder, Dr. Antonella Chada Santuccione, Dr. Susann Cattepoel, Dr. Christian Tackenberg, Dr. Gabriele Siegel, Dr. Maria-Teresa Ferretti, Dr. Marco Frey, Saoussen Ben Halima, Jitin Bali, Manuel Gersbacher, Lisa Strobel, Annette Trutzel, Diana Bundschuh, Garima Thakur, Barbara Siegenthaler, Nino Jejelava, Sebastian Zurbriggen, Vinod Udayar, Sonja Grinschgl, among others. In particular, I would like to thank Dr. Anita Szodorai for all the enjoyable moments within the 'Center of Evil' and for being, in many occasions, the voice of reason and good judgment! Lastly, I would like to give a special thanks to Dr. Cornelia Marty, Wiebke Buck, Michelle Rohr and Isabelle Leidi-Hegi, for all their support and assistance.

I would like to sincerely thank all the members (Daniel, Björn, Ramiro, James, Asanti, Alex) of the animal facility for their technical support and willingness to put up with Mr. President. Without your work and diligence none of our scientific work would be possible. Many thanks.

Equally important, I would like to extend my gratitude to Dr. Christopher R. Pryce for his expertise and support in establishing the various cognitive-behavioral tests used within this project. Always the gentlemen, it has been a pleasure to work alongside a world-leading behavioral specialist!

Furthermore, throughout my PhD I have had the pleasure to work on several exciting collaborations and would like to thank:

Prof. Christoph Hock, Prof. Roger M. Nitsch, Dr. Anton Gietl, Dr. Anita Szodorai, Dr. Husam Suliman, Dr. Henrike Wolf, Andrea Kälin, Marie-Louise Lüthi at Division of Psychiatry Research, University of Zurich: "Aβ-directed humoral immune responses in prodromal AD", "Novel blood and CSF biomarkers in MCI and AD", and "Amyloid (PIB) PET imaging in healthy elderly subjects".

Dr. Tobias Welt, Fabian Wirth at Division of Psychiatry Research, University of Zurich: "Immune and Inflammatory mechanisms in amyotrophic lateral sclerosis (ALS)" and "Muscarinic receptor agonists and their effects on APP metabolism *in vivo".*

Dr. Jan Grimm, Dr. Marcel Maier, Dr. Fabio Montrasio at Neuroimmune Therapeutics AG, Schlieren. "Preclinical research into human-derived antibodies against misfolded proteins in neurodegenerative diseases".

Dr. Luka Kulic, Claudia Späeni at Division of Psychiatry Research: "Adaptive immune responses in Alzheimer's disease".

Prof. Philip Scheltens, Dr. Charlotte Teunissen, Dr. Wiesje van der Flier, Dr. Sietske Sikkes at VUmc Alzheimercentrum, Amsterdam: "Identifying biomarkers for age-associated and neurodegenerative diseases" and "Mobile and Web-based Technologies for Dementia Care".

Prof. Annemieke Rozemuller, Prof. Elga de Vries, Prof. Jeroen Hoozemans, Anna Carrano at Department of Neuropathology, VU University Amsterdam: "Blood-brain barrier alterations underlying capCAA pathology".

Prof. John H. Growdon at MGH Memory Disorders Unit, Harvard, Boston, USA. “Mobile and web-based technologies for dementia care.”

Prof. Manuela Neumann, Thorsten Läufer at Experimental Neuropathology, University of Zurich: “TDP-43 and FUS mouse models representing ALS”.

PD Dr. Irene Knüsel at Institute of Pharmacology and Toxicology, University of Zurich: “Immune challenge as an environmental risk factor associated with neurodegeneration”.

Prof. A. Claudio Cuello, Prof. Roger M Nitsch, Dr. Tobias Welt, Benedetta Maimone at Department of Pharmacology, McGill University and Division of Psychiatry Research, University of Zurich: “Investigating synaptotoxicity in APP transgenic rats”.

Prof. Lawrence Rajendran, Dr. Zoe Goodger, Dr. Jenny Franberg, Dr. Gabriele Siegel, Saoussen Ben Halima, Jitin Bali at Systems and Cell Biology of Neurodegeneration, University of Zurich: “Characterizing the regulatory mechanisms of non-coding RNAs during aging and Alzheimer’s disease progression”.

Dr. Michael Linnebank, Melinda Farkas, Rebecca Derungs at Department of Neurology, University of Zurich: “Involvement of homocysteine and copper metabolism and in the development and progression of Alzheimer’s disease” and “Effects of B-vitamin deficiency on the progression of demyelinating CNS diseases”.

Lastly, I would like to thank Sharon, my partner in love and crime. We have travelled the world together and studied on three continents. It’s hard to believe that we have finally reached the end of this ‘student’ life. What will the future hold next for us? I don’t know, but I am comforted in knowing that it will be an unforgettable adventure shared with my best friend. Thanks for always supporting me and understanding the crazy work load that keep me so busy during the late nights, early mornings, weekends and holidays. I am not sure if I will finally get a chance to sleep in or take a day off, but at least I have completed my PhD!

To my parents (Don and Lois), family (JR, JD, JC, Mel, Jolene, Mick, Mitch, Micah, Mase, Case, Chris, Edwina and Kevin) and friends, thanks for all the love and encouragement. Could I kindly ask you all to call me (without laughter) Dr. Jordan from now on!

As a final comment, I would like to thank the, Forschungskredit (UZH), Zurich Neuroscience Zentrum (ZNZ) and the ENC-Network for financial support, education and training, and the collaborative environment to pursue my career as a young neuroscientist.

8 Curriculum Vitae

Name: Jordan W. McAfoose, BPsych Honours
Date of Birth: August, 1981, USA

Position/Title/Address:
PhD Fellow, University of Zurich
Division of Psychiatry Research and Psychogeriatric Medicine
August Forel-Strasse 1, 8008 Zurich, Switzerland
Tel. +41 44 634 88 48, jordan.mcafoose@bli.uzh.ch

Education

1995-1999	Cy-Fair Highschool, Houston, Texas, USA
1999-2003	Tomball College, Houston, Texas, USA
2004-2008	BPsych Honours, School of Psychology, James Cook University, Australia
2009-2012	PhD, Division of Psychiatry Research, University of Zurich, Switzerland
2010-2012	PhD, ENC-Network, VU Amsterdam, Netherlands

Academic Appointments

2006-2007	Research Assistant in Neurobiology, Comparative Genomics Centre, James Cook University
2007-2008	Principle Tutor for the Department of Psychology, James Cook University
2007-2008	Associate Lecturer, MBBS Honours Program, School of Medicine, James Cook University
2007-2008	Research Officer, Department of Psychiatry and Psychiatric Neuroscience, James Cook University
2009-2012	PhD Fellow, Division of Psychiatry Research, University of Zurich, Switzerland
2010-2013	PhD Fellow, ENC-Network, VU Amsterdam, Netherlands

Awards

2003	Dean's list for Academic Achievement, Tomball College
2004-2007	Golden Key International Honour Society
2007	Australian Psychological Society Prize in Psychology
2008	Dean's List for Academic Achievement, James Cook University
2008	Australian Psychological Society Prize in Psychology
2008	Academic Medal, James Cook University
2009	Forschungskredit Fellowship, University of Zurich
2010	ENC-Network Fellowship, Eramus Mundus, EU
2011	Gebert rüf Stiftung Venture Kick Stage 1

Professional Training

2008	Neuropathology, Department of Neuropathology, University of Sydney, Australia

2007-2008 Psychiatric Neuroscience, Department of Psychiatry and Psychiatric Neuroscience, James Cook University, Australia
2009-2011 Transgenic Mouse Models, Institute of Laboratory Animal Science, UZH, Switzerland
2009-2011 Neuroscience, Neuroscience Center Zurich, University of Zurich and ETH, Switzerland
2010-2012 Advanced Neuroscience Specialization, ENC-Network Neuroscience, EU

Membership
Erasmus Mundus Association
Swiss Society for Neuroscience
Federation of European Neuroscience Societies
International Brain Research Organization

Former
Australian Psychological Society
APS College of Clinical Neuropsychologists
Australian Neuroscience Society
Australian and New Zealand Society of Neuropathology

Research Areas of Interest
Neurodegeneration; Neuroimmune therapeutics; Transgenic models; Translational medicine; MedTech

Grant Support
Forschungskredit UZH, ENC-Network EU, Venture Kick, McGill-ZNZ

Corporate Activities
2010 TSE Systems, Development Partners
2010 Neurimmune Therapeutics AG, Development Partners
2011 imCare AG, Founder and CEO

Publications
Chadha Santuccione, A, Merlini, M., Shetty A., Tackenberg, C., Bali, J., **McAfoose, J.,** Kulic, L., Bernreuther, C., Grimm, J., Glatzel, M., Rajendran, L., Hock, C., Nitsch, R.M. (submitted). Active vaccination with the novel APP - interacting protein ankyrin G reduces beta-amyloid pathology in APP transgenic mice. *Molecular Psychiatry*.

Baune, B. T., Miller, R., **McAfoose, J**., Johnson, M., Quirk, F. & Mitchell, D. (2010). The role of cognitive impairment in general functioning in major depression. *Psychiatry Research*, 176, 183-189.

McAfoose, J. & Baune, B. T. (2009). Evidence for a cytokine model of cognitive function. *Neuroscience and Biobehavioral Reviews*, 33(3), 355-366.

McAfoose, J., Koerner, H. & Baune, B. T. (2009). The effects of TNF deficiency on age-related cognitive performance. *Psychoneuroendocrinology*, 34, 615-619.

Baune, B. T., **McAfoose, J**., Leach, G., Quirk, F. & Mitchell, D. (2009). Impact of

psychiatric and medical comorbid depression on cognitive function. *Psychiatry and Clinical Neuroscience*, 63, 392-400.

McAfoose, J. & Baune, B. T. (2009). Exploring visual-spatial working memory: A review of concepts and models. *Neuropsychology Review*,19, 130-142.

Janssen, D.G.A., **McAfoose, J.**, Schweizer A., Baxter, A., Verster, J.C., Deckert J., *et al.* (2008), The interaction between interferongammareceptors and the mapk6/8 signalling pathway is associated with antidepressant treatment outcome in depression, *Journal of Psychopharmacology,* 22 (suppl), 74.

Hager, K., Kenklies, M., **McAfoose, J.**, Engel, J., & Münch, G. (2007). α-lipoic acid as a new treatment option for Alzheimer's disease– a 48 months follow-up analysis. *Journal of Neural Transmission*, Suppl 72, 189-193.

Oral and Poster Presentations

McAfoose, J., Kulic, L., Welt, T., Späni, C., Pfister, A. & Nitsch, R. M. (poster presentation, July 2012). Effects of anti-TNF therapy on amyloid pathology and neuroinflammation in 12 month old arcAb mice. *AAIC Conference, Vancouver, Canada.*

Kulic, L., **McAfoose, J**., Welt, T., Späni, C., Hock, C. & Nitsch, R. M. (poster presentation, July 2012) A novel mouse model of interneuronal Aβ and CAA deposition. *AAIC Conference, Vancouver, Canada.*

McAfoose, J. (oral presentation - 2012, March). Effects of anti-TNF therapies on amyloid pathology and neuroinflammation in 12 month old arcAb mice. *8th Winter Brain Symposium*, *Division of Psychiatry Research and Psychogeriatric Medicine, University of Zurich, Sils Maria, Switzerland*.

Chadha Santuccione, A, Merlini, M., Shetty A., Tackenberg, C., Bali, J., **McAfoose, J.,** Kulic, L., Bernreuther, C., Grimm, J., Glatzel, M., Rajendran, L., Hock, C., Nitsch, R.M. (poster presentation – December, 2011). Active vaccination with the novel APP - interacting protein ankyrin G reduces b-amyloid pathology in APP transgenic mice. *Tag der Forschung*, *Psychiatric Universtat Klinik, University of Zurich, Zurich, Switzerland*.

McAfoose, J. (oral presentation - 2011, November). Identifying Biomarkers for Age-Associated and Neurodegenerative Diseases: Immune Surveillance Markers and Translational Approaches. *NUBIN Meeting*, *Alzheimerscentrum, VUmc Amsterdam, Netherlands*.

McAfoose, J. (oral presentation - 2011, November). Detecting and Monitoring Disease Progression in Super Slow Motion: TDP-43 pathologies. *Clinical Chemistry Meeting*, *VUmc Amsterdam, Netherlands*.

Wirth, F. Welt, T., **McAfoose, J.,** Späni, C., Jeske, A., Kulic, L., Nitsch, R. M. (poster presentation – September, 2011). Deciphering disease underlying mechanisms in

amyotrophic lateral sclerosis (ALS). *ZNZ Symposium 2011, Neuroscience Center Zurich, Switzerland*.

McAfoose, J., Hock, C., Scheltens, P. & Nitsch, R. M. (oral presentation – March, 2011). Identifying biomarkers for age-associated and neurodegenerative diseases. *ENC-Network Annual Meeting, Göttingen, Germany.*

Welt, T., **McAfoose, J**., Kulic, L., Hoey, S., Fisher, A. & Nitsch, R. M. (poster presentation, March 2011). Modulation of hippocampal muscarinin receptors influences APP processing – An in vivo microdialysis study. *AD/PD conference, Barcelona, Spain.*

Läufer, T., Welt, T., **McAfoose, J**., Naumann, R., Nitsch, R. M. & Neumann, M. (poster presentation, March 2011). Behavioral, biochemical and histological analysis of transgenic TDP-43 mice. *AD/PD conference, Barcelona, Spain.*

Wolf, K., Kulic, L., **McAfoose, J**., Lüthi, M. L., Kälin, A. M., Gruber, E. Nitsch, R. M., Hock, C. H. & Gietl, A. F. (poster presentation, March 2011). Serum levels of Beta-Amyloid-Peptides in patients with Alzheimer's disease (AD), Mild Cognitive Impairment (MCI) and Healthy elderly subjects. *AD/PD conference, Barcelona, Spain.*

Kulic, L., **McAfoose, J**., Welt, T., Späni, C., Jeske, A., Hock, C. & Nitsch, R. M. (poster presentation, March 2011). Familial Alzheimer's disease (AD) APP mutations at position 693 differentially affect Aβ accumulation and deposition in vivo. *AD/PD conference, Barcelona, Spain.*

McAfoose, J., Kulic, L., Späni, C., Jeske, A., Welt, T., Pfister, A., Zeller, S. & Nitsch, R. M. (poster presentation, March 2011). Effects of anti-TNF therapies on amyloid pathology and neuroinflammation in 12 month old arcAb mice. *AD/PD conference, Barcelona, Spain.*

McAfoose, J. (oral presentation - 2011, March). Effects of Anti-TNF therapies on amyloid pathology and neuroinflammation in 12 month old arcAb mice. *7th Winter Brain Symposium, Division of Psychiatry Research and Psychogeriatric Medicine, University of Zurich, Sils Maria, Switzerland*.

Welt, T., **McAfoose, J**., Kulic, L., Hoey, S., Fisher, A. & Nitsch, R. M. (poster presentation, November 2010). Modulation of hippocampal muscarinic receptors influences APP processing – An in vivo microdialysis study. *Society for Neuroscience, San Diego, California, USA.*

McAfoose, J. (oral presenation - 2010, March). Cognitive-behavioral phenotyping and disease mechanisms of transgenic AD mouse models. *6th Winter Brain Symposium, Division of Psychiatry Research and Psychogeriatric Medicine, University of Zurich, Sils Maria, Switzerland*.

McAfoose, J. Welt., T., Farinelli, M., Pryce, C., Mansuy, I. & Nitsch, RM. (oral presentation - 2009, December). Alzheimer's disease from an immunological

neuroscience perspective. *Tag der Forschung, Psychiatric Universtat Klinik, University of Zurich, Zurich, Switzerland*.

McAfoose, J. (oral presentation - 2009, March). Characterizing the expression of cytokines throughout aging, disease state and therapeutic intervention in an AD mouse model. *5th Winter Brain Symposium, Division of Psychiatry Research and Psychogeriatric Medicine, University of Zurich, Sils Maria, Switzerland*.

McAfoose, J., Koerner, H. & Baune, B. T. (oral presentation - 2008, December). TNF deficiency and age-associated cognitive performance – a mouse model. *Australasian Society for Psychiatric Research Conference, Newcastle, New South Wales, Australia.*

McAfoose, J., Koerner, H. & Baune, B. T. (oral presentation - 2008, January). The impact of TNF on cognitive function during aging processes. *The 28th Annual Meeting of the Australian Neuroscience Society, Hobart, Tasmania.*

Baune, B. T. & **McAfoose, J**. (oral presentation - 2008, January). The influence of IL-1beta, IL-6 and TNF-alpha polymorphisms on CNS function of cognitive performance, depression and antidepressant pharmacoresponse. *The 28th Annual Meeting of the Australian Neuroscience Society, Hobart, Tasmania.*